ACS Catalysis

pubs.acs.org/acscatalysis

Review

Enroute to the Carbon-Neutrality Goals via the Targeted Development of Ammonia as a Potential Nitrogen-Based Energy Carrier

Muhammad Asif Nawaz,* Rubén Blay-Roger, Maria Saif, Fanhui Meng, J. González-Arias, Baoji Miao, Luis F. Bobadilla, Tomas Ramirez-Reina, and J. A. Odriozola*

Cite This: *ACS Catal.* 2023, 13, 14415−14453

Read Online

ACCESS | Metrics & More | Article Recommendations

ABSTRACT: The reliance of a future carbon-free horizon is strongly aligned with the long-term energy storage avenues which are completely derived from renewable energy resources. Ammonia with its high energy content and density can perform as a decent candidate for buffering the short-term storage options. However, the current NH_3 production majorly feeding the current huge desire for ammonia is dominated by the conventional nonrenewable Haber−Bosch (H−B) process route, thus continuously damaging the target of carbon neutrality goals. High-purity hydrogen (H_2) gas is an essential precursor for the H−B process; however, it is a significant energy consumer (about 2% of the global energy supply) and contributes over 420 million tons of CO_2/annum. Therefore, the research on the renewable synthesis of nitrogen-based energy carriers (such as ammonia) from the direct electrochemical, photocatalytic, or plasma catalytic processes; its conversion; and utilization to the potential derivatives has been a hot topic in the past few decades. A prospective analysis of the highly appealing processes has been summarized in this study, which could facilitate the adaption of renewable alternatives as an effective approach for zero carbon emission, paving the excellent pathways along the road to the development of nitrogen-based energy technologies, especially the targeted development of ammonia. Further, this Review covers the current and future impacts of the H−B process, the development of aspiring ammonia synthesis routes (via electro, photo, bio, chemical loop, or plasma catalysis), and its conversion and utilization to the renewable derivatives in terms of fabrication of model catalysts, advanced characterization technology, and efficient device design.

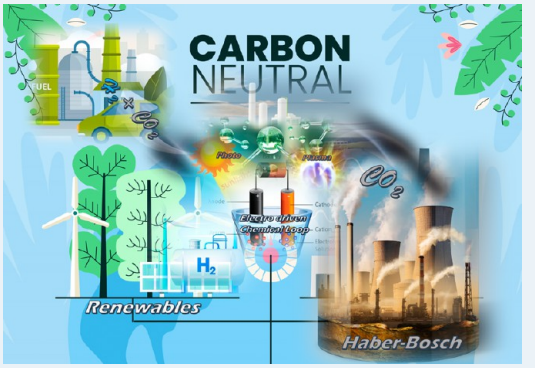

KEYWORDS: *nitrogen-based energy, Haber−Bosch process, NH_3, photoelectro catalysis, plasma catalysis*

1. INTRODUCTION

The exhaustion of fossil fuels and the deterioration of the ecological environment direly require the search for sustainable routes to meet future production desires. The steadily increasing demand in renewable resource-based industry and the growing anthropogenic climate change stipulate the utter replacement of extensive fossil fuels based industrial processes to the renewable and ecofriendly energy production systems.[1,2]

Obtaining high energy density liquid fuels such as methanol, liquid hydrogen, or liquid ammonia from renewable sources and converting them on site to the desired product can be a promising way of developing the narrative of a sustainable (net-zero carbon emissions) society. Among these, liquid H_2 can be the most important alternative for carrying the buffering seasonal fluctuations and satisfying the current desire for a large-scale energy storage. Its exceptional sustainable energy-based production can pave a palpable and economic path for decarbonizing future global energy systems. However, the liquefaction of hydrogen is an energy intensive mean, as a 1 kg production of H_2 in current electrolyzer needs an energy input of almost 50−56 kWh, leading to 26−30 kg of CO_2 emissions with an estimated power economy of 470 TWh a^{-1} and 254 Mt_{CO_2} a^{-1} equivalents.[3] The dissipation of (∼30%) energy content in the large-scale storage and boil-off losses during transportation over long distances would dictate its deployment in view of economic concerns and limited practical value. Ammonia (NH_3), with its carbon-free nature, high energy density (∼1.3 × 10^4 MJ m^{-3}, $\Delta_f H°_{298\ K}$ = −46 kJ mol^{-1}), and high hydrogen content (17.75 wt % than 12.6 wt % of

Received: May 28, 2023
Revised: October 5, 2023
Accepted: October 11, 2023
Published: October 26, 2023

methanol), can be evaluated as an ideal green fuel and intermediate for H_2 storage.[4,5] Being one of the most compelling industrial candidates in the sustainable community, NH_3 can be nominated as the second largest manufacturing chemical after H_2SO_4, with its substantial global production of 200 million tons per annum.[6,7] This supply for holding the industrial development requirements (in chemical intermediates, explosives, and refrigerant), majorly flourishes the food and agriculture sector with its 80% utilization in fertilizers.[8−10]

Having a low burning velocity, low ignition energy, a narrow flammability limit, high ease of liquefaction, and accessible dissociation chemistries, it can be counted as a promising candidate for H_2 carrier in advanced mobility and storage.[11] Currently, it is barely used as an energy carrier, while it can play a vital role in balancing the demand of other chemical commodities and substituting the conventional fossil fuel resources for future energy platforms. It would pave a bright path for the potential future uses as a zero carbon footprint and an efficient energy vector in the form of NH_3 and H_2 blends.[12] Enabling the molecule's prospect as a net-zero-carbon fuel via the emerging and renewable-electron-driven synthesis pathways would empower NH_3 to broad stationary transportation and energy applications. The deployment of environmentally friendly and energy-efficient alternatives is direly needed for large-scale industrial NH_3 production for ensuring the achievement of carbon neutrality goals. Therefore, as a distinctive nitrogen-based energy carriers, the sustainable synthesis of ammonia from the direct electrochemical, chemical loop, photocatalytic or plasma catalytic, its conversion and utilization to the renewable derivatives has been a hot topic in recent years.[13−18] The adaption of electrolyzing water, molten salt or solid-state electrolytic cell alternatives could pave their way in finding an imperatively better route than conventional H−B, along the road to the development of nitrogen-based energy technologies (especially for green ammonia).[19−23]

This Review presents an overview of the great efforts being devoted in recent times to the development of a green and sustainable nitrogen-based energy conversion and storage process (especially ammonia), powered by renewable sources. A round-trip efficiency of different routes of ammonia synthesis (thermal, electrochemical, chemical loop, plasma, and photocatalytic) along with its conversion and utilization as an energy vector has been deeply interpreted in terms of the advanced experimental devices, catalysts design, and developed characterization technology.

2. AMMONIA: AN OLD-COMPASSIONATE LAD

Ammonia (NH_3) is a poisonous, colorless gas with an intimate toxic odor that has been known since ancient times. It was identified by a number of distinguished chemists Carl Wilhelm Scheele (Sweden/Germany), Claude Louis Berthollet (French), Joseph Priestley (England), Peter Woulfe (Ireland), and Joseph Black (Scotland) in the early 17th−18th century.[24] As an essential element of society and a fundamental building block in every aspect of life from fertilizer to the manufacturing of plastics, explosives, dyes, fabrics, refrigerant, stabilizer, neutralizer, purifier in food transport, water treatment applications, pharmaceuticals and a vital source of energy carrier, it naturally occurs all around the environment (in the air, soil, plants water and animals).[25−27] NH_3 is an extremely precious commodity in various sectors; however, as a basic building block of NH_4NO_3 and the major source of N_2, 90% of NH_3 produced worldwide is used in fertilizer for providing the essential nutrients (such as zinc, selenium and boron).[28] With its profound global impact, ammonia has been a pillar of the chemical industry, where it currently ranks among the topmost chemicals produced globally with the recent estimated worldwide ammonia production capacity of 224 million tons (Mt).[29,30]

The industrial ammonia synthesis process via the catalytic reaction of N_2 + H_2, was first ever developed by Fritz Haber and Carl Bosch (German chemists) in 1909, being nominated as Nobel laureates (Haber in 1918 and Bosch in 1931) for their work in Chemistry.[11] That unprecedented invention was a milestone in the instigating catalytic field that established the basis for the entire chemical engineering science and harnessed the genesis of a new industrial catalysis era. Since then, the preeminent H−B bench reactor was converted by Carl Bosch in 1913 with amazing speed into the first commercial ammonia plant in Oppau, Germany, making 20 tons of ammonia per day.[28] This commercial production of NH_3 in the early nineties, owes its existence to the successful evolution of a fused iron catalyst as an effective applicant of a great technical achievement in early stage, where the enormous efforts in the successful progress of synthetic ammonia industry with several new techniques and strategies, led to a precedent for today's prevalent innovation,[24,31,32] including the most recent Nobel Prize in Chemistry awarded to Gerhard Ertl[33] in 2007 for his achievements in surface science, particularly at the gas−solid interface. Even though the current industrial ammonia synthesis (H−B) process is a nongreen and fossil fuel-derived hydrogen product, it is still considered the backbone of widespread agriculture manufacturers. However, the conventional synthesis route direly needs to be replaced by the new green horizons of environmentally friendly ammonia via overcoming the major challenges of low-cost sustainable approaches of hydrogen and nitrogen resources at industrial scale.

2.1. Current Ammonia as the Major Source of Carbon Emission. The tremendous advancement in heterogeneous catalysis over the last 50 years, and the accredited technical improvement in the process engineering could encourage the expanded production (∼2200 tons) of ammonia per day from a single plant.[31] In view of the sources adopted for ammonia production, they can be categorized into the following three aspects: The source being derived from the fossil fuel as the feedstock with higher carbon emissions can be regarded as brown ammonia. The source being adopted from the brown ammonia while applying some effective measures of carbon capture and storage technology to the production process can be categorized as low-carbon ammonia or blue ammonia. However, the ammonia being made with the entire sustainable route such as electricity, water and air can be nominated as the green ammonia or zero-carbon ammonia.[34] Therefore, it can be interpreted that the overall ammonia being synthesized in this regard is similar in basic aspects, while it is the carbon emission in the synthesis route that resolves it into different zones. The current traditional synthesis route (N_2+3H_2 ⇌ 2NH_3) by Haber−Bosch (H−B) process, ΔH 400 °C = −104 kJ mol^{-1}, is not only composed of an energy-intensive mean but also incorporated with crucial environmental impacts.[24,35] It could be one of the most astonishing industrial chemical process ever developed; however, it represents the significantly largest carbon dioxide emitting chemical industry process as well.[29] Since the highly carbon and energy-intensive H−B

https://doi.org/10.1021/acscatal.3c02410
ACS Catal. 2023, 13, 14415−14453

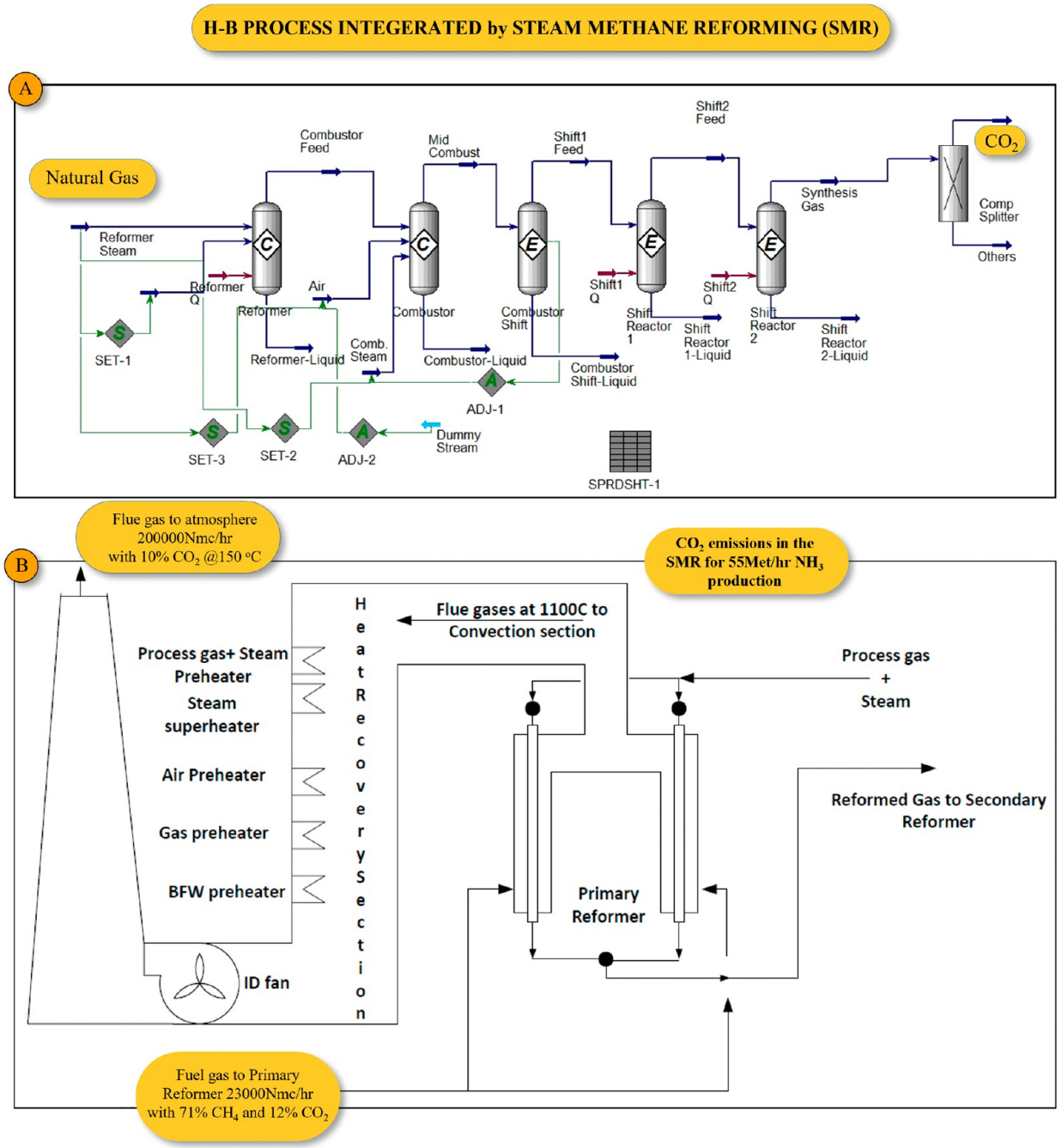

Figure 1. Process flowchart of primary reformer producing ample amount of CO_2 using fossil feedstock (data acquired from different running industrial sectors).

process of converting H_2 and N_2 to ammonia, appearing in the brown ammonia category, is usually operated under harsh reaction conditions while consuming huge amounts of energy per ton. Notably, 2−3% of the global power generation is utilized every year in the industrial H−B process while engendering the huge (430 million tons) CO_2 emissions.[34] H_2 as a requisite precursor of the H−B process is an exceptional energy consumer being syndicated with high levels of carbon emissions through typically steam methane reforming (SMR) route, acquiring the typical reaction conditions to be maintained for the activation of inert N_2 molecule.[35−37]

The exothermic reaction ($\Delta H = -46$ kJ mol^{-1}) nature of ammonia synthesis ($N_2(g) + 3H_2(g) = 2NH_3(g)$) involving a decrease in entropy, favors the high pressures and lower temperatures as the key factors of forward reaction.[38] However, the strong energy barrier of inert N≡N bond and the sluggish reaction rate, makes the synthesis reaction to be maintained at typical reaction conditions (450 °C, 200 bar) adopting an Fe-based catalyst.[28] Sustainable ammonia synthesis is the process of making ammonia 100% renewable and carbon-free, while the SMR process via water and air to produce hydrogen generates approximately 90% of the carbon dioxide. Natural gas (NG), coal, or oil as the major sources of hydrogen production for ammonia synthesis, adopt the processes that release 1.6, 3.0, and 3.8 tons of CO_2 per ton of NH_3, and the best practice energy consumption values of

https://doi.org/10.1021/acscatal.3c02410
ACS Catal. 2023, 13, 14415−14453

7.9, 11.1, and 12.2 MWh, respectively.[24] Where a rough estimation from different current industrial sectors revealed that each of the single working plants synthesizing NH_3 from hydrocarbon feedstocks, would emit 3000−4000 N mc (calculation as industrial flow) flue gases every single hour to the atmosphere only from the primary reformer section with a major contribution (10−15%) of CO_2 at 150 °C temperature for each Nmc/Met production of ammonia as shown in Figure 1. Hydrogen is produced on-site via SMR with a typical reformer or gasifier initially installed for the conversion of raw feed (fuel) to the syngas ($CH_4 + H_2O \rightarrow CO + 3H_2$) in combination with the water−gas shift (WGS) reaction by the shift reactors to separate the CO and hydrogen mixture ($CO + H_2O \rightarrow CO_2 + H_2$). This consists of the following steps: combining the H_2O and CO from syngas to form CO_2 and more H_2; methanation to convert leftover CO to methane; acid gas removal for isolating the hydrogen and CO_2; compression of the $H_2 + N_2$ gas mixture to synthesis pressures; and finally, ammonia synthesis in the H−B reactor indicate the hectic measures of this route, releasing the ample amount of CO_2 at various steps along the way. Despite the huge technological advancement in the process, that massive carbon footprint goes well beyond its energy demands and has always been an energy-hungry route of sucking up about 2% of the world's total energy production. The energy utilized in the manufacturing of NH_3 is usually associated with the plant size, region, and source of H_2 extraction. Although the reaction itself is exothermic, significant energy is primarily consumed in the reactant purification, compression and H_2 production in strongly endothermic SMR process operated at 800−1000 °C, while applying excess steam (at 350−550 °C) in the shift reactor to eliminate CO from the effluents and enhancing H_2 yield through the slightly exothermic water gas shift (WGS) reaction (as shown in the following).

$$CH_4 + H_2O \rightarrow CO + 3H_2,\ \Delta H^\circ R,\ 298\ K = +206.1\ kJ\cdot mol^{-1} \quad (1)$$

$$CO + H_2O \rightarrow CO_2 + H_2,\ \Delta H^\circ R,\ 298\ K = -41.2\ kJ\cdot mol^{-1} \quad (2)$$

Therefore, as the source of around 1/3 of global emissions, quantifying the CO_2 footprint and providing the necessary basis for targeted emission management is the most urgent task for achieving climate goals and the significant reduction of greenhouse emissions. The H−B route could be the most instigating process ever developed; however, the industrial NH_3 production is also the biggest CO_2 emitting source than any other chemical industry, thus requiring an overall decent integrated system based upon a low-carbon energy process. The current desire for ammonia fertilizer is increasing day by day in this techno economic era, where the huge consumptions in crops and daily life products may leach the remainder into the air, water and soil to cause the widespread eutrophication, biodiversity, and stratospheric ozone loss, adding to the greenhouse emissions. It can be stated that as ammonia is produced today, our food is effectively a nonsustainable fossil-fuel product for majorly relying on the nitrogenous fertilizer.[28] Therefore, minimizing the ammonia emissions from agriculture and CO_2 needs some effective measures to find new applications to improve the resulting air pollution and to prevent any additional emissions through deposition for implementing the net-zero carbon emissions plan.

3. ENROUTE TO THE ZERO-CARBON ARTIFICIAL AMMONIA SYNTHESIS

Keeping in view of the intensive utilization (80%) of ammonia in fertilizers likely to be increased to ∼270 million tons per year by 2050, the current predictive analysis combined with the requirement of decarbonizing the H−B process reflects that these carbon-intensive means of industrial NH_3 production must be sorted through significant greener alternatives.[34] Therefore, harnessing the low-carbon narrative by deploying some low-cost renewable (electrifying, solar, or wind) means would efficiently reduce those exhaustive carbon emissions. Several investigations are being appraised to make a sustainable ammonia synthesis in a fully decarbonized manner. Possible tactics include the following: powering the reaction with renewable sources; conventionally manufacturing it with the desolation of CO_2; generating H_2 without fossil fuels in a modified small-scale H−B units by water electrification (wind, solar, and tidal wave, etc.); and adapting the efficient renewable production strategies by electro, photo, bio, or plasma catalysis, could pave their way in finding an imperatively decent route than conventional H−B. The diversity in the ammonia synthesis sector would fantastically grow quickly with the formulation of those new smart integrated plants with notable potential for rationally concerning the dramatical reducing costs by renewable energies.

3.1. Electrifying the Haber−Bosch Process Using Renewable Energies. The adaption of H_2 through water electrolysis in a renewable electrochemical Haber−Bosch (eHB) process, contrasting with that of conventional utilization of fossil fuel resources in large-scale H−B processes, could be the catastrophic approach of zero carbon emission entity. The electrochemical synthesis of ammonia is majorly dependent on the type of electrolyte, where the three basic categories such as solid oxide electrolyte, aqueous solution electrolyte, and molten salt electrolyte perform the vital role in transporting the N/H-containing ions to the electrode surfaces, in which ammonia synthesis takes place.[39−41] Centralizing the small-scale islanded herb units with efficient catalytic activity at mild conditions in the designated electrification process could be of great significance for deviating the dynamic supply of hydrogen, dwindling the intensive energy requirements, and reducing the involved safety risks. Therefore, the enticing approach in electrochemical process is the adaption of renewable H_2 atoms from H_2O molecules instead of molecular hydrogen,[2] where the smart process operating at optimal process conditions could beat the utter desire of fossil fuels both in power generation and hydrogen production.[42] Therefore, it could present a decent means of settling a trade-off between reaction rates and yields that is usually encountered for running the H−B process. The dynamic relation of increasing the voltage (even in fractions of a volt) instead of pressure in an electrochemical system can achieve the desired limits, which is normally taken by hundreds of bar pressure. Immense efforts have been devoted in flourishing the small-scale green eHB route to substitute the synthesis loop of commercial H−B process,[43] which are being discussed with the following aspects.

3.1.2. The High-Temperature Route (>500 °C): Solid-State Electrochemical Ammonia Synthesis (SSEAS). Being aspired

https://doi.org/10.1021/acscatal.3c02410
ACS Catal. 2023, 13, 14415−14453

by the natural enzymatic N_2 fixation of synthesizing ammonia at ambient conditions by microorganisms over nitrogenase metallo-enzymes, NH_3 could be synthesized via electron/proton interactions in the electrochemical process.[38,44,45] However, the typical requirement of NH_3 synthesis process being conducive at high temperature, is usually unfavorable for general electrolytes to operate in that high-temperature region.[46−48] Because the idea of electrons and protons in the natural process could be combined with the high-temperature protonic conductors, that could be connected in turn with the solid-state electrochemical ammonia synthesis (SSEAS) approach.[49] Usually in a simple electrochemical process of synthesizing ammonia at a lower pressure, a voltage is applied across a solid-state electrochemical cell to carry out the redox reaction. H_2O is oxidized at the anode catalyst to convert H_2 into protons, by the following scheme: $3H_2 \rightarrow 6H^+ + 6e^-$(anode), which migrate to the cathode and react with N_2 at a different catalyst, reducing it to produce NH_3: $N_2 + 6H^+ + 6e^- \rightarrow 2NH_3$(cathode). The overall scheme lies in entailing the grand challenge of dinitrogen (N_2) fixation to its fully hydrogenated product, ammonia (NH_3), by overcoming the high energy barrier (941 kJ/mol) of thermodynamically strongest (N≡N) triple bond.[50] Typically, two porous electrodes (anode and cathode) are separated by a dense solid electrolyte in SSEAS system, to accelerate the ion transport while hindering the gas diffusion within the cell.[51] The fundamental study on the highly proton-conductive solid-state materials demonstrating the electrochemical synthesis of NH_3 from N_2 and H_2 using a solid proton conductor and working at high temperatures was first discovered in the late nineties.[49,52] Since then, numerous approaches have been employed in broad aspects of SMR, WGS, hydrogen purification, and ammonia synthesis, significantly identifying the main challenges of integrating the protonic ceramic membrane reactor (PCMR) to the crucial divisions of the conventional plant.[53−58] The principal aspect of designing the device (electrolyte) lies in a way that the catalytic activity could exhibit adequate electronic conductivity toward ammonia synthesis while allowing sufficient proton fluxes and suppressing the side reaction of hydrogen evolution (HER). Therefore, investigating the electrochemical N_2 reduction, could not only promote the enhanced NH_3 synthesis but also encourage the reliance of renewable sources by compensating the power consumption in electrical grids. NH_3 production in solid electrolytes or molten salts has been achieved in early studies at elevated temperature with relatively high production rate of 10^{-8} mol cm^{-2} s^{-1};[51] however, the N_2 fixation in liquid electrolytes at ambient conditions has been a recent factor of interest, especially for the harvesting of NH_3 from renewable resources.[59] The Mo-based nitrogenase in this concern was designed by Hoffman, Brown, and co-workers, comprising of two-protein components acting as electron-transfer media (iron protein) and N_2-binding and reduction site (iron−molybdenum protein).[50,60] It was found that the reduction of a N_2 molecule followed by the reductive elimination of one molecule of H_2 could result in the higher production rate of NH_3 through the accumulation of $8e^-$ electrons while moving from a pair of $C_{10}H_{16}N_5O_{13}P_3$ molecules to the iron−sulfur cluster during reaction.[61,62] Nevertheless, the poor Faradaic efficiencies (FE) in response to the higher unfavorable HER activity and poor electronic conductivity in most of the electrocatalysts for ammonia synthesis, make it a mystifying step to select an effective catalyst at industrial scale.[53−56] Marnellos and co-workers[52] using a $SrCe_{0.95}Yb_{0.05}O_3$ (SCY) perovskite, designed the porous polycrystalline Pd electrodes on both sides of the SCY electrolyte that resulted into the ammonia synthesis rate (ASR) of 4.5×10^{-9} mol/(cm^2 s), working at a current efficiency (CE) of 78%, atmospheric pressure and 570 °C temperature. Xie and co-workers studied the proton conduction properties of different kind of Ca^{2+}-doped pyrochlore-type oxides ($La_2M_2O_7$ (M = Ce, Zr)), and fluorite-type oxide ceramics $Ce_{0.8}M_{0.2}O_{2-\delta}$ (M = Sm, Gd, Y, La,) in the solid states proton conducting cell reactor, achieving a high yield of NH_3 formation rate ranging from 1.3×10^{-9} for $La_{1.95}Ca_{0.05}Ce_2O_{7-\delta}$, 2.0×10^{-9} for $La_{1.95}Ca_{0.05}Zr_2O_{7-\delta}$, 8.2×10^{-9} for $Ce_{0.8}Sm_{0.2}O_{2-\delta}$, 7.7×10^{-9} for $Ce_{0.8}Gd_{0.2}O_{2-\delta}$, 7.5×10^{-9} for $Ce_{0.8}Y_{0.2}O_{2-\delta}$, and 7.2×10^{-9} mol s^{-1} cm^{-2} for $Ce_{0.8}La_{0.2}O_{2-\delta}$.[63−65] Similarly, Chen[66] and Liu [16] co-workers fabricated the $BaCe_{1-x}Gd_xO_3$-α ($0.05 \leq x \leq 0.20$) and $BaCe_{0.90}Sm_{0.10}O_{3-\delta}$ perovskite-type oxides working at a temperature range of 300 to 650 °C, which exhibited the high proton conductivity for the 4.63×10^{-9} mol s^{-1} cm^{-2} and 5.82×10^{-9} mol s^{-1} cm^{-2} ASR, respectively. Various other approaches on proton-conducting electrolyte materials such as pyrochlore-type oxides,[63,64] fluorite-type oxides,[65] perovskite-type oxides,[67,68] polymers[69−71] and composite electrolytes[72,73] have also been provided by other groups.

However, most of the electrolytes were associated with high-temperature proton conductors at atmospheric pressure for NH_3 synthesis, which could cost high energy consumption with the decomposition of NH_3 as well. Solid polymers could be a good approach for proton conductors at low temperature and atmospheric pressure SSEAS in this concern. Kyriacou and co-workers[74] using Pt (anode) and Ru (cathode) electrolytes, which were first introduced in a Nafion membrane as a solid polymer electrolyte cell (SSEAS), sustaining an ASR of 1.3 μg h^{-1} cm^{-2} at −1.02 V and 90 °C with a CE of 0.24%. Similarly Liu's group[69] adopted perovskite-type $SmFe_{0.7}Cu_{0.3-x}Ni_xO_3$ (cathode) and $Ce_{0.8}Sm_{0.2}O_{2-\delta}$ fluorite-type (anode), respectively, in a Nafion-based SSEAS at 90.4% CE, yielding a fast NH_3 synthesis rate of 1.13×10^{-8} mol s^{-1} cm^{-2} at −2 V and 80 °C. Similarly, a tubular protonic ceramic cell of $BaCe_{0.2}Zr_{0.7}Y_{0.7}O_{3-\delta}$ (<30 μm) electrolyte was successfully developed by Robinson and co-workers[75] for PCMR applications, exhibiting the significant mechanical strength, chemical stability and high protonic conductivities.[76−79] An efficient approach has been proposed by Kyriakou and co-workers,[80] designing a $BaZr_{0.8}Ce_{0.1}Y_{0.1}O_{3-x}$ solid electrolyte based PCMR that separated the Ni-$BaZr_{0.7}Ce_{0.2}Y_{0.1}O_{3-x}$ anode and vanadium nitride (VN)-Fe porous (cathode) electrodes, operating at temperatures between 550 and 650 °C and ambient pressure. It was demonstrated that the $CH_4 + H_2O$ reactant mixture could be converted to CO_2 and H^+ in the anode compartment, that would react with the lattice nitrogen after being transported through the membrane to the cathode compartment, achieving a high rate of 68 mmol NH_3 h^{-1} m^{-2} via a Mars−van Krevelen mechanism at 600 °C and 0.63 V with 5.5% FE to NH_3. In this concern, density functional theory (DFT) calculations could be an efficient way of realizing the promising metal mononitrides for NH_3 synthesis, where the dissociated N_2(gas) would occupy the lattice vacancy via protons reaction with lattice nitrogen.[81−84] VN can perform well among the auspicious nitrides, experimentally verifying their potential in acidic solutions to form NH_3 at low applied bias.[81,85−87] An integrated protonic ceramic fuel cell

https://doi.org/10.1021/acscatal.3c02410
ACS Catal. 2023, 13, 14415−14453

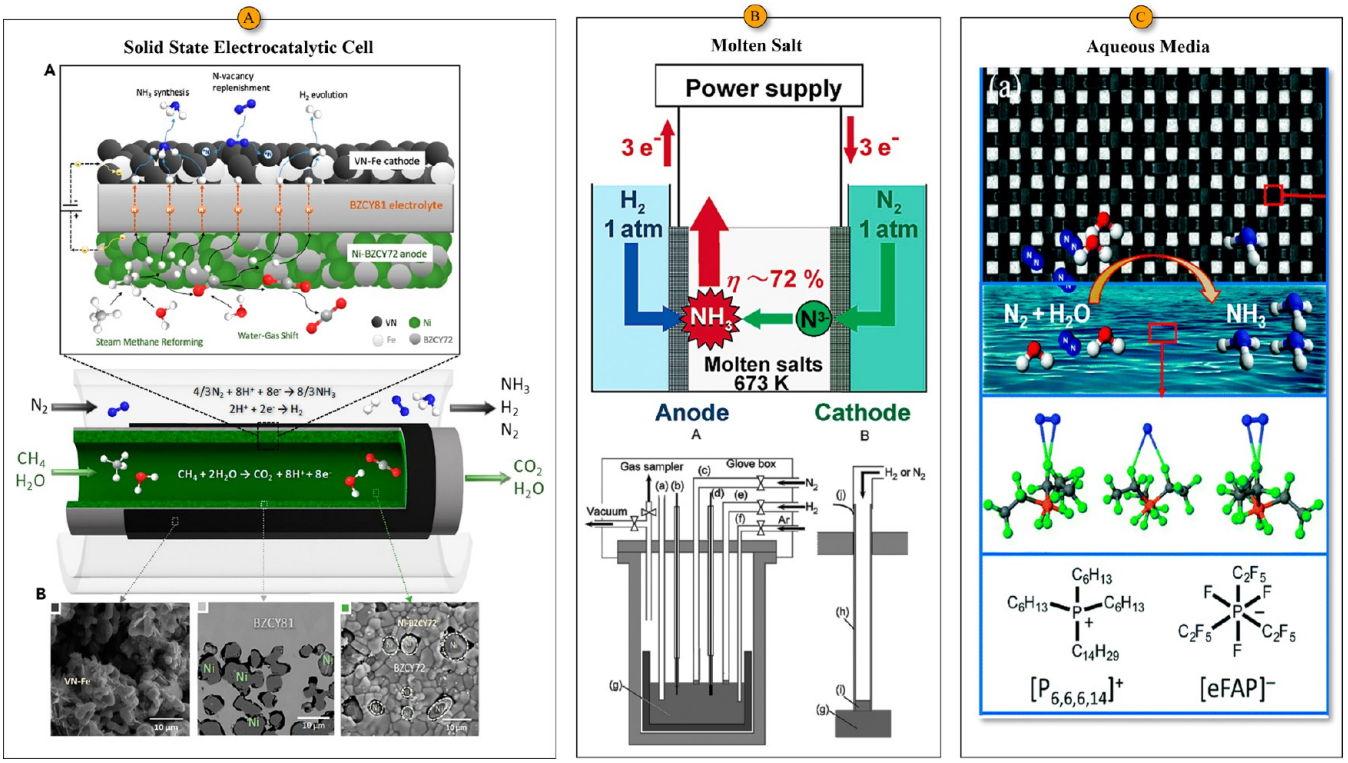

Figure 2. Ammonia synthesis. (A) By integrated protonic ceramic fuel cell (PCFC) operating at atmospheric pressure in protonic ceramic membrane reactor (PCMR). Reproduced with permission from ref 80. Copyright 2020 Elsevier. (B) Molten salt. Reproduced with permission from ref 90. Copyright 2003 American Chemical Society. (C) Aqueous media. Reproduced with permission from ref 91. Copyright 2017 Royal Society of Chemistry.

(PCFC) operating at atmospheric pressure in PCMR reactor by Kyriakou and co-workers[80] could substitute the commercial H−B units, generating the H_2 over Ni-composite anode and synthesizing the ammonia over a VN-Fe cathode via purifying the product through a $BaZrO_3$-based electrolyte (Figure 2A). The efficient deviation of thermodynamically limited CH_4 conversions by extracting H_2 from reforming chamber and subsequently transforming it to CO_2 instead of CO at atmospheric pressure and 550−650 °C temperature, enhanced the H_2 yield in a single device, thereby pumping the accelerated (5%−15%) protons to NH_3. The PCMR combined with PCFC in the designed electrochemical unit, eradicating the essential requirement of the downstream shift reactor, could exploit the residual H_2 and efficiently refine the N_2 from ambient air while retrieving the electricity usage. This proposed electrochemically designed cell could hold the promise of potentially lower energy (4 times) consumption at 0.3 V, notable conversions under milder conditions for increasing the cathode catalyst's Faradaic efficiency (FE) to NH_3 to at least 35%, and significantly cutting (50%) CO_2 emissions than its conventional H−B contenders (500 kJ $molNH_3^{-1}$).

In addition to the proton-conducting electrolytes for high temperature route, oxide-ion (O_2^-) conductive solid-electrolyte-based systems, could also realize the NH_3 production from N_2 and H_2O simultaneously at the cathode irrespective of the charge carrier. Among the two different classes of solid oxide electrochemical cell for NH_3 synthesis, the one containing a proton conducting electrolyte, is a promising candidate in which H_2 is converted into H^+ on the anode and combined with N_2 at cathode by traveling through the electrolyte for NH_3 synthesis. While H_2O splits into H^+ and H_2 which react with activated nitrogen to synthesize NH_3 in the oxide ion conducting cell while generating oxygen molecules with the traveling of O_2^- ions through the electrolyte to the anode due to H_2O splitting by applying a combined stream of N_2 and H_2O at the cathode. Since, getting pure O_2 as a byproduct at the anode in the oxide ion cell is a key value to the process, where CO_2 emissions are nullified from the process by using pure H_2O instead of H_2 as the H^+ source. Although electrochemical NH_3 production from N_2 and H_2O is theoretically less energy intensive and a carbon-free path rather than producing H_2 from natural gas reforming, the low conductivity of O_2^- and weak reducing power greatly restrict the NH_3 yield. Amar and co-workers[88] demonstrated the NH_3 synthesis in an O_2^--conducting composite electrolyte working at 375 °C 1.4 V and 3.87% CE, achieving a maximum NH_3 synthesis rate of 4.0×10^{-10} $mol.cm^{-2}.s^{-1}$ on a $La_{0.75}Sr_{0.25}Cr_{0.5}Fe_{0.5}O_{3-\delta}$-$Ce_{0.8}Gd_{0.18}Ca_{0.02}O_{2-\delta}$ composite cathode. The nature of the working electrode (based upon H^+ and O_2^- conducting cells) was much sensitive to the NH_3 synthesis rates, especially the working electrode configuration of Ru catalyst increased by an inner layer of Ag, resulting in the significantly decreased FE and synthesis rates in response to the generated surface hydrogen species in H_2O electrolysis. Similarly, Stoukides's and co-workers[89] obtained an ASR of 1.50×10^{-13} $mol.cm^{-2}.s^{-1}$ at 650 °C and atmospheric pressure, adopting the yttria-stabilized zirconia (8% Y_2O_3/ZrO_2) as O_2^--conducting electrolyte for SSEAS using N_2 and H_2O as feed gases. The electrokinetic influence associated with limitations in conductivity at high temperature and significant positive (>70 kJ mol^{-1}) Gibbs free energy need more efficient catalysts

https://doi.org/10.1021/acscatal.3c02410
ACS Catal. 2023, 13, 14415−14453

in this approach to improve the selectivity. The substantially boosted conductivity and hastened reaction kinetics of electrolytes usually adopt elevated temperatures in the solid-state electrolytes to achieve an appreciable (8^{-10} mol·cm^{-2}·s^{-1}) NH_3 synthesis rate, thus making it thermodynamically unfavorable while necessitating the trade-off for maximizing NH_3 yield. Since, the investigations have usually been conducted in high temperature electrocatalytic NH_3 synthesis in solid oxide electrolytes, possibly related to the lower rates in those counterparts; however, it is a promising candidate in electrocatalytic process with added incentives of producing pure oxygen.

3.1.3. The Intermediate-Temperature Route (100−500 °C): Molten Electrolytes. Using N_2 and H_2 as the reactants, a flourishing interest in electrochemical NH_3 synthesis by SSEAS, could achieve the maximum NH_3 generation rate in the order of 10^{-9} to 10^{-8} mol·cm^{-2}·s^{-1} with considerable CE. However, the high energy consumption rate or carbon intensive nature of this process in large cell potential[69] and high temperature conditions[52] may limit its frequent utilization. Molten electrolytes (NaOH/KOH) on the other hand could achieve enhanced ionic conductivity while reducing the operating temperature (200−400 °C) with a faster NH_3 synthesis rate. Since, presumably exhibiting the higher ion conductivity, it could be emerged as another class of promising electrolyte working at intermediate temperatures and facilitating the higher overall performance. Where the stabilized N^{3-} in molten alkali metal salts can be adopted as an alternative to the protic solvents, thus avoiding the competitive HER. The electro-cleavage of H_2 or N_2 sources initially occurring on the electrode surfaces in molten salts, proceed toward the diffusion of N^{3-}/H^+-containing ions for ammonia synthesis (Figure 2B). The adoption of molten salt composition and H_2 sources are governing factors that greatly influence the reactions on the electrodes' surfaces and diffusion of ions in electrolytes, thus dictating the overall Faradaic efficiency and ammonia synthesis rate.

Ito and co-workers[90,93−96] working on LiCl-KCl-Li_3N and LiCl-KCl-CsCl-Li_3N electrolytes in molten eutectic melts and molten salt system, achieved the highest ASR of 3.33×10^{-8} mol·cm^{-2}·s^{-1} in a CE of 72% and 400 °C temperature using N^{3-} as the charge carrier from nitrogen at the cathode, while traveling through the electrolyte and reacting with H_2 at the anode. It was demonstrated that a lower ASR could occur in accordance with the H_2 partial pressure in the gas electrode with the dissolution of a portion of NH_3 to imide (NH_2^-) and amide (NH_2^-) anions in the rate-determining step. However, some other means for the hydrogen sources such as H_2O,[97−100] CH_4,[101] H_2S,[102] and HCl[103] have also been selected instead of pure H_2, for electrochemical NH_3 synthesis in LiCl-KCl-CsCl eutectic melts to increase the overall reaction yield. Where the competitive undesired HER reactions can be suppressed, facilitating the high FE due to the series of different processes carried out in separated vessels while avoiding the metal contact with air as the source of inefficiency. McEnaney and co-workers[99] substantially inhibited the undesired HER by circumventing the direct N_2 protonation from nitrogen and H_2O in a Li-mediated cycle strategy for ammonia synthesis system at atmospheric pressure and an initial high (88.5%) CE. Although the catalyst optimizations, molten salt compositions, and electrode reactions have been widely explored, the lower ammonia yield and lower faradaic efficiency are still common problems being encountered by the undesirable side reactions of concomitant hydrogen evolution on cathode.[104] Since, a clear demonstration of the N_2 cleavage reaction mechanism occurring on three phase interfaces (gaseous N_2-electrode-molten salt), advanced characterization approaches and a well-defined microstructure electrocatalyst are still in high demand to enhance the synthesis rate by constraining those side reactions on electrode.

3.1.4. The Low-Temperature Route (<100 °C): Liquid Electrolytes. The low-temperature NH_3 generation in aqueous electrolytes using ubiquitous H_2O as the proton source, could substantially reduce the process cost and the energy consumption and potentially inhibit the greenhouse gas emission for producing NH_3 at ambient conditions. Where, the abundance of H_2O molecules in aqueous media leads to an extremely competitive electrolysis to hydrogen as compared to that of solid or molten salt systems. Since, its flexibility of harvesting NH_3 from N_2 and H_2O in aqueous electrolyte could expand the tempting goal of sustainable development at ambient conditions (Figure 2C), nonetheless, the insufficient activity of the most electrocatalysts in electrocatalytic conversion of N_2 to NH_3 via the N_2 reduction reaction (eNRR) and extremely challenging process of the competitive N_2 activation, hardly exceed 5−10% CE and (10^{-12} mol.cm^{-2}.s^{-1}) synthesis rate. The complex exposed faces and defects generated by the surface reconstruction of certain nanosized metal catalysts during reactions under reduction potentials, necessitate the delineation of efficient electrocatalysts design.[105−111] Using aprotic solvents could be a notable strategy of reducing the H^+ availability and accelerating the CE; but a low NH_3 yield would be generated by the extremely small operating current density.[91,112−114] Nitrate (NO_3^-) ions which are usually regarded as the widespread water pollutants could also be classified as an attractive nitrogen source instead of inert N_2 to synthesize NH_3 through electrochemical process.[115] Keeping in view the carcinogenic aspects of nitrite ions (NO_2^-) with extensive deployment in fertilizers, the conversion of these ions into useful products can be a tremendous approach for renewable resources. Where, the selective reduction of NO_2^- to N_2 or NH_3 in a concentrated H_2 atmosphere through noble catalytic (Pd, Rh, or Ir) hydrogenation could demonstrate high yield.[116−118] While, owing to its thermodynamic readiness and higher solubility in H_2O, selectively reducing NO_2^- to NH_3 by employing electrons as the reductant could avoid the use of H_2 with improved reaction efficiency, thus reducing the operating cost and solving the problem of eliminating water pollution lead to a promising strategy of realizing the green NH_3 synthesis.[38,119−121]

While, considering the deoxygenation and hydrogenation phenomenon in NO_2^- reduction, an efficient catalyst along with the excellent electrical conductivity and low biological toxicity, should resist the excessive hydrogen coverage to nullify the interference of HER.[122] In a recent study by Anthony and co-workers, a promising electrocatalyst of iron−phosphorus nanoarrays (FeP NA|Ti) was deployed in a single-chamber cell of neutral pH for selectively reducing NO_2^- to NH_3, while circumventing the potential hazard of H_2 accumulation.[123] Calculating the adsorption energy barriers by DFT studies and providing a suitable reaction mechanism, they suggested a potential pathway of eliminating and recycling the NO_2^- pollutants in H_2O bodies while achieving a high FE of 82.5 ± 2.3%. The eNRR process of ammonia synthesis can

https://doi.org/10.1021/acscatal.3c02410
ACS Catal. 2023, 13, 14415−14453

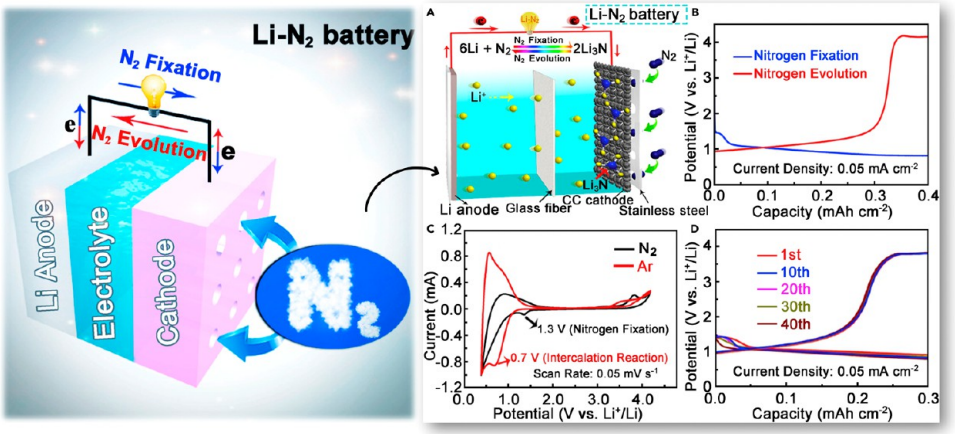

Figure 3. N_2-to-NH_3 conversion by a rechargeable Li−N_2 battery assembly with an ether-based electrolyte, Li anode, and a carbon cloth cathode working on the advanced N_2/Li_3N cycle strategy. Reproduced with the permission from ref 92. Copyright 2017 Elsevier.

be substantially pursued in a confined region of negative potentials with a highly active electrocatalyst. Where, the deep mechanistic understanding of a certain electrocatalytic system may explicit the strong binding pathways of N_2 molecule to overcome the adverse desorption of reaction intermediates. In addition to electrolysis, battery configuration is also a crucial factor in diverting new directions toward N_2 fixation. As similar to the natural biological nitrogen fixation process in an associative manner by nitrogenase enzymes under ambient conditions, ammonia can be synthesized in diazotrophic microorganisms' route, where molecular hydrogen is obtained from some bio sources or water splitting process governed by renewable resources.[124] Since, two proteins in the nitrogenase enzymes act as an oxidizing and reducing unit, where the available protons from the medium are conveyed to nitrogen and the electrons could come from the protein in a metal-centered catalytic cofactor. Where, a successful illustration of a reversible nitrogen cycle by Ma and co-workers[92] based on a rechargeable Li−N_2 battery assembly with an ether-based electrolyte, Li anode, and a carbon cloth cathode has been presented in Figure 3. The advanced N_2/Li_3N cycle strategy suggesting a reversible reaction of $6Li + N_2 \leftrightharpoons 2Li_3N$, endowed the exclusive features of Li−N_2 rechargeable batteries for exhibiting an encouraging electrochemical CE of 59%. The state-of-the-art eNRR system entirely driven by renewable resources must be competitive enough to provide the energy acquired for H_2 generation in ammonia synthesis reaction ΔH° = 22.5 MJ $kg_{NH_3}^{-1}$ in a sustainable route.

Since, an enzymatic fuel cell (EFC) constituted upon the nitrogenase/cathode and hydrogenase/anode was adopted by Minteer and colleagues[125] using methyl viologen electron donor to mediate NH_3, while simultaneously making electrical energy. A current efficiency of 26.4% was obtained on this H_2/N_2 enzyme-assisted coupling by electron transfer between the electrodes, demonstrating a charge of 60 mC across the EFCs with 286 nmol NH_3 mg^{-1} ammonia synthesis rate. While, a general strategy was suggested by Hao and co-workers[126] using Bi nanocrystals and K cations in expanding the electrochemical reduction of stable molecules library to simultaneously promote eNRR selectivity and activity. The strong interplay between N 2p orbitals and Bi 6p band with the stabilized key N_2-reduction intermediates by K cations and regulated H^+ transfer, exhibited exciting results in aqueous media for a high FE of 66% with 200 mmol g^{-1} h^{-1} NH_3 yield. Since, the overall scheme requires a robust scientific and engineering design with exceptional mechanistic insights to solve the operating potential window about thermodynamics. The electrochemical N_2 fixation albeit veto its upscaling, the limiting phenomena of efficiency gains, dwindling electrical and catalytic activity, drifted materials design and kinetics, and the temperature regime problems are still hindering the emergence of potential electrocatalytic route in substituting the industrial process. In contrast to the high-temperature-operated units, the lower temperature ammonia synthesis tolerating the flexible configurations at convenient operating conditions and viable current densities could achieve high selectivity. While, regarding the equipment and operational costs, low temperature (<100 °C) electrochemical ammonia synthesis could be a preferable choice, where water functioning as a proton carrier could perform well in connecting the redox half-reactions in the liquid electrolyte at the ambient pressure and the favorable thermodynamics may sustain a stable ammonia phase. However, the electrokinetic limitation, irrespective of the catalyst type, may visualize the low FE (<10%) due to the side reaction of hydrogen formation. Meanwhile, the desire of large overpotentials causing the drop of energy efficiency values at high current densities and the lack of stability in long-term operation are the leading obstacles in the propitious molten eutectic-based strategies.

3.2. Photocatalytic Ammonia Synthesis. Adapting the sustainable alternatives for the green NH_3 synthesis from N_2 and H_2O by effectively capturing solar energy in a photocatalytic mean could be an effective strategy of decarbonizing the H−B process.[127,128] The abiotic photo fixation of N_2 in sands and soils being introduced in the pioneering studies by Dhar and Schrauzer and co-workers, can be adopted as the vital source of natural N_2 fixation as similar to the biological mean.[129−131] Being operated under ambient conditions, water and air are the major renewable feedstocks in this carbon-free method, relying only on sustainable energy input (light). Since, generating the electrons and holes via the absorption of light (UV/vis/IR) by a photocatalyst is a common mean, where these photogenerated charge carriers then activate N_2 from the air, followed by the generation of ammonia by the protonation of the activated nitrogen with H_2 in water (as shown in the following equations). The solar-driven N_2 fixation is a significant mean of modulating the nitrogen cycle, ultimately

https://doi.org/10.1021/acscatal.3c02410
ACS Catal. 2023, 13, 14415−14453

meliorating the accessibility of fertilizer in isolated regions[132,133]

$$\text{absorption of light: photocatalyst} + h\nu(>E_g) \rightarrow e^-_{CB} + h^+_{VB}$$

$$\text{nitrogen reduction (NRR): } N_2 + 6H^+ + 6e^-_{CB} \rightarrow 2NH_3$$

$$\text{water oxidation (OER): } 2H_2O + 4h^+_{VB} \rightarrow O_2 + 4H^+$$

Despite various privileges in the nitrogen photoreduction, the poor efficiency of this process, little advancement in comprehending the fundamental reaction mechanisms, kinetically unfavorable and high cost nature of electron-donating scavenger to consume photogenerated holes, low ammonia yield, and inactive photocatalysts are the major hurdles of its wider deployment in renewable energy sector.[23,134−143] The weak adsorption tendency of nitrogen molecules on the surface and the oxidation of the reaction products by the holes usually lead to a lower rate of photochemical reduction of semiconductor catalysts. Even though the enhanced NH_3 yield to mmol h^{-1} g^{-1} from the lower order of μmol h^{-1} g^{-1} in photocatalyst systems has been realized in some lab scale platforms, but far lagging to that in eNRR. It could restrain the commercial deployment of this process, making the comparative evaluation of different studies unviable in terms of their catalytic performance and energy conversion efficiency. However, the development of robust measurement and unique product quantification protocols to synthesize new high-activity catalysts and dispensing the advanced operando characterization techniques may orient efforts toward developing interest in this regard to small-scale photocatalytic systems for distributed ammonia synthesis (described later in the catalyst development section). A brief description of some examples in this aspect would include a demonstration of bridging Fe hydrides as precursors and an active site of MoFe-nitrogenase for catalytic N_2 reduction to ammonia which could stimulate the N_2 activation via reductive elimination of H_2.[144] The light-enhanced process of photolysis of NH_3 synthesis by triphos-supported $Fe(N_2)H_x$ catalysts from a new (I) $[P_2^{P,Ph}Fe(H)]_2(\mu\text{-}N_2)$ complex, could provide the increased NH_3 yields at atmospheric conditions from N_2 and H_2 (Figure 4).[144]

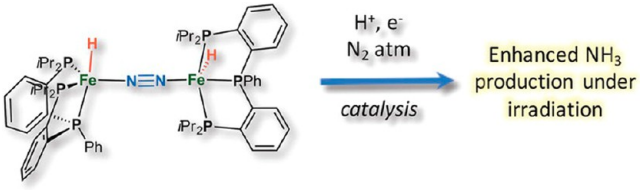

Figure 4. Light-enhanced eNRR synthesis of NH_3 by a triphos-Fe catalyst under photolysis irradiation of a mercury lamp. Reproduced with permission from ref 144. Copyright 2017 John Wiley and Sons.

The synthesis and characterization of these new $P_2^{P,Ph}Fe(N_2)(H)_x$ systems illustrated that the presence of mercury lamp irradiation significantly increased the ammonia yields as much as 180% improvement, suggesting the photoelimination of H_2 as a mean of activity enhancement. The structural and functional mimic of nitrogenase through enzymatic processes has been considered in various recent studies to produce ammonia, where the different ligands and clusters are carried out in multiprotein complex nitrogenase for molecular electron relay centers in fast redox catalysis.[145−148] The decentralization of ammonia production can be achieved as an effective strategy for the future by splitting the N≡N bond using solar illumination, where heat triggers the photocatalytic activity by lowering the electron−hole pair rejoin and thus increased the exciton timespan for the enhanced NH_3 synthesis. In a recent study by Foster et al., Fe decorated on 2D MoS_2 photocatalysts as inorganic [Fe−S_2-Mo] motifs were developed for light-driven N_2 fixation to NH_3 at high temperatures (270 °C), with an attached structure like the nitrogenase cofactor (FeMoco) by accommodating the Fe atoms on a single MoS_2 molecular layer at different loadings.[149] The fabricated catalytic material along with a solar furnace, functionally mimics the nitrogenase by the solar light concentrator to divert N_2 to NH_3 and H_2 in water under visible-light illumination without adding any sacrificial agent (direct thermal energy), demonstrating the facile deployment of an exciting facility for the decentralization of NH_3 fertilizer in local farmlands.[6,124,150] Detailed inspection indicated that priorly fascinating the photoelectron transfer to N_2 in place of H_2 at elevated temperatures, encouraging the boosted N_2 adsorption at high temperature, significantly altered the overall NH_3 synthesis rate as compared to that of water photolysis. It was demonstrated that the effective strategy of deploying high temperatures triggers the photocatalytic heat derived from the solar absorption, achieving the superior high activity of 0.24% ammonia energy efficiency and selectivity while suppressing the electron−hole pair reattachment in MoS_2. However, another strategy of Mo_3Si thin film sputtered on graphite paper was suggested to be favorable for NH_3 synthesis under ambient conditions, finding an enhanced (6.69%) FE and ASR of 2×10^{-10} mol s^{-1} cm^{-2} at −0.4 V and −0.3 V in 0.1 M Na_2SO_4 vs. RHE.[151] DFT calculations revealed that the enhanced N_2 adsorption and activation while further transferring proton−electron reaction in synthesizing NH_3 at high electrochemical and structural stability, could be a reason for efficient synergistic interaction between the accelerated chemical activity of exposed molybdenum species and metallic conductivity of Mo_3Si.

Similarly, a unique Si-based aerophilic-hydrophilic heterostructured photocathode was designed by Zhang et. al[152] being composed of poly tetrafluoroethylene (PTFE) porous framework as the gas-diffusion layer, Si as the photo absorber, and Au nanoparticles (NPs) as the active sites, exceeding the energy conversion efficiency of nitrogen fixation for photoelectrochemical NH_3 synthesis. It was demonstrated that the enriching N_2 concentration at the highly dispersed Au active species and PTFE porous framework of the aerophilic-hydrophilic heterostructure manipulated the proton activity under aqueous media while suppressing the excessive HER. DFT calculation further illustrated that lowering the NRR energy barrier could result in a FE of 37.8% and an NH_3 yield rate (ASR) of ∼18.9 μg cm^{-2} hr^{-1} at −0.2 V versus the reversible hydrogen electrode (RHE) in ambient condition. A potential means of applying nanostructured photoelectrochemical solar cell of plasmon-enhanced black silicon in the presence of sulfite as a reactant for nitrogen reduction was also proposed by Ali et. al,[139] decorating gold NPs on black silicon (bSi) based photo absorber as the reduction catalysis sites with a Cr hole-sink layer. The autonomous electrochemical device being composed of multilayer structure and powered by photoexcitation could carry out oxidation and reduction reactions on different areas of the device (Figure 5A), achieving an ammonia yield of 13.3 mg m^{-2} h^{-1} under 2

https://doi.org/10.1021/acscatal.3c02410
ACS Catal. 2023, 13, 14415−14453

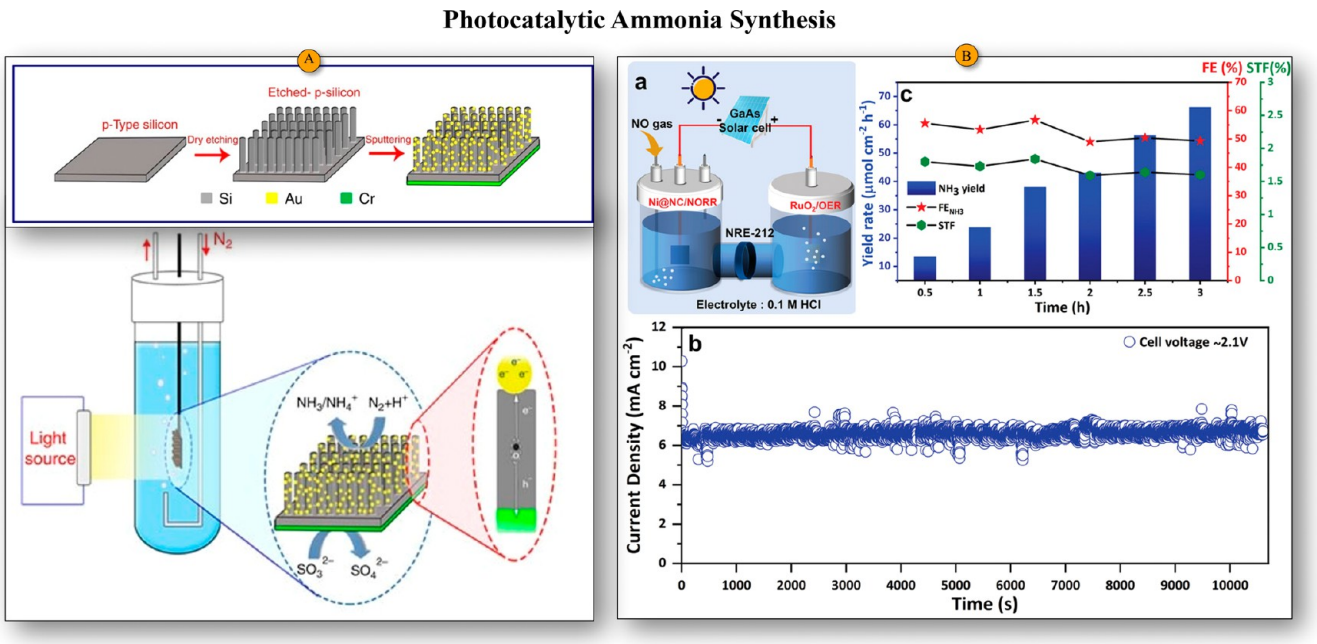

Figure 5. (A) Schematic illustration of fabricating and implementing the photoelectrochemical solar cell of plasmon-enhanced black silicon in the presence of sulfite as a reactant for nitrogen reduction. Reproduced with permission from ref 139. Copyright 2016 Nature. (B) Strategy of solar-to-fuel conversion system with PV-electrolyzer system to obtain stable operating current, and NH_3 yield rate. Reproduced with permission from ref 154. Copyright 2022 John Wiley and Sons.

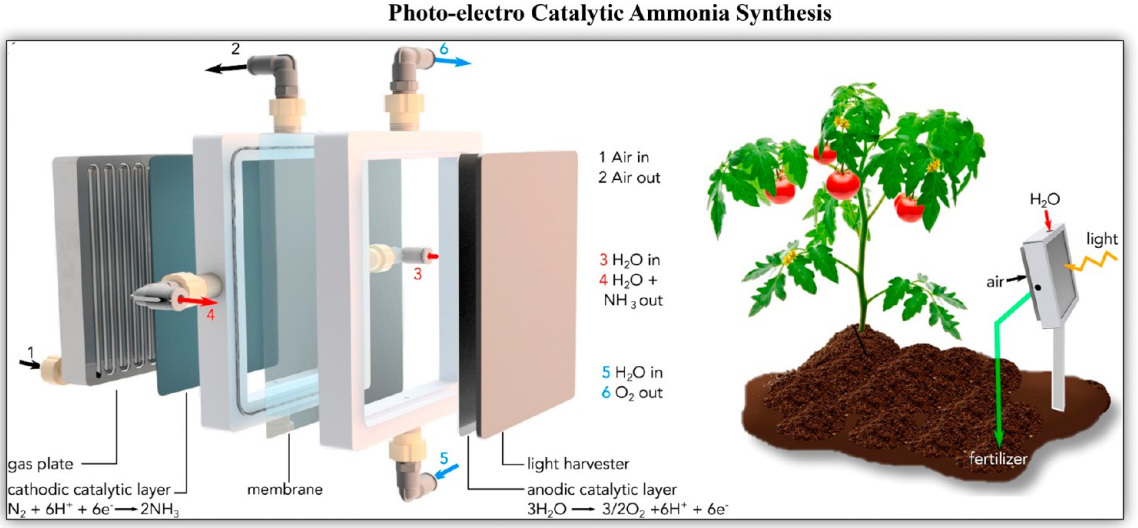

Figure 6. A photoelectrocatalytic approach of eN_2RR via coupling the electrode and photon absorber at a device scale. Reproduced with permission from ref 58. Copyright 2019 Elsevier.

suns illumination, which could be increased to 60 mg m^{-2} h^{-1} by increasing pressure 7 atm. Jang et al.[153] illustrated that a poor water reduction catalyst of CuO and Cu_2O photocathodes could efficiently compete the photoelectrochemical nitrogen reduction to ammonia in a scheme of solar water reduction reaction. It was demonstrated that the photoexcited electrons in designed photocathodes can reduce the amount of energy required for NH_3 production for $15NH_3$ with 17% and 20% FE in a 0.1 M KOH solution at 0.6 and 0.4 V, respectively, under simulated solar illumination vs the RHE.

Sridhar et al.[154] suggested a solar energy-mediated approach of rationally integrating an electroreduction process with solar energy for the sustainable ammonia synthesis by utilizing nitrogen oxide air pollutant. In the strategy of solar-to-fuel conversion, a fuel-cell electrolyzer was constructed for delivering a stable performance at 1.5 V over 20 cycles by integrating the oxygen evolution reaction at the RuO_2 anode and NRR at the Ni@NC cathode (Figure 5B). It was demonstrated that a substantial amount of (72.3%) FE could be attained at 0.16 V_{RHE} by integrating the PV-electrolyzer cell with a Ni core residing in the nitrogen-doped porous carbon shell (Ni@NC), ensuring long-term catalyst stability by preventing the dissolution of Ni NPs. While, a photoelectrocatalytic strategy of eN_2RR was suggested by Martín and co-workers,[58] that could be a feasible approach in developing the advanced strategies of NH_3 synthesis via

https://doi.org/10.1021/acscatal.3c02410
ACS Catal. 2023, 13, 14415−14453

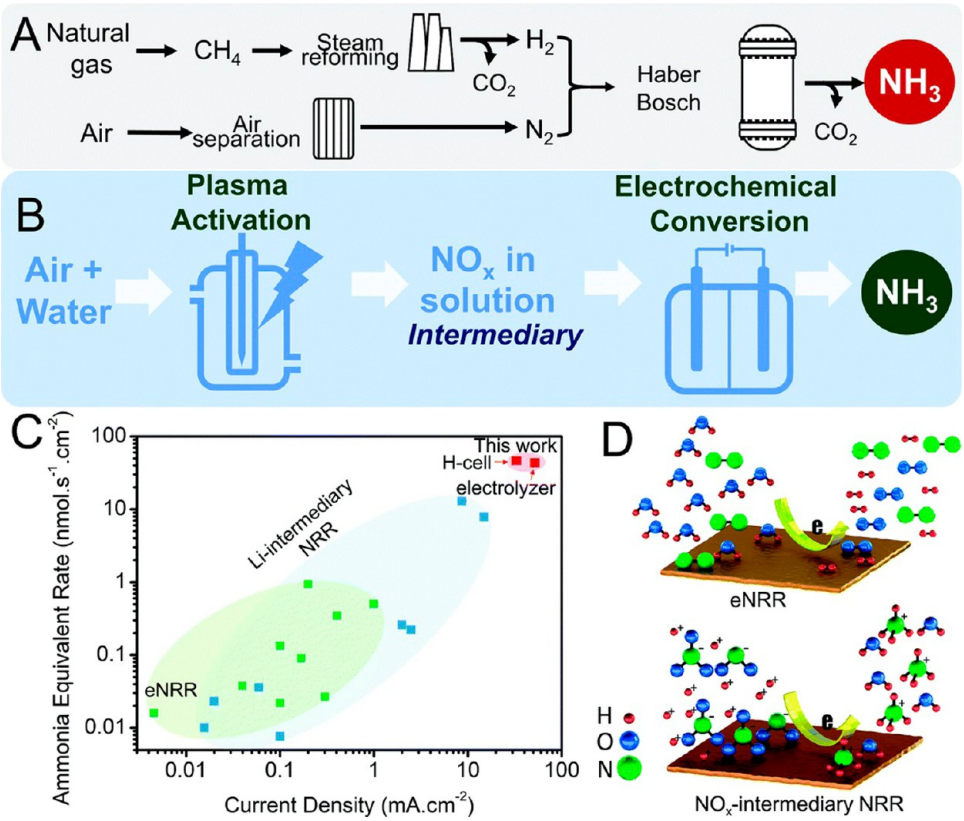

Figure 7. Comparative schematic illustration of hybrid plasma-electrochemical technology for renewable NH_3 synthesis. (A) conventional H−B process. (B) NH_3 synthesis approach by nonthermal plasma and electrochemical ammonia synthesis system. (C) NH_3 equivalent synthesis rate and current densities for the reported hybrid systems, and (D) NRR products from N_2 versus NO_x intermediary. Reproduced with permission from ref 166. Copyright 2021 Royal Society of Chemistry.

coupling the electrode and photon absorber at a device scale. The equipment suggested by for that strategy could be comprised by a light harvester, proton-conductive liquid electrolyte, the gas-diffusion electrode, and ion-permeable membrane, conceiving a dark cathode (N_2 reduction) and photoanode (anodic reaction) as shown in Figure 6. This efficient high-temperature eN_2RR would rely on a complex interaction among the major impacts of thermally driven processes, materials' conductivity, catalytic activity, and selectivity. However, some significant catalytic challenges may also be encountered in case of oxygen presence in the cathodic compartment, leading to the inefficient reduction reaction while running at a large overpotential of usually higher than 1.1 V.

3.3. Plasma Catalysis for Ammonia Production. Plasma catalysis could be a sustainable approach in feasibly substituting the commercial H−B process, where the non-equilibrium plasma being generated by ionizing the source gases, can activate N_2 molecule through an electric discharge without a catalyst by generating highly energetic molecular, ionic, atomic, or radical species.[155,156] The collisions between high-energy electrons and reactant molecules resulting in the highly excited species lead to a relatively low background temperature by the huge mass discrepancy. Because of the small mass of electrons, the temperature could reach only 105 K by nonthermal plasmas since the exothermic NH_3 synthesis process could be favored at low temperature while reducing the sintering or coking of catalysts. Plasma could also be combined with solid catalysts, where the highly reactive atoms may enhance the ASR at ambient conditions via boosting the kinetics and extending the time span of short-lived active species.[121,157,158] However, the correlations between the energies of elementary steps in heterogeneous catalytic reaction and complicated plasma characteristics may also impose a challenging phenomenon in controlling the plasma-incorporated process for changing the electric field distribution and limiting the rates of thermally catalyzed reactions at surfaces.[159] Different studies deploying the N_2 vibrational excitations based upon microkinetic models in a dielectric-barrier-discharge (DBD) plasma suggested that these obstacles can be removed by introducing the catalysts to nonthermal plasma reactor (NTPR).[160,161] It was postulated that the required activation energy for N_2 dissociation could be decreased via plasma-induced vibrational excitations, thus overcoming the scaling issues by converting the nitrogen into electronically or vibrationally excited states without affecting the subsequent reaction steps. The ammonia synthesis rates could be greatly enhanced on the metal sites that weakly bind the N_2 molecule and thermally activate it in a DBD plasma reactor. An enhanced (2.3 g NH_3/kWh) energy efficiency could be achieved on a Ru catalyst with carbon nanotubes (CNT) support and Cs promoter using Amberlyst 15 and Molecular Sieve 13X microporous absorbents, supplying N_2/H_2 ratio of 3:1 at an applied voltage of 6000 V, and a frequency of 10,000 Hz in an NTPR induced by DBD.[162] Similarly, an effective wool-like copper electrode was designed in different reports to accelerate the ASR of 3.3 g NH_3/kWh with and energy efficiency of 3.5%, using nonthermal atmospheric-

https://doi.org/10.1021/acscatal.3c02410
ACS Catal. 2023, 13, 14415−14453

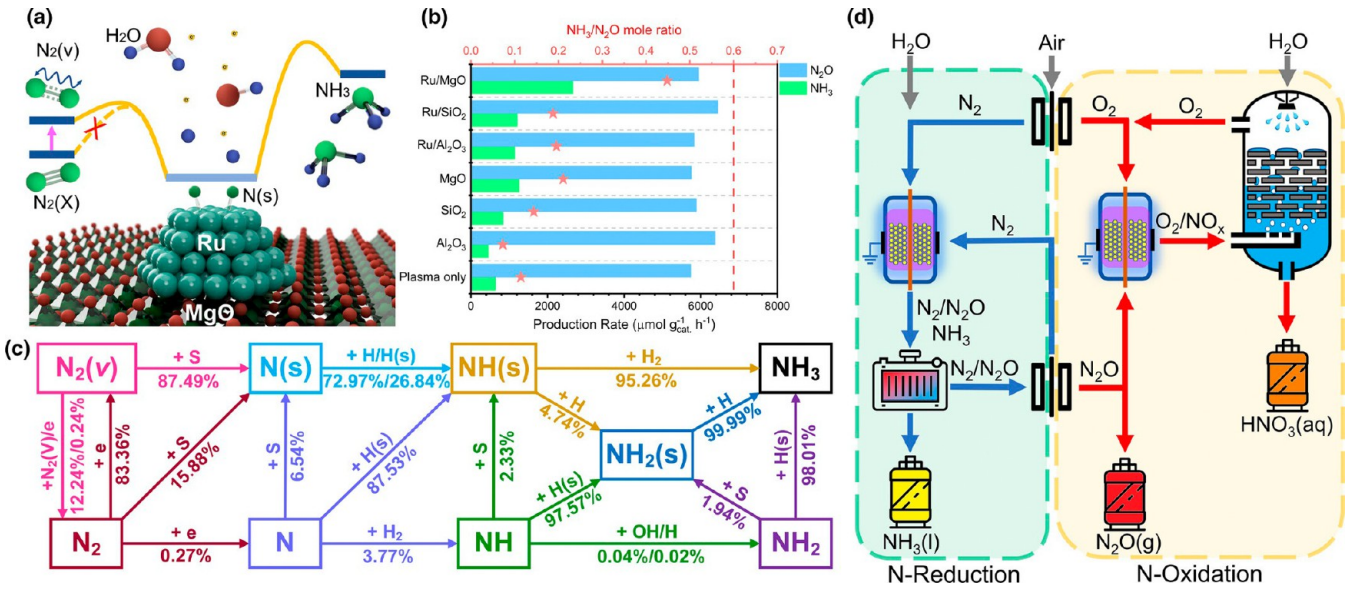

Figure 8. (a) DFT calculations, (b) thermal catalysis performance tests, (c) mechanistic insights of ammonia formation, (d) experimental configurations of different types of plasma reactors for ammonia synthesis. Reproduced with permission from ref 167. Copyright 2022 John Wiley and Sons.

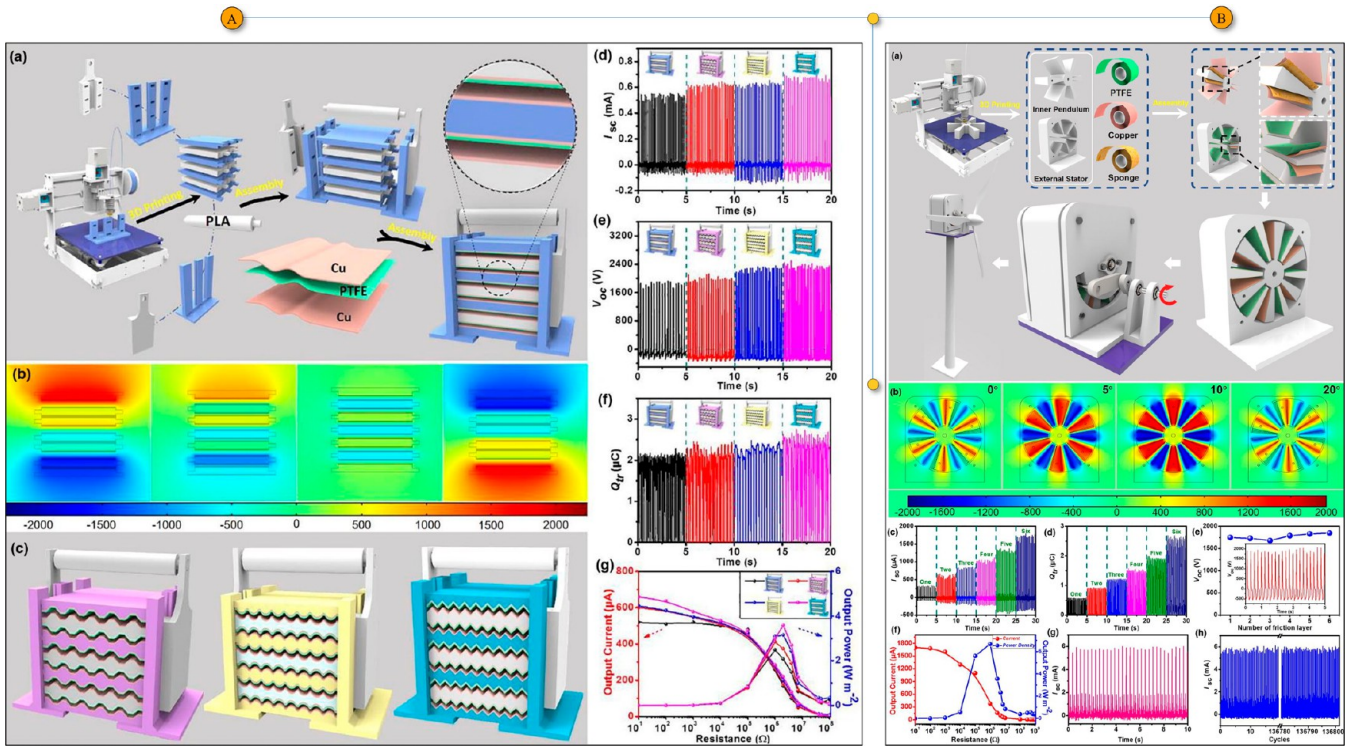

Figure 9. Schematic illustration of basic structure and fabrication process and performance data of the triboelectric nanogenerator (TENG). Reproduced with permission from ref 170. Copyright 2019 Elsevier.

pressure plasma by glow discharge.[163,164] Hawtof et al.[165] designed a hybrid electrolytic system for the synthesis of NH_3 from N_2 and water at ambient temperature and pressure adopting a gaseous plasma electrode in the absence of any material surface. A Pt electrode immersed in the solution (H_2SO_4) operated as the anode for H^+ supply to reduce N_2 and trap the produced ammonia, while the metal cathode was substituted by plasma generated in a gas gap between the solution surface and a stainless-steel nozzle. The solvated electrons (as the powerful reducing agents) were generated at a gas−liquid interface by using only electricity, thus giving a record-high (up to 100%) FE and large (0.44 mg/h) production rate. Distinct from other plasma-based processes, the conditions were regulated by using a gas purge to remove the air and treating the solvated electrons with H_2O containing acid. Similarly, a hybrid system of plasma-driven NO_x intermediary generation coupled with an electrocatalytic reduction process was introduced by Sun et al.[166] that could be inherently compatible with the small scale decentralized ammonia synthesis. The system coupled the plasma-activation

https://doi.org/10.1021/acscatal.3c02410
ACS Catal. 2023, 13, 14415−14453

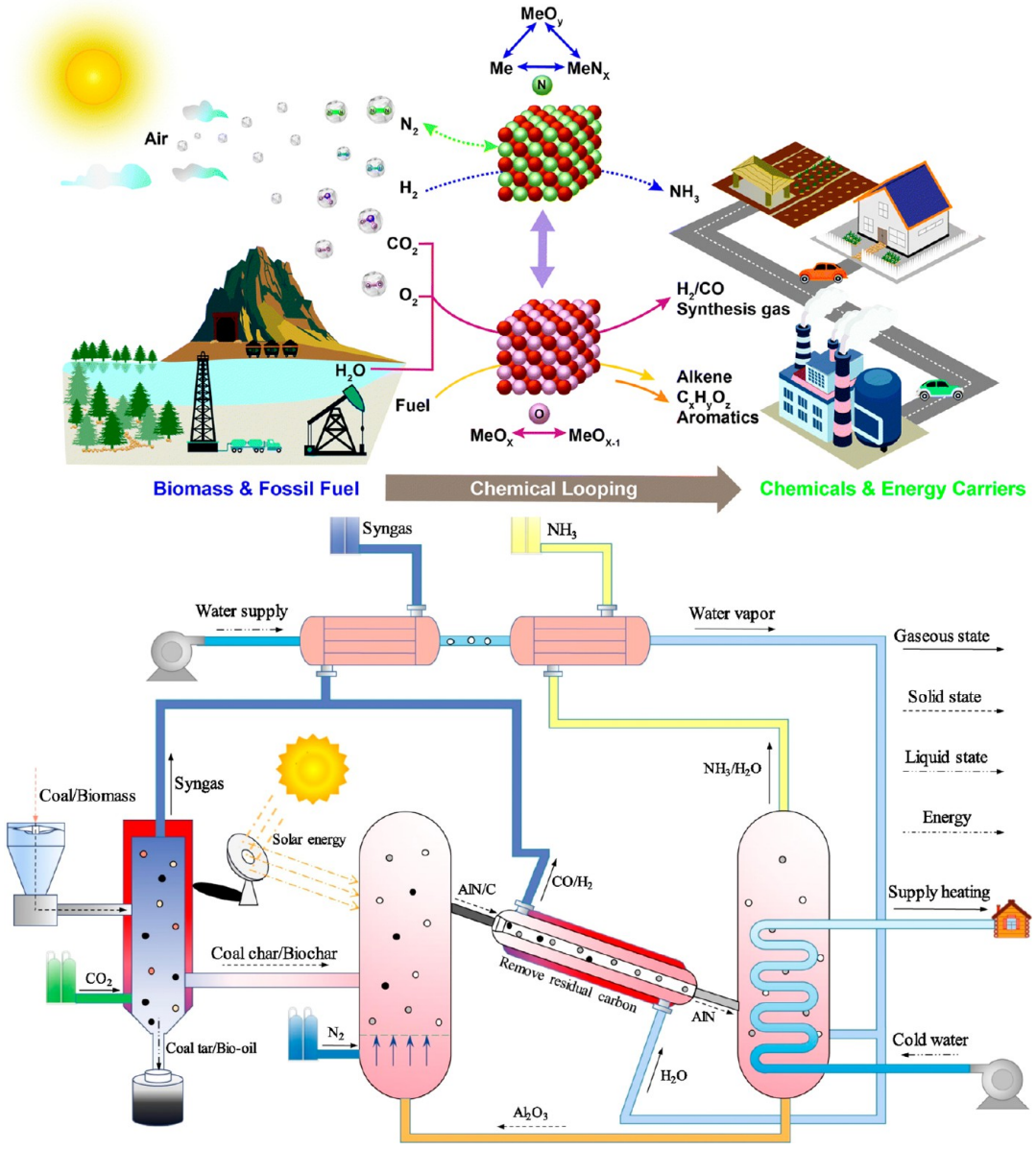

Figure 10. Green chemical looping NH_3 synthesis process. Reproduced with permission from the refs 17 and 186. Copyright 2020 Royal Society of Chemistry and Copyright 2022 Elsevier, respectively.

for water and air to produce NO_x intermediates at low specific energy consumption of 3.8 kW h mol^{-1} by a nonthermal plasma bubble column reactor in a dual reactor configuration of multiple discharge schemes and bubble dynamic control (Figure 7). Meanwhile those NO_x intermediates would be subsequently reduced to highly efficient and scalable green ammonia synthesis with a rate of 42.1 nmol cm^{-2} s^{-1} in an electrolyzer working under ambient conditions. While, an excellent plasma-catalytic NH_3 synthesis was achieved by Zhang and co-workers[167] to significantly decrease the N_2 and H_2O dissociation barriers on the catalyst surface in a nonthermal plasma discharge reactor via the dissociation of H_2O and N_2 under mild conditions while utilizing plasma-induced vibrational excitation (Figure 8). The efficient process designs of different reactor configurations, gas flow rates, catalysts, and discharge powers with different saturations of H_2O vapor, resulted in the significant synthesis rate of 2.67 mmol $g_{cat.}^{-1}$ h^{-1} at MgO supported Ru catalysts. DFT calculations and spectroscopic analysis confirmed that the plasma-catalyst interactions in response to the reduced activation energy (1.07 eV) of dissociative N_2 adsorption attributing to the efficient dissociative adsorption of vibrationally excited $N_2(v)$ and H_2O, enhanced the NH_3 synthesis rate for predominantly leaping the "unfavorable" reaction through Eley−Rideal reactions.

A triboelectric nanogenerator (TENG) has emerged as one of the most prominent innovations in energy harvesting technologies, which can take mechanical energy from the environment and efficiently convert it into electric energy.[168] The construction of a complicated nanoscale structure in a printable manner by 3D printing technology being incorporated by the efficient integration with computer-aided design software, could efficiently meliorate the wide availability of TENG in a customized system for high synthetic NH_3 efficiency.[169] An energy and cost-effective design approach of tactically integrating the 3D printing technology with

https://doi.org/10.1021/acscatal.3c02410
ACS Catal. 2023, 13, 14415−14453

personalized fabrication of printed TENGs was introduced by Gao et al.[170] for a flexible and shape-adaptive 3D-printed self-powered N_2 fixation system to achieve an ambitious breakthrough in the synthetic NH_3 industry (Figure 9A,B).

This pioneering step toward perfectly engaging the digital manufactured TENGs by 3D printing with self-powered sustainable metal-free NRR under ambient conditions using melamine-sponge-based precursor for cathode catalyst resulted in an NH_3 yield of 36.41 $\mu g\, h^{-1}\, mg_{cat}^{-1}$ and an output power density of 1.48−6.7 $W\, m^{-2}$ with 10 Hz working frequency. While, in view of some other practical implications illustrated in the policy briefing the NH_3 as a zero-carbon fertilizer, fuel and energy store by The Royal Society in February 2020, recently the JGC company has captured the scientific interest for achieving 25−50 kg per day production of NH_3 at one of its green NH_3 demonstration plants. The process runs on solar power and at a much lower pressure (around 5 MPa), and it produces hydrogen through water electrolysis using a new Ru catalyst in the ammonia synthesis step. Similarly, in another reported collaborative work of the Science and Technology Facilities Council (STFC), UK and Siemens company, a test system has been launched to run a demonstration plant for a smart H−B process, by powering it with wind to produce a considerable amount of renewable ammonia (25−30 kg per day). However, there are still bigger challenges and opportunities to be overcome for manufacturing the anticipated green ammonia in the future goal of carbon neutrality, which needs the deep mechanistic illustration of various catalytic materials and the deployment of new device configurations.

3.4. Chemical Looping Ammonia Generation. Chemical looping is another energy efficient and high product selectivity process, being employed in gasification, reforming, combustion, and air separation for oxygen supply that usually avoids the undesired characteristics of alternative synthesis techniques while utilizing the nitrogen carrier (NC) materials at mild reaction conditions.[171−173] Chemical looping ammonia synthesis (CLAS) by efficient fixation/release of NC at ambient pressure is currently a promising alternative route that could produce energy via several continuous reactions or the regeneration of chemical intermediates by simply decoupling the overall reaction scheme of NH_3 synthesis into various spatially separated subreactions mediated by a nitrogen carrier.[174−176] The overall scenario of intensive reaction conditions in H−B process (450 °C, 200 bar), primarily lies in entailing the grand challenge of overcoming the high energy barrier (941 kJ/mol) of the inert and nonpolar N≡N molecule, its sluggish reaction rate and the scaling coordination existing on the catalyst surface.[177−179] The CLAS process performed at atmospheric pressure is a simplified ammonia synthesis route, which enhances energy efficiency and reduces the carbon footprints as compared to that of H−B process, by circumventing the severe process conditions and scaling problems by avoiding the trade-offs in heterogeneous catalysis of competitive N_2 and H_2 (or H_2O) adsorption.[180,181] The cyclic operation of storing fixed nitrogen is usually a way of encountering intermittent renewable power sources, energy requirements for process heating and compression, and relocation of the centralized and integrated large-scale ammonia synthesis units. CLAS processes could be a possible way of energy storage, making it feasible to synthesize ammonia on site at atmospheric pressure rather than transporting it long distances. The processes usually splits into two or three different steps of first activating N_2 by generating a bulk metal imide or nitride as the NC, and then synthesizing NH_3 by the reaction of N_2 carrier materials with H_2 or H_2O, or sometimes going through the regeneration/reuse of intermediate(s) required in the first step[182] (Figure 10). Metal nitrides are usually considered to be highly active catalyst and support materials under ammonia synthesis conditions.[183−185] However, together with the compatibility of suitable thermodynamic, kinetic properties and good stabilities in intermittent operations of CLAS, the identification and development of highly efficient NC is the key step of making the feasible, high-selectivity, and high-yield NH_3 production approach.

In the subsequent discussion, according to the NC and the hydrogen source, CLAS processes are usually categorized into metal imides or metal nitrides (MNs) as the NC and H_2 or H_2O as the hydrogen source or sometimes through metal reduction by electrolysis. NC is usually regarded as a nitrogen storage medium for activated nitrogen being first dissociated and stored in a material, while through discharging and charging nitride lattices, the ammonia synthesis reaction is completed with a hydrogen source. Usually the H_2 required in the CLAS process is provided via sustainable routes of water electrolysis based on green energy resources, solar driven thermochemical water splitting, or directly from the reactants used in one of the CLAS loops (e.g., water), while NC regeneration can also be adopted as a reductant through biochar in some CLAS processes. The development of efficient NC materials is the key to the CLAS process, where MNs are generally categorized as highly active catalyst and support materials under mild ammonia synthesis conditions.[183−185] In the metal nitride mediated CLAS using H_2O as the H source, N activation of a metal to generate a bulk metal nitride followed by the NH_3 formation via hydrolysis of metal nitrides to metal oxides and finally the reduction of the metal oxide to metal. In the metal nitride-mediated CLAS process adopting H_2 as the H source and metal nitrides as NC, NH_3 is generated via the hydrogenation of N-rich MNs; however, it is sometimes difficult to achieve mild-condition nitrogen fixation and NH_3 synthesis using a solo metal nitrides material as NC.[180] While the regeneration of metal nitrides from their corresponding oxides is also thermodynamically unfavorable. It has been demonstrated that the coupling of alkali or alkaline earth metal hydride-imide with the transition metal catalysts can significantly promote the performance of the lithium hydride-lithium imide (LiH-Li_2NH)-mediated CLAS process.[187,188] The evolution of different reaction pathways of the LiH-Li_2NH mediated loop through a series of intermediates $LiZn_x$, and Li_2NH compounds as nitrogen carrier, with a ternary metal nitride (LiZnN), could significantly enhance the kinetics of N_2 fixation and the ammonia production rate (956 $\mu mol\, g^{-1}\, h^{-1}$) by lowering the apparent activation energy (from 102 kJ mol^{-1} to 50 kJ mol^{-1}). While alkali or alkaline earth metal hydrides and imides have been demonstrated to be another type of nitrogen carriers using H_2 as the H source.[188−191] Metal imides are feasible NC for the significant NH_3 yield via the nitridation of alkali or alkaline earth metal hydrides with N_2 in the metal imides mediated process using H_2 as the hydrogen source, which usually follows the denitridation of these imides with H_2 to regenerate the metal hydrides and simultaneously generate NH_3.[189,192,193] However, the slow reaction rate of nitrogen fixation on the hydrides and the low equilibrium concentration of ammonia in the

https://doi.org/10.1021/acscatal.3c02410
ACS Catal. 2023, 13, 14415−14453

Table 1. Catalytic Activity of Different NH_3 Synthesis Catalytic Systems

Catalytic system	Temperature [°C]	Pressure [MPa]	NH_3 yield	TOF [s^{-1}]/FE [%]	ref
Ru/C12A7:e^-	350	0.1	2757 μmol g_{cat}^{-1} h^{-1}	0.197 s^{-1}	228
Ru/C12A7:O_2^-	350	0.1	546 μmol g_{cat}^{-1} h^{-1}	0.038 s^{-1}	228
Cs−Ru/MgO	350	0.1	2264 μmol g_{cat}^{-1} h^{-1}	0.013 s^{-1}	228
Ba−Ru/AC	350	0.1	148 μmol g_{cat}^{-1} h^{-1}	0.003 s^{-1}	228
Ru/CaO	350	120.1	158 μmol g_{cat}^{-1} h^{-1}	0.006 s^{-1}	228
Ru/C12A7:e^-	340	53.0	2290 μmol g_{cat}^{-1} h^{-1}	0.0239 s^{-1}	229
Co/C12A7:e^-	340	49.5	912 μmol g_{cat}^{-1} h^{-1}	0.00213 s^{-1}	230
Ru/Ca_2N:e^-	3402	60	1674 μmol g_{cat}^{-1} h^{-1}	91.5 s^{-1}	231
Ru/CaNH	340	110	53 μmol g_{cat}^{-1} h^{-1}	2.0 s^{-1}	231
Ru/C12A7:e^-	340	51	745 μmol g_{cat}^{-1} h^{-1}	24.9 s^{-1}	231
Cs−Ru/MgO	340	120	697 μmol g_{cat}^{-1} h^{-1}	4.2 s^{-1}	231
Ru/CaH_2	340	51	2549 μmol g_{cat}^{-1} h^{-1}	98.0 s^{-1}	231
7% Fe/CeO_2	100	0.1	155 μmol g_{cat}^{-1} h^{-1}	-	232
20% Co-BaH_2	300	0.1	1866 μmol g_{cat}^{-1} h^{-1}	-	188
20% Fe-BaH_2	300	0.1	1703 μmol g_{cat}^{-1} h^{-1}	-	188
Fe(95%)Co(5%)	400	0.1	820.07 μmol g_{cat}^{-1} h^{-1}	–	233
Fe(85%)Ni(15%)	400	0.1	334.354 μmol g_{cat}^{-1} h^{-1}	–	233
Fe_3Mo_3N	400	0.1	95 μmol g_{cat}^{-1} h^{-1}	-	234
Ni_2Mo_3N	400	0.1	29 μmol g_{cat}^{-1} h^{-1}	-	234
δ-MoN	400	0.1	4 μmol g_{cat}^{-1} h^{-1}	-	234
Co_3Mo_3N	400	0.1	167 μmol g_{cat}^{-1} h^{-1}	-	234
Fe/$BaCeO_{3-x}H_yN_z$	400	0.9	6800 μmol g_{cat}^{-1} h^{-1}	-	235
Fe/LiH	350	1	11 428 μmol g_{cat}^{-1} h^{-1}	-	179
10% Fe/C	400	1	14 400 μmol g_{cat}^{-1} h^{-1}	-	236
80% Fe/$Ce_{0.8}Sm_{0.2}O_{2-\delta}$	450	1	8700 μmol g_{cat}^{-1} h^{-1}	-	237
$CoRe_4$	400	0.1	943 μmol g_{cat}^{-1} h^{-1}	-	238
Co_3Mo_3N	400	0.1	652 μmol g_{cat}^{-1} h^{-1}	-	239
$NiCoMo_3N$	400	0.1	166 μmol g_{cat}^{-1} h^{-1}	-	240
Ni-LaN	400	0.1	5543 μmol g_{cat}^{-1} h^{-1}	-	241
$Ni_{1.1}Fe_{0.9}Mo_3N$	500	0.1	354 μmol g_{cat}^{-1} h^{-1}	-	242
CeN NPs	400	0.9	1450 μmol g_{cat}^{-1} h^{-1}	-	184
$K_2[Mn(NH_2)_4]$	400	1	11141 μmol g_{cat}^{-1} h^{-1}	-	243
$SrZr_{0.9}Y_{0.1}O_{3-\alpha}$	450	-	6.50×10^{-12} mol s^{-1} cm^{-2}	<1%	244
$BaCe_{0.9}Ca_{0.1}O_{3-\alpha}$	480	-	2.69×10^{-9} mol s^{-1} cm^{-2}	50%	245
$BaCe_{0.85}Gd_{0.15}O_{3-\alpha}$	480	-	5.00×10^{-9} mol s^{-1} cm^{-2}	70%	246
$BaCe_{0.85}Y_{0.15}O_{3-\alpha}$	500	-	2.10×10^{-9} mol s^{-1} cm^{-2}	≈60%	247
$La_{0.9}Ca_{0.1}Ga_{0.8}Mg_{0.2}O_{3-\alpha}$	520	-	1.63×10^{-9} mol s^{-1} cm^{-2}	47%	248
$La_{1.9}Ca_{0.1}Zr_2O_{7-\delta}$	520	-	1.76×10^{-9} mol s^{-1} cm^{-2}	≈80%	249
$BaCe_{0.85}Y_{0.15}O_{3-\alpha}$	530	-	4.10×10^{-9} mol s^{-1} cm^{-2}	60%	250
$BaZr_{0.7}Ce_{0.2}Y_{0.1}O_{3-\delta}$	550	-	2.86×10^{-9} mol s^{-1} cm^{-2}	6.2%	251
$La_{0.9}Sr_{0.1}Ga_{0.8}Mg_{0.2}O_{3-\alpha}$	550	-	2.37×10^{-9} mol s^{-1} cm^{-2}	≈70%	252
$ScCe_{0.95}Yb_{0.05}O_{3-\alpha}$	570	-	4.50×10^{-9} mol s^{-1} cm^{-2}	78%	253
$Ce_{0.9}Gd_{0.1}O_{2-\delta}$	600	-	3.67×10^{-11} mol s^{-1} cm^{-2}	4.53%	254
$BaZr_{0.7}Ce_{0.2}Y_{0.1}O_{3-\delta}$	620	-	1.70×10^{-9} mol s^{-1} cm^{-2}	2.7%	78
8% Y_2O_3/ZrO_2	650	-	1.50×10^{-13} mol s^{-1} cm^{-2}	<1%	255
LiCl-KCl-CsCl	300	-	0.72 mol h^{-1} m^{-2}	23%	98
$SrCe_{0.95}Yb_{0.05}O_{3-\alpha}$	650	-	1.4×10^{-5} mol h^{-1} m^{-2}	–	255
$Ce_{0.8}Gd_{0.18}Ca_{0.02}O_{2-\delta}/Li_2CO_3-Na_2CO_3-K_2CO_3$	375	-	0.014 mol h^{-1} m^{-2}	3.9%	256
$Ce_{0.8}Gd_{0.2}O_{2-\delta}/Li_2CO_3-Na_2CO_3-K_2CO_3$	400	-	0.004 mol h^{-1} m^{-2}	5.3%	257
$BaZr_{0.8}Y_{0.2}O_{3-\delta}$	550	-	0.0018 mol m^{-2} h^{-1}	0.46%	258
d-TiO_2/TM	RT	-	1.24×10^{-10} mol cm^{-2} s^{-1}	9.17%	259
TiO_2/Ti	RT	-	9.16×10^{-11} mol cm^{-2} s^{-1}	2.50%	260
Ru/TiO_2 -Vo	RT	-	2.11 μg cm^{-2} h^{-1}	0.72%	224
Fe-doped TiO_2	RT	-	25.47 μg $mg_{cat.}^{-1}$ h^{-1}	25.6%	261
$MnO_2-Ti_3C_2T_X$	RT	-	34.12 μg $mg_{cat.}^{-1}$ h^{-1}	11.39%	262
Au@CeO_2	RT	-	10.6 μg mg_{cat}^{-1} h^{-1}	9.5%	263
$Cr_{0.1}CeO_2$	RT	-	16.82 μg $mg_{cat.}^{-1}$ h^{-1}	3.84%	264
Cu-CeO_2-3.9	RT	-	5.3×10^{-10} mol cm^{-2} s^{-1}	19.1%	265
$Bi_4V_2O_{11}/CeO_2$	RT	-	23.21 μg $mg_{cat.}^{-1}$ h^{-1}	10.16%	266
Ru/2H-MoS_2	50 °C	-	1.14×10^{-10} mol cm^{-2} s^{-1}	17.6%	267
$RuCe_{2.4}$/BN	400	-	14.6 mmol g_{cat}^{-1} h^{-1}	-	268

https://doi.org/10.1021/acscatal.3c02410
ACS Catal. 2023, 13, 14415−14453

Table 1. continued

Catalytic system	Temperature [°C]	Pressure [MPa]	NH_3 yield	TOF [s^{-1}]/FE [%]	ref
Pt_1-Pt_n-TiN	280	-	121 μmol g_{cat}^{-1} h^{-1}	-	18
Ni@NC	-	-	34.6 μmol cm^{-2} h^{-1}	72.3%	154
Zn−LiH−Li_2NH	350	-	956 μmol g^{-1} h^{-1}		269
LiCl−NaCl−KCl	400	-	914 μmol g^{-1} h^{-1}	-	194
MnFeAl	600	-	166.3 μmol. g^{-1} h^{-1}		196
FeNp	450−750	-	420.9 μmol g^{-1} min^{-1}	-	212
Li_3N	510	-	0.025 μg s^{-1}	-	221
Ni/SiO_2	155	-	109.3 μmol g-cat^{-1} min^{-1}	-	270
Ru/TiO_2	RT	-	10.4 μg_{NH3} cm^{-2} h^{-1}	40.7%	271
CuCoSP	RT	-	1.17 mmol cm^{-2} h^{-1}	93.3%	272
Ru/LaCoSi	250−400	-	18.5 mmol g^{-1} h^{-1}	-	214
Mo_3Si thin film	-	-	2×10^{-10} mol cm^{-2} s^{-1}	6.69%	151
$Ru_{1.7}$/CeScSi	300	-	0.58 mmol g_{cat}^{-1} h^{-1}	-	273
LaCoSi	400	-	5.8 mmol g_{cat}^{-1} h^{-1}	-	274
CoPPi	-	-	159.6 μg mg_{cat}^{-1} h^{-1}	43.37%	275
BaH_2/Ni−Mg−O	350	-	6160 μmol g^{-1} h^{-1}	-	276
Fe/$BaTiO_{3-x}H_x$	400	-	8.9 mmol g_{cat}^{-1} h^{-1}	-	277
Co/CeN NPs	200	-	0.4 mmol g^{-1} h^{-1}	-	278
Co-based $BaAl_2O_{4-x}H_y$	430	-	500 mmol g_{cat}^{-1} h^{-1}	-	279

hydrogenation of imides to NH_3 and hydrides at atmospheric pressure may hinder their frequent adaption.[194] While the transition metals with their corresponding nitrides or oxides (Mn_4N, Fe_2O_3, TiO_2, etc.) have also been found in playing an important role of unconventional NH_3 synthesis rate for CLAS processes by promoting the N_2 fixation, hydrogenation, or hydrolysis reactions.[195,196] One of the typical examples is the transformation of Mn among different nitride forms in the manganese nitride mediated CLAS process. Various efforts have been devoted in the improvement of slow kinetics of nitridation and hydrogenation reactions of Mn nitrides and hydrogenation reactions.[197−201] Similarly, molybdenum nitride (Mo_2N) has also been widely applied as an efficient transition-metal-nitride-based NC material for generating NH_3 directly with H_2,[202−206] (usually 3−4 times higher) than that of thermo-catalytic ammonia synthesis route, where the enhanced the reaction kinetics between Mo and N_2 could accelerate the N-fixation step, while facilitating the NC regeneration.[207]

Increasing efforts have been devoted to improving the efficiency of CLAS process, using the electric or photon energy,[99,194,208] structure modulation of NC,[99,194,198,200,208] and kinetics enhancement by adding catalyst.[209,210] Similarly, the strong cooperative reactivity of the composite Mn based nitrogen carrier (Mn_4N and LiH or BaH_2Mn nitride), could result in the exceptional catalytic activities for ammonia synthesis under mild conditions as compared to that of their parent elements by catalyzing the N_2 fixation and hydrogenation reactions.[179,191,211] Suggesting new chemical looping reaction pathways could be another strategy of improving the CLAS process,[18,173,186,209,212−218] where the easy alloying characteristics of lithium and group 14 elements (Li_xM) could provide some interesting results in N_2 fixation through the generation of ternary nitrides.[219−221]

4.0. Catalytic Evolution in Developing the Ammonia Synthesis Catalyst. Synthetic NH_3 production relies on the energy-intensive H−B process. The invention of fused Fe as one of the most investigated catalysts has instigated a catalytic ammonia synthesis industry, which is still considered well consolidated for occupying the absolute position in industry with some technological breakthroughs. However, Ru, Co, or Mo based bimetallic nitride catalysts are also getting new places in expressing the idea of seeking technical advancements. Anyhow, developing more active catalysts for a mild reaction environment is of vital scientific importance for substituting the current well-developed H−B process. In this concern, the conductivity of the bulk/oxides or doped catalyst in the solid electrolytes could be postulated as the governing factor for an active catalytic system. Recent studies in developing an optimized perovskite-based or fluorite-based electrolytes for significant proton conductivity, positively correlated the performance with the tolerable current densities at credible overpotentials, demonstrated a high (10^{-9} mol-s^{-1} cm^{-2}) overall reaction rate toward NH_3 accompanied by substantial (up to 60%) FE toward H_2. Adopting a similar perovskite nature of both (cathode and anode) components with the fabrication of an effective interface in a highly conductive protonic solid electrolytes could be approached for efficient performance over a broad range of temperatures. In response to the limiting factors in the low, medium, and high temperature zones, the PCMR obviously could be preferred in a high-temperature regime (>500 °C); however, poor electrolyte/catalyst conductivity, high HER rates for protons' recombination in the cathode cell, and the NH_3 decomposition may still have some surging limitations (as can be seen in Table 1). Catalytic evolution in eNRR to ammonia has always been a hot topic for potentially competing with the H−B process and mitigating the associated carbon emissions. However, the lack of specificity toward nitrogen fixation by most electrocatalyst surfaces limited the significant progress. Developing an emerging class of potential catalysts and delineating the possible reaction pathways (NO_2, NO_2^-, NO, N_2O, N_2, NH_2OH, NH_3, and NH_2NH_2) in the NO_3^- reduction to NH_3 through investigating the molecular catalyst structure, could bring a renewed attention to the recycling of reactive N-containing species (e.g., NO and nitrate) to NH_3.[1,15,55,222−227]

Transforming the brown H−B process to the green alternatives needs robust catalytic design by illustrating the advanced scientific investigations and developing a mechanistic understanding of complex species and catalytic surfaces in

https://doi.org/10.1021/acscatal.3c02410
ACS Catal. 2023, 13, 14415−14453

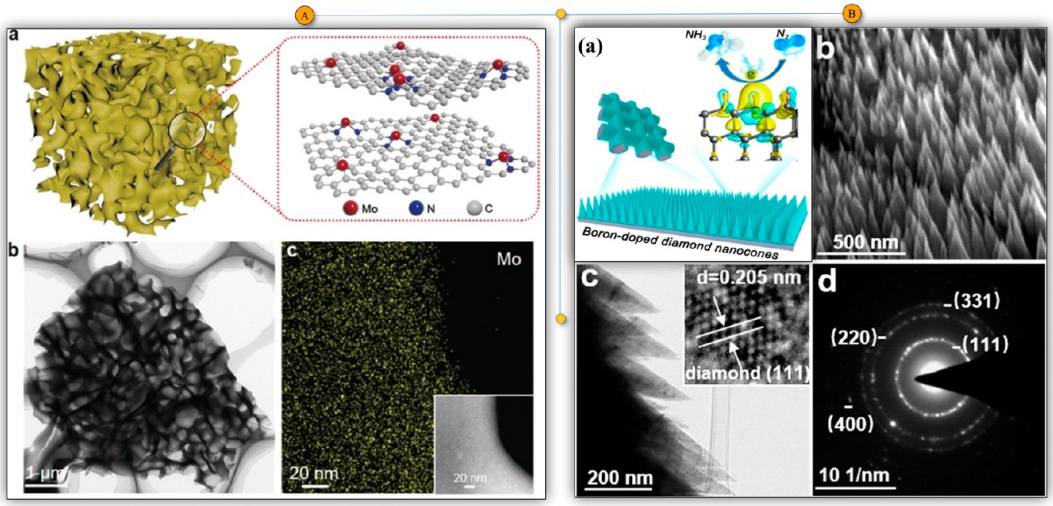

Figure 11. (A) Demonstration of atomically dispersed Mo single atom on N-doped porous carbon with its corresponding atomic structure model, and TEM, EDS HAADF-STEM micrographs, respectively. Reproduced with permission from ref 305. Copyright 2019 John Willey and Sons. (B) Morphology and structural representation of Boron-doped nanodiamond (BND) films/Ti electrode with its corresponding SEM, TEM, HRTEM images, and SAED pattern, for a high-efficiency electrocatalyst, respectively. Reproduced with the permission from ref 312. Copyright 2020 American Chemical Society.

nitrogenase-promoted or molecular catalyst-promoted NH_3 synthesis. Various characterizations have been adopted to realize the different characteristics of the catalytic species and reaction intermediates. The profound insights into revealing the vital role of the potential-driven variations in morphology, crystal structure, and chemical state during electrochemical redox reactions have been interpreted by deploying advanced in situ/operando routes in various recent investigations. Enlightening the recent advancement made in the catalytic insights in terms of numerous catalysts developed for renewable NH_3 synthesis, the following sections would briefly describe those investigations being made in this scenario while illustrating the conducted characterization approaches. Extracting N_2 from air is one of the main sources in the renewable eNRR route, demonstrating a sustainable platform of large-scale NH_3 manufacturing. However, still challenging to firmly attributing the effective eNRR process to drive high-rate NH_3 synthesis due to the nonpolar and extremely stable nature of N≡N triple bond (941 kJ mol^{-1}), thus suffering from low ASR (mostly <200 $\mu g\ h^{-1}\ mg_{cat.}^{-1}$) and low FE.[55] A variety of different catalytic materials including noble-metal nanostructures, oxides, sulfides, nitrides, nitrogen- and boron-doped carbon, and carbides have emerged as promising and active eNRR catalysts for modulated activity and significant stability.[15,87,260,280−283] However, the higher eNRR activity in most of the catalytic materials is usually impeded by their intrinsic deficiencies in conductivity and considerable active sites.[174,284,285] NO_x (NO and NO_2), as a major air pollutant by heavy diesel vehicle or power plant emissions has inauspicious impacts on the environment and injurious to human health, leading to photochemical smog and acid rain while directly damaging the respiratory system, since need the stringent legislation for control.[286−288] Various types of transition metals (Fe, Mn, and Cu) and rare earth metals oxides or zeolites have been investigated for the selective catalytic reduction (SCR) reaction of NO_x with NH_3, as a strategy of controlling NO_x emissions from stationary or mobile sources.[289] It is of great importance to develop the effective, durable, and cost-effective electrocatalysts via rationally tuning the microstructures of the catalytic surfaces to promote the FE and accelerating the NRR kinetics with different modifications of heteroatom doping, carbon supports, defect engineering and structural engineering.[290−294] As iron has been an old lad occupying the ammonia industry for a longer time, different modulations on Fe single atom could lead to an active and selective catalyst in the eNRR system. Revealing the reaction mechanisms and the potential limiting steps by DFT calculations for nitrate reduction on atomically dispersed Fe sites could further illustrate the governing factors of NO* reduction to HNO* and HNO* reduction to N*. A recent study has demonstrated that the lack of neighboring metal sites in the developed Fe single atom catalyst on a standard glassy carbon electrode can effectively promote the ammonia product selectivity via preventing the N−N coupling step required for N_2.[85] Thus, a maximal ammonia yield rate of 20,000 $\mu g\ h^{-1}\ mg_{cat.}^{-1}$ and ∼75% FE was achieved at −0.66 V vs RHE, with ∼100 mA cm^{-2} NH_3 partial current density at −0.85 V. Similarly, progress on zeolite-based passive NO_x adsorbents (PNA) has emerged recently as selective catalytic reduction catalysts by actively participating in adsorption of nitrogen oxide species. Where, different studies revealed that the unique shape and excellent properties of zeolite, make them persistent candidates in providing the new opportunities as profitable catalysts in NO_x emission control for diesel engines.[295] Zeolite-supported copper catalysts (Cu-zeolites) have been extensively applied in the past decade in SCR, demonstrating that the correlation between the catalytic cost, structure, performances, and stability are the crucial factors for their implications in various sectors. However, the challenges about the adjustment of the Al location, tailoring the hydrothermal stability, and reducing the capital investment still need to be overcome.

4.1. Mechanistic Insights by Advanced Characterization Tools. A variety of different noble and non-noble metals have been developed for NRR electrocatalysts at ambient conditions with aqueous electrolytes.[188,266,280,281,290,296−303] A higher ASR (3.9 $\mu g\ h^{-1}\ cm^{-2}$) and a corresponding higher FE of 30.2% by hollow gold nano cages could surpass the noble metals group,[280] however

https://doi.org/10.1021/acscatal.3c02410
ACS Catal. 2023, 13, 14415−14453

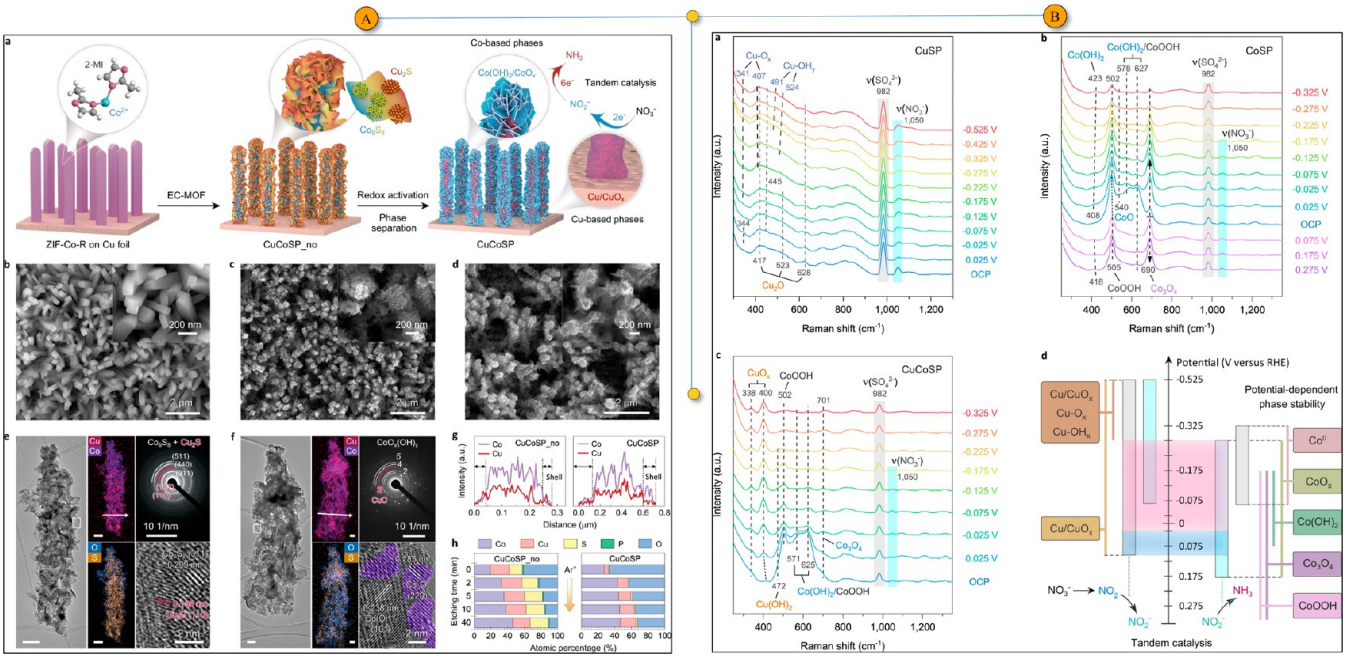

Figure 12. (A) Design scheme with SECM micrographs. (B) In situ Raman spectra of core−shell Cu-CuO_x & Co-CoO phases generated multifunctional NO_3RR electrocatalysts. Reproduced with permission from ref 272. Copyright 2022 Nature.

strained by high material costs. While the highest FE of 10.16% and ASR of 23.21 μg h^{-1} $mg_{cat.}^{-1}$ achieved by $Bi_4V_2O_{11}$/CeO_2[296] non-noble-metal-based hybrid material, and the highest ASR of 26.57 μg h^{-1} mg_{cat}^{-1}. with a corresponding FE of 15.95% presented by Boron Carbide (B_4C) nanosheets[290] among the alternative materials of metal-free catalysts, could be a better fit of demonstration. It has been established that the size of metal-based nano catalysts majorly influencing the catalytic activity, need to be regulated simultaneously in relation to the increasing fraction of metal atoms with unsaturated coordination sites.[304] Since, an efficient and robust nonprecious-metal single molybdenum atom catalyst was anchored on nitrogen-doped porous carbon (SA-Mo/NPC), exhibiting high electrocatalytic activity and stability for N_2 fixation, owing to its well-dispersed single molybdenum atoms architecture, high porosity, and conductive carbon support.[305] The abundance of single active sites and the 3D hierarchically porous carbon frameworks, resulted in a high FE of 14.6 ± 1.6% in 0.1 $_M$ KOH and an enhanced ASR of 34.0 ± 3.6 μg h^{-1} $mg_{cat.}^{-1}$ at room temperature and −0.3 V vs RHE in 0.1 $_M$ HCl, without losing the current drop during a 50,000s NRR.

Carbon-based materials on the other hand are also a promising electrocatalyst group for NRR, where the incorporation of heteroatoms (such as B and N)[306−308] can stimulate the inert atmosphere of pure carbon by modulating the electronic structures of adjacent carbon atoms and providing the electrocatalytically active sites for N_2 electro-reduction.[299,309] The sp^3-configured diamond possessing the high electron and hole mobilities, excellent chemical inertness, extremely wide electrochemical potential window and wide a band gap of 5.5 eV diamond, surpassed the other carbon family members (e.g., graphene and CNT) in suppressing the HER, and enabling a high FE of NRR.[310,311] A novel effort was made on the fabrication of boron-doped nanodiamond (BND) films for a high-efficiency electrocatalyst in NH_3 synthesis while elucidating the roles of substitutional B atoms and charge accumulation on the nanostructured Ti meshes surface with theoretical simulations (Figure 11A,B).[312] These substitutional BND atoms could initiate the NRR active centers to afford a high ASR of 19.1 μg h^{-1} cm^{-2} and an enhanced FE of 21.2%, thus suppressing the reaction free energy on certain surfaces for the NRR rate-determining step and lasting the reaction up to a stable eight-day operation under ambient conditions. While the Cu-based oxide having excellent capability of binding the NO_3^- ion and efficiently converting NO_3^--to-NO_2^-, have been widely explored in NO_3RR reduction reaction.[313−316] Where, considerable exertions have been recently deployed in various studies via regulating the catalytic activity of Cu-based nanostructures by modulating the binding strengths of partially reduced intermediates adsorbed on copper centers and tuning the proton/electron-transfer. Cu_3P NPs embedded in reduced graphene oxide (Cu_3P-rGO) hybrid served as an efficient electrocatalyst toward NH_3 synthesis in an efficient effort by Zhao et al.[317] achieving a high FE of 10.11% and a large NH_3 yield of 26.38 μg h^{-1} $mg_{cat.}^{-1}$ at −0.45 V vs. RHE in 0.1 M HCl, with high electrochemical stability. Similarly, in response to their great potential, excellent properties, and significant catalytic activity toward gas molecules and a variety of energy-related electrocatalysis applications,[318−323] Co-based materials could be anticipated as the efficient NRR catalysts. A hollow nanocages cobalt phosphide (CoP HNC) cathode in hierarchical structure was recently employed by Xu and co-workers[324] as a noble-metal-free high-efficiency NRR electrocatalysts, achieving an exciting performance of 10.78 μg h^{-1} NH_3 yield, and FE of 7.36% while potentially suppressing the excessive HER at −0.4 V vs. RHE under ambient pressure and room temperature.

Similarly, a pyrolysis-phosphorization approach was adopted by Zhang and co-workers[325] using ZIF-67 precursor to manufacture the CNT embedded cobalt phosphide nanocomposites (CoP/CNs) NRR catalysts, attaining an ASR of 48.9 μg h^{-1} mg_{cat}^{-1} with a FE of 8.7% at −0.4 V (vs. RHE) in 0.1 M Na_2SO_4. However, in a combined investigation of

https://doi.org/10.1021/acscatal.3c02410
ACS Catal. 2023, 13, 14415−14453

theoretical simulations and experimental techniques by Chu and co-workers,[326] CoO nanostructures were found to be the representative of most superior NRR electrocatalysts. DFT calculations as a tool of predicting the potential of CoO for the NRR catalyst revealed that CoO possessed poor HER activity and favorable NRR activity. The RGO served as a support material for CoO quantum dots (QDs, 2−5 nm) to fabricate the CoO QD/RGO hybrid material, demonstrating the great potential of 8.3% FE at −0.6 V and a high NH_3 yield of 21.5 $\mu g\ h^{-1}\ mg^{-1}$ vs. RHE, with excellent selectivity and stability under ambient conditions. Similarly, the ambient NH_3 synthesis with excellent selectivity and durability was enabled by an eNRR catalyst of CoP_3 nanoneedle array on carbon cloth (CoP_3/CC), achieving a large NH_3 yield of 3.61×10^{-11} mol s^{-1} cm^{-2} and high FE of 11.94% at −0.20 V vs. RHE in 0.1 M Na_2SO_4, with high durability.[327] However, the strong adsorption of the NO_3RR intermediates (e.g., NO_2^- and NO) may lead to the rapid deactivation of pure Cu/Co catalysts and generally encountered the scaling relations.[313,314,328] A design concept of interactive active sites facilitating the cascade conversion of NO_3^--to-NH_3 via a facile electrochemically driven phase-separation strategy was revealed by Wenhui and co-workers[272] by integrating the intermediate states of Cu/Co metals residing at low applied overpotentials. This electrochemically modulated phase-separation technique of configuring copper−cobalt binary sulfides into potential-dependent core−shell Cu-CuO_x and Co-CoO phases generated multifunctional electrocatalysts for NO_3RR process. Combining the kinetic studies and various catalytic and characterization results including in situ scanning electrochemical microscopy (SEM) (Figure 12A) along with the help of in situ Raman spectra (Figure 12B), revealed that in situ fabricating the various active intermediate phases and rich phase interfaces could be an efficient approach of expeditious spillover and conveying of reaction intermediates. The instant reduced amount of NO_2^- generation with the substantial NH_3 production was demonstrated to be significantly enhanced at the border (X ≈ 600 μm) between the Cu and $Co(OH)_2$ layers, The SEM results unequivocally confirmed that the NO_3^- reduction to NO_2^-, was tentatively preferred at the inner phases of Cu/CuO_x while the outer-layer shell of Co/CoO phases was selectively responsible for rapid reduction of NO_2^- to NH_3. This superior integrated catalytic approach outperforming the previous report studies generated a high ASR of 1.17 mmol cm^{-2} h^{-1}, 93.3 ± 2.1% FE and ∼36% half-cell energy efficiency in 0.1 M NO_3^- at −0.175 V vs RHE in a wide range of NO_3^- concentrations at 13 pH, while avoiding the generally encountered scaling relations. The available d-orbital electrons in transition metals for π back-donation of N−N, originates the high NRR activity for promoting the adsorption and activation of N_2.

The different metal-based oxides, sulfides, nitrides, and carbides have delivered comparable NRR performances. Nevertheless, the enhanced adsorption of *H from the d-orbital electrons of transition metals to form strong metal-H bonds compromised the FE of eNRR accelerated HER. The research being captured on different elements with weak hydrogen adsorption could be of great value for achieving desired NRR activity. On the other hand, the common perception toward Fe-, Ru- and Co-based catalysts for ammonia synthesis over the decades could be the reason for inefficient behavior of other metals in normal condition.[228,329−334] In some aspects, the early 3d metals are considered catalytically inactive for ammonia synthesis, which can bind N_2 too strongly that hinders its subsequent hydrogenation to ammonia.[335−337] The strong N adsorption energy (E_N = −1.8 eV) on the clean Cr(110) metal surface, having the capability of dissociative adsorption of N_2 with the generation of too stable Cr nitride surface to be hydrogenated to NH_3 at ambient conditions, impede its wider application in ammonia synthesis. However, different treatment methods and techniques could be employed to make them active for a suitable ammonia synthesis catalyst. A recent report by Guan et al.[338] envisaged an intrinsic strategy to "activate" Cr under lower temperatures for effectively rendering a highly active ammonia synthesis catalyst by constructing a unique composite of BaCr nitride-hydride, $[HBa_6]$ $[CrN_4]$ octahedral and tetrahedral units, respectively. Since, an observable amount of ammonia was produced in positive reaction orders of nitrogen and hydrogen at 373 K and 1 bar with low (50.1 kJ mol^{-1}) apparent activation energy. While a four times higher ammonia synthesis rate (6.8 $mmol_{NH3}$ g_{cat}^{-1} h^{-1}) than that of reference Cs−Ru/MgO catalyst was achieved at 10 bar and 573 K. Deeper investigations revealed that inactive nature of these early transition metals could be accelerated in effective ammonia catalysis by generating the reactive nitrogen and hydrogen in the active phase of Ba_5CrN_4H-like structure. Meanwhile, the excellent electrocatalytic properties of SnO_2 widely employed in various energy related fields can be considered in eNRR electrocatalysts. However, only a few works have been reported on the SnO_2 based sub micrometer particles for NRR, obtaining low ammonia yield and FE, being attributed to the low conductivity of SnO_2 sub micrometer particles and limited active sites. A recent study based upon experimental techniques and DFT calculations for RGO supported SnO_2 quantum dots (QDs), endowed a promising electrocatalyst for NRR at ambient conditions.[339] The ultrasmall SnO_2 QDs (2 nm) grown on RGO exhibited a fascinating NH_3 yield of 25.6 $\mu g\ h^{-1}\ mg^{-1}$ (5.1 $\mu g\ cm^{-2} h^{-1}$) and an FE of 7.1% in 0.1 M Na_2SO_4 at −0.5 V together with inferior HER activity, where the outstanding stability outperformed the most recently reported NRR electrocatalysts. It was interpreted that the strongly electronically coupled SnO_2/RGO provided the abundant sites for efficient N_2 adsorption and brought about the enhanced conductivity with the decreased work function, considerably reducing the energy barrier in rate- determining step ($*N_2 \rightarrow *N_2H$).

Similarly, the unique properties of bismuth-based materials with intrinsic electronic structures encouraged a wide exploration of Bi nanocrystals,[126] mosaic Bi nanosheets,[340] and flower-like β-Bi_2O_3[341] in response to their poor HER activity, and exhibiting the fascinating NRR performances with usual high FE. As described earlier in a strategy of Hao and co-workers[126] deploying Bi nanocrystals and K cations, exciting results (66% FE with 200 mmol g^{-1} h^{-1} ASR) of simultaneously promoting eNRR selectivity and activity were obtained in aqueous media under ambient conditions with the stronger interplay of N 2p orbitals and Bi 6p band. However, the complex chemical and structural variations under the reaction potentials still need a clear reaction mechanism and deeper illustration of various active sites. Where a recent study on the in situ reduced nanorod-like Bi-based MOF and fragmented into densely embedded Bi^0 nanocrystals under applied potentials were carried out by different approaches of complementing the electron microscopy and in situ Raman spectroscopy, exploring the structural and chemical transformation of the Bi species during the NRR.[342] The generation

https://doi.org/10.1021/acscatal.3c02410
ACS Catal. 2023, 13, 14415−14453

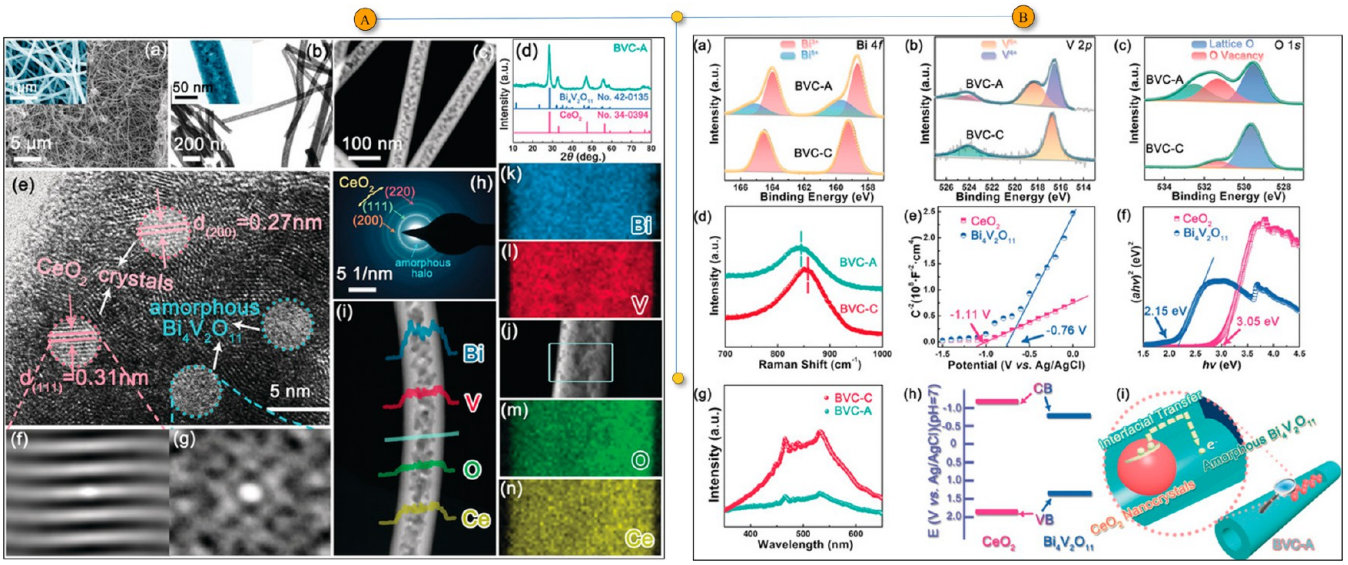

Figure 13. Various characterization approaches (A) SEM (a), TEM (b), HAADF (c), and XRD (d) HRTEM (e–g), SAED pattern (h), EDX (i), mapping (j–n) ; (B) XPS (a–c), Raman (d), Mott–Schottky plot (e), Kubelka–Munk plot (f), PL spectra (g), band alignment (h), and interfacial charge transfer (i), of noble-metal-free $Bi_4V_2O_{11}/CeO_2$ hybrid as a unique NRR electrocatalyst. Reproduced with permission from ref 296. Copyright 2018 John Wiley and Sons.

of different reaction species on different catalytic sites during NRR was confirmed by in situ Raman spectroscopy with fluorescence optical responses, ascribing the accumulation of generated NH_3 with increased peak intensity and applied overpotentials. The detection of the intermediate (such as $*NH_2$*NH_2) species at molecular level by could further unveil that the associative alternating mechanism could mainly be driven by the dual-metal sites in realizing the N_2 reduction pathways. Online differential electrochemical mass spectroscopy (DEMS), on the other hand, providing complementary direct illustration on electrocatalytic mechanisms, was applied in tracking the NRR process via monitoring the volatile intermediates and products. The in situ mass-resolved determination of volatile reaction species analyzed by DEMS, revealing the reaction route on the Bi metal catalyst through a two-step reduction and decomposition process, confirmed the outstanding NRR activity. Tuning the geometric and electronic structures of the catalytic species under NRR conditions resulted in an excellent NRR performance of 3.25 ± 0. 08 $\mu g\ cm^{-2}\ h^{-1}$ ammonia yield at −0.7 V by fragmented Bi^0 NPs in both neutral and acidic electrolytes, and a FE of 12.11 ± 0.84% at −0.6 V vs RHE in 0.10 $_M$ Na_2SO_4.

4.1.1. Surface Tuning and Defect Engineering for Oxygen Vacancy Mediated Catalysts. Defects' engineering and the mediation of surface oxygen vacancies (V_o) are ways of introducing active centers in metal oxides (or hydroxides) for an effective and flexible route to tune the reactant adsorption and activation as well as the stabilization of reaction intermediates[343] for various processes of oxygen reduction reaction,[344,345] CO_2 conversion[346−349] and N_2 photo fixation.[350−353] Owing to its acid–base interaction, oxygen storage and unique redox properties, ceria (Ce) has been deployed in various sectors as support, promoter, or main active component, among which NH_3–SCR catalysts or as a vital element in three-way catalysts for automotive emission control have been prominent requisitions.[354,355] Various recent studies demonstrated the ceria-based NH_3–SCR catalysts as the effective candidate in terms of excellent catalytic performance and NH_3 yield. However, due to the loss of surface area by sintering and high reduction temperature, pure ceria is usually not suitable as a support for NH_3–SCR catalysts, thus requiring some additional components (such as CeO_2–ZrO_2) to significantly increase the oxygen storage capacity and the thermal stability of the oxide.[356] The strong interplay with metals, abundant oxygen vacancies, and governable manufacturing with different exposed crystal facets make the CeO_2 nanomaterials as one of the effective catalytic support materials in heterogeneous catalysis. Ceria based nanomaterials are highly efficient catalysts applying with the uniqueness of CeO_2 supports with noble-metal single atoms or nanoclusters, where the highly dispersed noble-metal sites result in the extraordinary catalytic performances of CH_4 conversion, hydroformylation, CO_2 valorization, WGS activities, CO oxidation, and ammonia synthesis or decomposition process.[357] A unique NRR electrocatalyst based on noble-metal-free $Bi_4V_2O_{11}/CeO_2$ hybrid catalyst (regarded as BVC-A) was designed by constructing the amorphous $Bi_4V_2O_{11}$-crystalline on CeO_2 hybrid material via a spinneret electrospinning process with subsequent calcination (Figure 13A,B).[296] The role of critical mole ratio was found to be important in establishing the amorphous and crystalline phase, where CeO_2 restrained the heat transfer rate, and induced the amorphization of $Bi_4V_2O_{11}$ when employing moderate mole ratios of Ce/Bi (≥1:2). However, the amorphous effect was diminished, giving rise to the crystalline $Bi_4V_2O_{11}$ phase in counterpart BVC-C as the mole ratio of Ce/Bi dwindles to 1:4 in this hybrid. Scanning/transmission electron microscopies (SEM)/(TEM) Figure 13A(a-b), high-angle annular dark field (HAADF) Figure 13(c), and X-ray powder diffraction (XRD) Figure 13(d), were carried out to depict the different morphological changes and to prob the phase composition of different catalytic surfaces. The images of the $Bi_4V_2O_{11}/CeO_2$ hybrid in the diameter range of 60 nm, depict the hollow nanofibrous morphology (amorphous BVC-A phase). XRD examination revealed only CeO_2 with no obvious diffraction peaks of $Bi_4V_2O_{11}$, implying the amorphous state of the later

https://doi.org/10.1021/acscatal.3c02410
ACS Catal. 2023, 13, 14415−14453

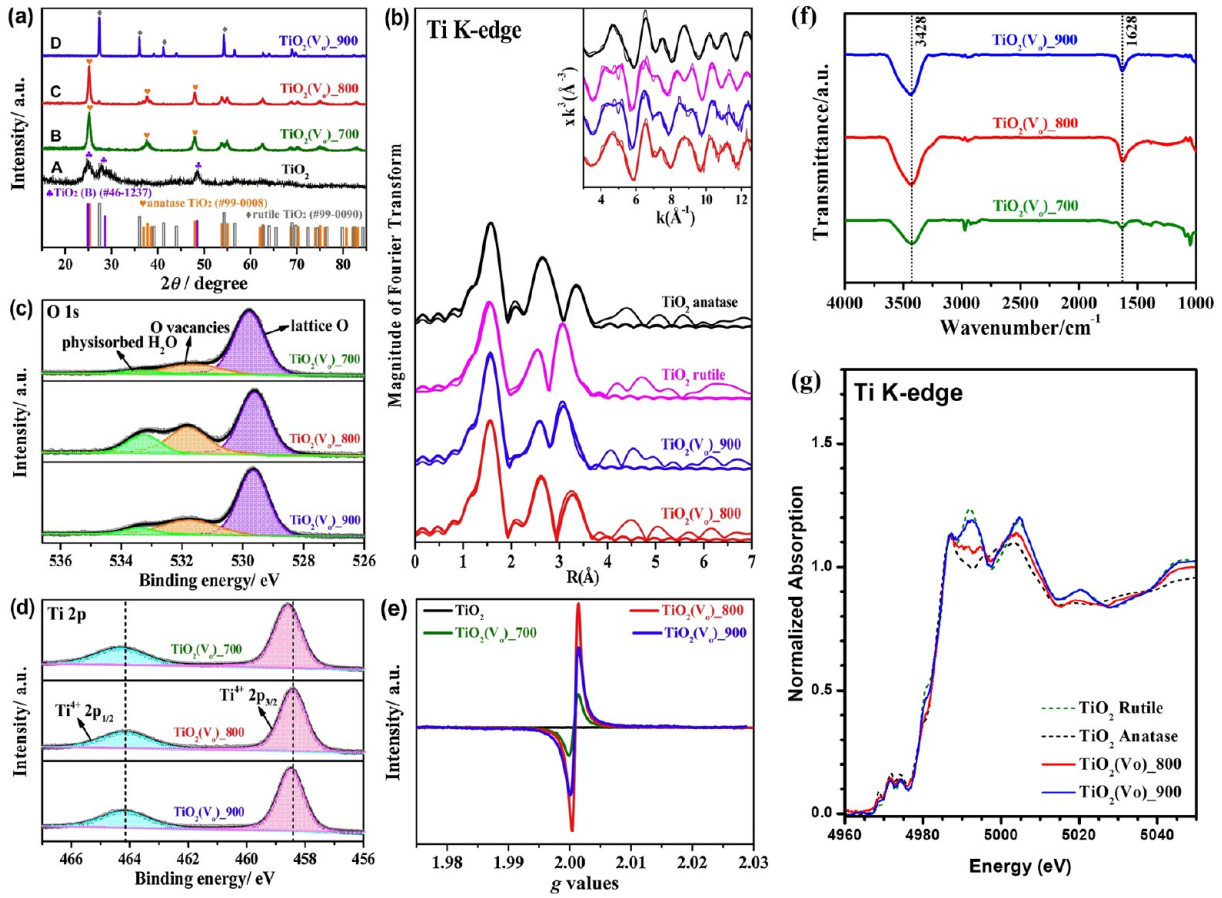

Figure 14. Various characterization approaches in revealing the deep mechanistic insights of NH_3 synthesis catalysts, (a) XRD patterns, (b) EXAFS, (c,d) XPS, (e) ESR, (f) FTIR, and (g) XANES, spectra of different Ti based catalysts, respectively. Reproduced with permission from ref 363. Copyright 2019 Elsevier.

phase. CeO_2 inducing the amorphous structure could establish the band alignment with $Bi_4V_2O_{11}$ for rapid interfacial charge transfer, while the high amounts of defects as active sites in the amorphous $Bi_4V_2O_{11}$-crystalline CeO_2 hybrid catalyst could accelerate the N_2 fixation rate. Since, a remarkable FE of 10.16% and an NH_3 production yield of 23.21 $\mu g\ h^{-1}\ mg_{cat.}^{-1}$ were exhibited by the BVC-A hybrid catalyst under ambient conditions. The X-ray photoelectron spectroscopy (XPS) spectra of Figure 13B(a-c) indicated that the high-valence Bi defect could be recognized by extracting oxygen ions from $[VO_{3.5}]^{2-}$ layers during the amorphization phenomenon, thus encouraging the abundant generation of reduced vanadium species and enriched oxygen vacancies. Such a disordered structure renders amorphous $Bi_4V_2O_{11}$ rich in dangling bonds were also determined by Raman spectra Figure 13B(d), indicating that inducing the sufficient active sites and reducing the required energy barrier, could hold an efficient NRR process.

In response to the efficient calibers of abundance, chemical and stability nontoxicity of a typical n-type semiconductor, TiO_2 can be regarded as a promising candidate in eNRR. It is widely explored in different studies that tuning the surface oxygen vacancies significantly enhances the electrocatalytic ambient nitrogen fixation of TiO_2,[358−361] provide substantial ASR and FE in a wide potential range. Nevertheless, the lower activation of TiO_2, weak N_2 adsorption and low conductivity could impede its NRR catalytic activity.[260,362] The electronic structure, density of unoccupied states, and bonding geometry of different X-ray absorbing atoms can be analyzed by *Operando* X-ray absorption spectroscopy (XAS) to deliver deeper mechanistic insights for better catalytic activity.

In a recent study by Han et. al,[363] the activation of TiO_2 surface was carried out by engineering surface oxygen vacancies for accelerated NRR activity to synthesize NH_3 under moderate conditions. DFT calculations unveiled that significantly reducing the free energy for the NRR reaction on the defective sites by the creation of surface oxygen vacancies over pristine TiO_2, stabilizing the high potential, determining, and destabilizing the reaction intermediates (*NNH), could efficiently enhance the ammonia yield. Fourier transformed extended X-ray absorbance fine structure (EXAFS) Figure. 14A(b) and Ti K-edge X-ray absorption near-edge structure (XANES) in Figure. 14A(g) further illustrated the rutile and anatase formation in $TiO_2(V_o)$_900 and $TiO_2(V_o)$_800, respectively. Similarly, the ESR Figure. 14A(e) analysis presenting the symmetric distribution in a pair of sharp peaks further corroborate the presence of V_o in all three annealed TiO_2 samples in a well agreement with a V_o signal at $g = 2.003$ as shown in Figure 14A(c), demonstrating the trapping of electron at oxygen vacancies. Fourier-transform infrared (FTIR) spectra indicating a broad band at 3428 cm^{-1} illustrate the existence of bridging surface hydroxyls (i.e., V_o) and/or physiosorbed water in all the cases with the following sequence of peak intensity $TiO_2(V_o)$_800> $TiO_2(V_o)$_900> $TiO_2(V_o)$_700 (Figure 14A(f), being well accredited with the trend of V_o percentage. It could be demonstrated that the

https://doi.org/10.1021/acscatal.3c02410
ACS Catal. 2023, 13, 14415−14453

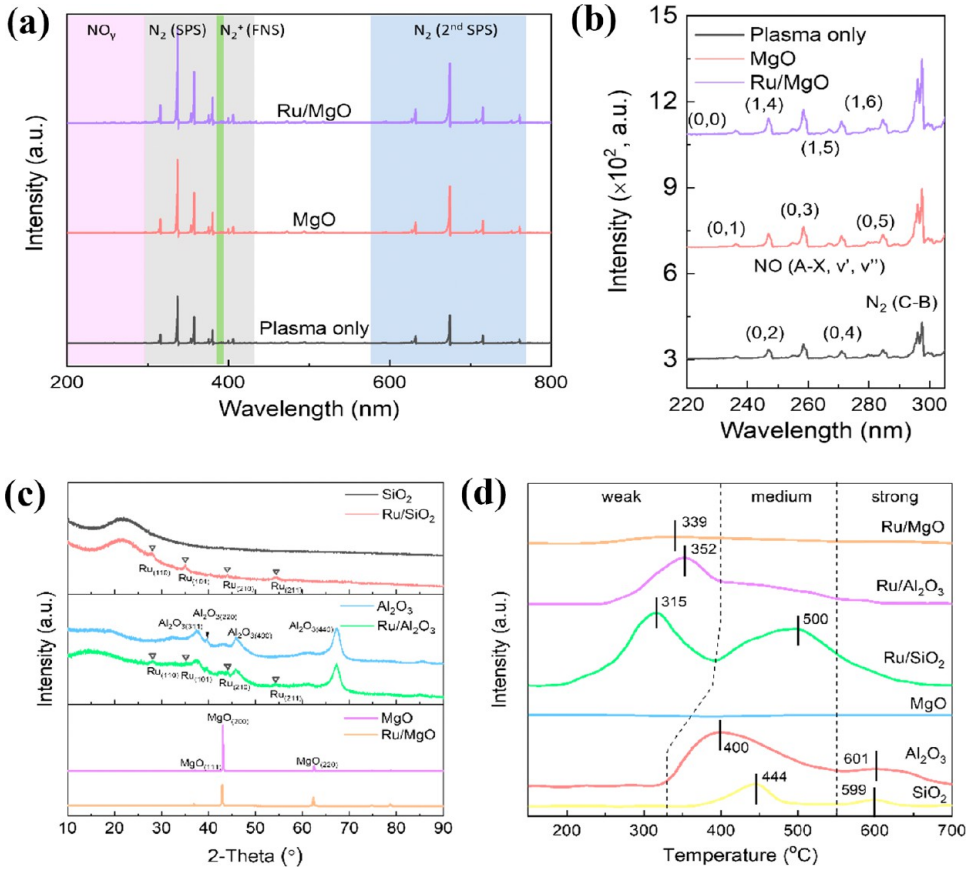

Figure 15. (a) Plasma induced overall OES pattern, (b) emission spectrum, (c) XRD patterns, and (d) NH_3-TPD profiles of different MgO and Ru/MgO packed catalysts, respectively. Reproduced with the permission from ref 167. Copyright 2022 John Wiley and Sons.

readily tuned V_o level of TiO_2 by mediating the annealing temperature, makes it possible to activate the first protonation step and also permits the significantly enhanced N_2 chemisorption (corresponding to *H). An accelerated ASR of ca. 3.0 $\mu g_{NH_3}\, h^{-1}\, mg_{cat.}^{-1}$ was achieved with a FE of 6.5% at −0.12 V (vs. RHE), substantially outperforming the pristine TiO_2, while being capable of maintaining a surprising high FE of 9.8% at a (80 mV) low overpotential.

While another effective way of enhancing the required yield is to dope the TiO_2 with metal heteroatoms of Cu, Zr, V, Fe, or La, where La_2O_3 can perform well as an effective dopant in activating the N_2 reduction electrocatalyst.[364−366] In a recent study by Li and co-workers,[367] vacancy-rich La-doped TiO_2 nanorods were demonstrated as a significant high electrochemical stable catalyst in ambient NH_3 synthesis with a negligible activity decay in 48 h test. Revealing the mechanism by DFT calculations, they found a large ASR of 23.06 $\mu g\, h^{-1}\, mg_{cat.}^{-1}$ and a high FE of 14.54% by optimized La-TiO_2 catalyst at −0.70 V vs RHE in 0.1 M $LiClO_4$. In another strategy of growing Ru NPs on the rutile TiO_2 support by Cai and co-workers[271], a general approach of modulating the binding strength of reactive intermediates was found via interface engineering, demonstrating that the first protonation of N_2 was greatly promoted by the synergistic interaction of electronic coupling between TiO_2 support and Ru NPs. A greatly improved ammonia yield of 10.4 $\mu gNH_3\, h^{-1}\, cm^{-2}$ was achieved at room temperature and ambient pressure via an associative mechanism in the eNRR with a FE of 40.7% at −0.15 V while suppressing the HER, vs RHE in 0.5 M K_2SO_4 aqueous solution. Moreover, a ternary Ru complex hydride being composed of electron-and hydrogen-rich [RuH_6] anionic centers (Li_4RuH_6 and Ba_2RuH_6) was reported by Wang et al.,[368] for a nondissociative eNRR process. The dynamic and synergistic interaction of all the constituents in the ternary complex, transporting the electrons and protons between the centers by hydridic hydrogen and stabilizing the N_xH_y intermediates by the Li/Ba cations, led to the superior activity of ammonia production under mild conditions via promoting an associative reaction mechanism with the perfectly balanced kinetic barriers and narrow energy span in the multistep process. While, Rh could also be inferred to proceed with the excellent NRR activity, generating an N_2H_2 intermediate via a two-electron transfer pathway, which could be subsequently decomposed in the electrolyte to synthesize NH_3. However, Chen et al.[302] recently compared the NH_3 electrosynthesis of Fe supported CNTs electrocatalyst at temperatures below 100 °C directly from water and N_2 at ambient conditions in a flow electrochemical cell, obtaining a stable ASR of 2.2×10^{-3} g $m^{-2}\, h^{-1}$ for 60 h, at under −2.0 V applied potential and a 0.28% FE. The obtained activity was associated with the specific carbon sites (as the main active sites) generated at the interface between CNT and Fe NPs, being capable of activating the N_2 molecule toward hydrogenation. The outperforming ASR and FE values were claimed to be higher than the most reported enhanced rate of noble metals based (Ru/C) of 1.9×10^{-7} g $h^{-1}\, cm^{-2}$ by Kordali and co-workers[74] work under comparable reaction conditions at 20 °C and −1.10 V, maintaining a total high (95.1%) FE with the potential hydrogen gas. While, in a recent study by Yang and

https://doi.org/10.1021/acscatal.3c02410
ACS Catal. 2023, 13, 14415−14453

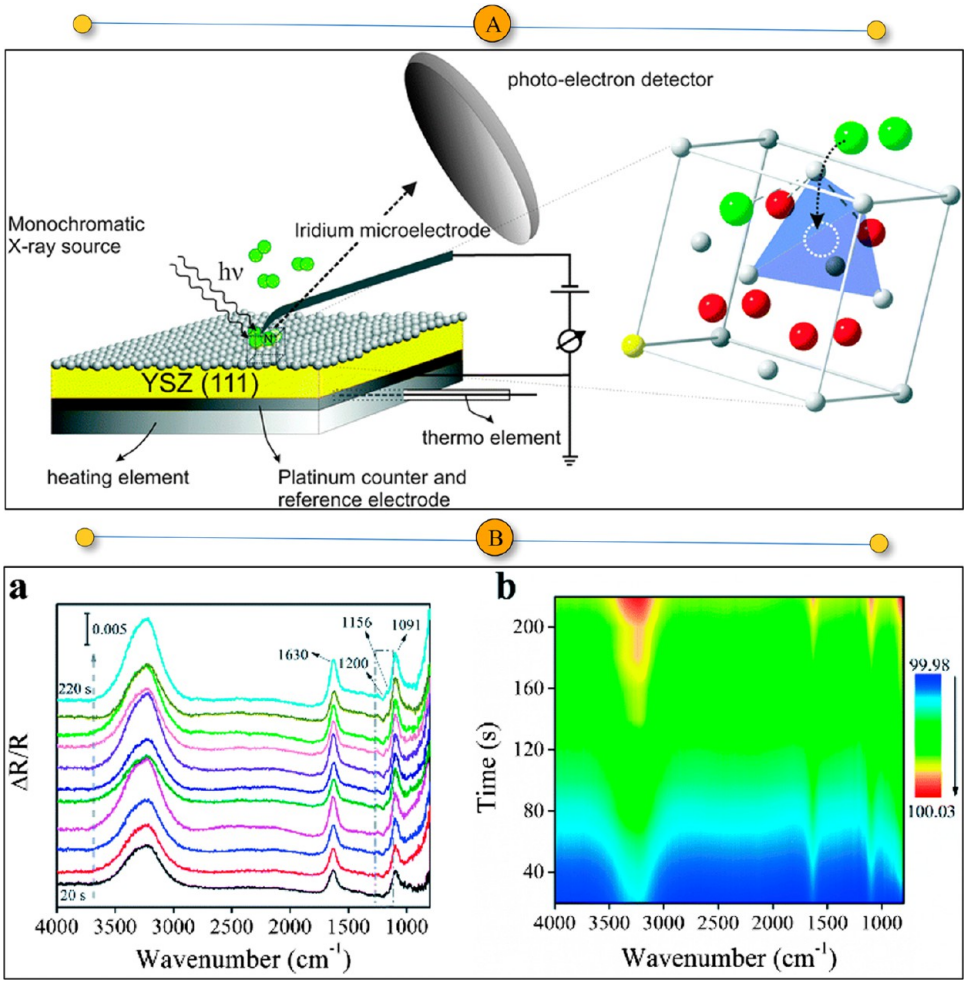

Figure 16. (A) Cell arrangement of in situ XPS experiments. Reproduced with the permission from ref 369. Copyright 2011 Royal Society of Chemistry. (B) In situ electrochemical-FTIR spectra on the Ni−Fe−MoS_2 NC catalyst. Reproduced with the permission from ref 370. Copyright 2020 Royal Society of Chemistry.

co-workers,[85] vanadium nitride (VN) NPs were found to be active and stable eNRR catalysts with 6.0% FE and an eNRR rate of 3.3×10^{-10} mol s^{-1} cm^{-2} and at −0.1 V within 1 h, maintaining an ASR of 1.1×10^{-10} mol $^{s-1}$ cm^{-2} for 116 h, with a steady-state turnover number of 43182. A Mars−van Krevelen mechanism eNRR was followed by $^{15}N_2$ as the feed to give both $^{14}NH_3$ and $^{15}NH_3$, where the $VN_{0.7}O_{0.45}$ species investigated by Ex situ XPS and Operando XAS were found to be the governing factors of catalyst deactivation. Meanwhile, the advances of Spectro electrochemical cells with the help of in situ time-resolved studies such as surface X-ray scattering technique would make a feasible approach of illustrating the structural changes of electrode surface or dynamic motions of microstructures, providing deep insight into active reaction sites accompanying the NRR activity. Meanwhile, the deployment of optical emission spectra (OES) indicated that the hydrogen-rich environment of larger Ni particle size, could lower the ASR due to substantial surface coverage by hydrogen (Figure 15.[167] Since, the higher TOF (s^{-1}) were obtained by NPs (Ni/SiO_2−SOG ∼ 5.6 nm), resulting in a higher ASR of 109.3 μmol min^{-1} g-cat^{-1} than that of the Ni bulk and other larger nanoparticle size catalysts and at equimolar composition with 7.92 g-NH_3/kWh energy yield.

By adopting in situ XPS, Valov and co-workers[369] manifested that N_2 can be activated electrochemically at the junction between an iridium microelectrode, the reactant molecule N_2, and yttria stabilized zirconia electrolyte (YSZ, (111)-oriented) at a temperature of 450 °C,10^{-5} Pa pressure and more negative (E = −1.25 V) potentials (Figure 16A). Similarly, deeper analysis of the possible active species and reaction routes can be probed by in situ XPS investigations while illustrating the adsorbed intermediate species and valence states. An associative alternating mechanism was deduced by Zeng et al.[370] by exploring the in situ FTIR studies for NiFe-MoS_2 nano cubes working at −0.3 V vs. RHE in 0.1 M Na_2SO_4 solution, where the two negative-going peaks located at 1156 and 1200 cm^{-1} were assigned to the NH_2 rocking vibration and N−H stretching modes (Figure 16B), respectively. In situ electrochemical TEM as a powerful emerging technique with some technical advances, could further provide a unique possibility of interpreting the atomic scale morphological and microstructural deviations in NRR reactions.[342] Direct experimental evidence of particle size effect in cold plasma NH_3 synthesis at ambient conditions was provided for the first time by Gorky et al.[270] by applying DBD plasma over silica supported Ni NPs by surface organometallic grafting (Ni/SiO_2−SOG). The existence of various synergistic interactions between metal NPs and plasma generated species (such as the hydrogen sink behavior of Ni) was helpful in

https://doi.org/10.1021/acscatal.3c02410
ACS Catal. 2023, 13, 14415−14453

dictating the ammonia synthesis rate under equimolar plasma gas phase compositions.

5.0. Ammonia as an Energy Vector and the Techno-Economic Viability of Its Green Alternatives. Recalling that as an essential element of society, ammonia can be adopted as a fundamental building block in every aspect of life from fertilizer to the manufacturing of plastics, explosives, dyes, fabrics, refrigerant, stabilizer, neutralizer, purifier in food transport, water treatment applications, pharmaceuticals and a vital source of energy carrier.[25−27] Synthetic ammonia is one of the most produced chemical products in the world, where its high-value utilization also requires a growing impetus for a highly energy-efficient catalytic process and hybrid system. Switching to renewable electricity for green ammonia is the main window of combating the twin challenges of the 21st century's environmental issues that could save over 360 million tons per year of carbon dioxide worldwide. It is an essential raw material in modern society as a promising carbon-free energy vector, where its future large-scale synthesis and utilization will be continued, as a never-ending story. H_2 is considered an efficient energy carrier because of its abundance, high energy density, zero emission and ubiquity; however, economical, safe, effective, and regulated storage of hydrogen in bulk is expensive and difficult, requiring the special need of high-pressure cylinders or cryogenic tanks in the narrative toward a low-carbon economy. Furthermore, its compression and liquefaction also consume much energy due to its low boiling point and relatively large compressibility factor. Ammonia is cheaper, easier to store and transport, readily "cracked", purified to on-site production of hydrogen, and contains 50% more H_2 upon liquefaction by volume than liquid hydrogen, all of which can be adopted as the long-distance transportation carriers of high energy densities. Ammonia as an energy vector and hydrogen carrier could be converted back into different downstream products or simply could be adopted in the flowing way of energy derivatives:

- Direct fuel for -fuel cells and internal combustion engines/turbines
- Hydrogen carrier
- Energy storage
- Energy transportation
- Feedstock for chemical processes
- Direct agricultural application
- Production of nitrogen-based fertilizers

5.1. The Clean, Green Hydrogen Fuel Cell. Ammonia can be adopted as a practical hydrogen energy vector and its pre-existing industry infrastructure is occupying the market to kick-start the hydrogen economy, producing, storing, and trading millions of tons of ammonia every year.[371] It can combat climate change by controlling the challenges (political commitment, economical storage, and safety concerns) that currently impede the realization of the full potential of hydrogen gas as a clean fuel. The economic viability of green ammonia is bright, possessing the lowest source-to-tank cost (up to USD$4.50/gasoline gallon equivalent) in terms of energy content among the fuels produced from renewable resources.[372] As an energy or hydrogen source carrier, ammonia mainly includes three aspects: green synthesis of ammonia; separation, storage and transportation of ammonia; and utilization and conversion of ammonia.[373,374] In recent years, it has been deployed by many governments, research institutions, and well-known enterprises, with various new methods, progresses, and new materials. Adopting ammonia as a fertilizer is one possibility, but turning it into electrical or thermal energy is more captivating. Ammonia is thermally decomposed to release hydrogen gas for energy generation via two paths of catalytically cracking ammonia to produce hydrogen for use in fuel cells or directly using it by eliminating the intermediate process of converting ammonia into hydrogen. As a H_2-rich (17.6% content) compound, it can be used as a raw material for hydrogen production in fuel cells, while as a zero-carbon-emission fuel (only producing water and dinitrogen upon complete combustion), it dominates the significant advantages over H_2. An ammonia fuel cell (operating with ammonia and oxygen gas or air) is a power generation device that can directly convert the chemical energy contained in fuel to electrical energy. The required chemical raw materials are supplied from the outside and are not stored inside the battery, because ammonia has high hydrogen content, high energy density, and simple reforming hydrogen production device, which surpass the other derivatives which contain CO_x as a serious issue of fuel cell poisoning.

Ammonia could also be deployed directly in some applications without further processing, where high efficiencies are desired by liquid hydrogen or synthetic hydrocarbons such as solid oxide fuel cells (SOFCs).[375,376] It can be fed directly to the anode in an SOFC, where the high temperature conditions (700−900 °C) effectively crack the ammonia molecule into its constituent elements before the oxidation of H_2 into water.[374] NH_3 decomposition catalysts with new advanced SOFCs and novel solid-state electrolytes can develop durable and high-performance direct ammonia SOFCs, where its power generation efficiency could be higher than that of H_2−SOFC and liquid electrolytes in the temperature range of 400−900 °C. Recent developments have significantly enhanced the cell efficiency and durability, as compared to that of hydrogen fuel cells.[377] The synthesis and decomposition of ammonia which often sharing a rate-determining step are composed of a similar reaction appearing in opposite directions via the adsorption/desorption of dinitrogen at different reaction conditions. However, it is also noteworthy that an ideal catalyst for NH_3 synthesis may not be appropriate in reverse for the decomposition reaction, for the different reaction species and their relative concentrations on the catalyst surface present in both (forward and reverse) cases.[378] Since, the traditional ammonia cracking/decomposition reaction is highly endothermic, critically achieving at 600−950 °C and maintaining at high flow rates with inexpensive materials such as iron or nickel catalyst. Although the decomposition with the most active Ru-based catalysts doped with K, Ba and Cs supported on various oxides and carbon supports may obtain an appropriate H_2 production rate at temperatures higher than 500 °C, however, it could be influenced by the change in reaction condition. The progress in the category of abundant and cheaper materials (such as $NaNH_2$-based ammonia cracking systems) may promote the adaptation of ammonia in sustainable energy storage purposes. However, owing to the nature of catalytic material, the variation in the rate-limiting step, the nature of the support and promoters and the geometry of active sites may prompt a new definition of complex intermediates, leading to the unfavorable reaction routes. Different reaction mechanisms have been proposed on various transition metals for the decomposition of NH_3, approaching advanced characterization techniques and theoretical bases for future catalyst design, integrating with electronic ideal supports and

https://doi.org/10.1021/acscatal.3c02410
ACS Catal. 2023, 13, 14415−14453

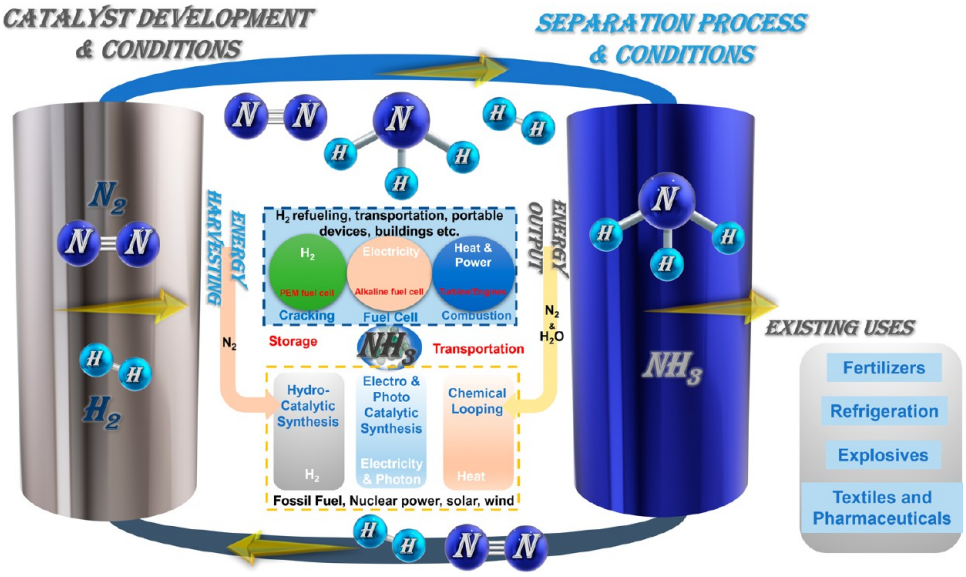

Figure 17. Ammonia decomposition and restoration schemes into variable derivatives reproduced with permission from refs 378 and 385. Copyright 2021 and 2017 Elsevier, respectively.

catalytic promoters. Since, the lower temperature (400−600 °C) decomposition currently involves the active research and innovation programs based on amide ($-NH_2$) and imide ($-NH$) materials or advanced metallic monolith catalyst support to replace the rare-metal catalysts, showing significant promises in reducing the energy costs, and achieving admirable NH_3 cracking by optimizing pressure drop at high flow rates.[379] The $Na/NaNH_2$ system using a simple flow reactor in variable-temperature NH_3 decomposition experiments, shows superior catalytic activity of producing onsite hydrogen on the supported Ni and Ru catalysts, reaching a decomposition efficiency of 99.2% at 530 °C, adopting only 0.5 g of $NaNH_2$ in a 60 sccm NH_3 flow.[380]

While it could also be implemented indirectly by integrating proton-exchange membrane fuel cell (PEMFC) stacks with NH_3 decomposition reactors into a compact system that works with some metal based NH_3-decomposition catalyst, thus reducing the huge amount of heat supply.[381] However, several approaches being developed in electrochemical and photochemical NH_3 decomposition for hydrogen production, require significant consideration in the postcracking purification for obtaining a usable H_2 stream before utilizing it in PEMFC.[12] Moreover, recycling the tail gas from PEMFC for heating, NH_3 decomposition is an effective pathway for better heat integration, lower cost power generation and vehicle application, where the carbon-free PEMFC systems integrated with NH_3 decomposition reactors could be highly competitive in both energy efficiency and economic feasibility than those gasoline-fueled heat engines, indirect methanol PEMFC or H_2-fueled PEMFC systems. In the indirect ammonia supply fuel cell system, ammonia is first catalytically decomposed into hydrogen and nitrogen through the reforming device: $2NH_3 \rightarrow N_2+3H_2$, and then, the hydrogen is supplied to the fuel cell. The ammonia decomposition hydrogen production device is simple, efficient, low-cost, and easy to carry, where it only needs to add a reformer at the inlet of the fuel cell to achieve ammonia decomposition. In addition to developing a fast and efficient ammonia decomposition catalyst system, the length of the insulated metal tube equipped with a spherical catalyst can also be appropriately increased to promote full contact between ammonia and the catalyst, thereby improving the efficiency of ammonia decomposition to produce hydrogen. Therefore, ammonia is particularly suitable as a hydrogen supply carrier for fuel cells and is widely used in new energy vehicles. However, the high operating temperature of SOFCs (550−900 °C) may only be suitable for continuous stationary applications that do not require frequent switching. Therefore, SOFC can be used in heavy-duty vehicles, such as aviation, shipping, trucking, etc. In addition, the SOFC anode material responsible for catalytically decomposing ammonia into hydrogen should be stable, durable and high-temperature resistant during continuous operation. However, the degradation of anode materials is still a major obstacle to SOFC commercialization. Further improvements in SOFC and ammonia decomposition technology are necessary to realize such a concept. At present, the efficiency and power density of direct ammonia fuel cells are not ideal. In addition, for environmental protection considerations, the exhaust gas generated needs to be processed to concentrate and recover the residual ammonia. The additional heat exchange devices required by this process increase the complexity of the system. The aim of creating a unique infrastructure that supports the sustainable and cost-efficient approach of treating both the ample amount of generated carbon wastes (CO_2) and the renewable hydrogen attained in ammonia industry to the sustainable synthetic aviation fuels would further contribute toward the decarbonization of the full transport system. Targeting the development of disruptive technologies by overriding the idea of combining CO_2 emissions with sustainable H_2 could follow the spirit of circular economy for generating the next generation synthetic fuels by integrating advanced catalytic technologies as described in the themed picture of this article. The flexible scalability of these technologies will allow their implementation in decentralized processing plants, thus favoring flexibility for production cycles within a circular economy concept.

5.2. Ammonia Energy as a Fuel for Vehicles and Internal Combustion Engines/Turbines System. Ammonia is a carbon-free compound that only produces water, nitrogen and a small amount of nitrogen oxides when burned,

https://doi.org/10.1021/acscatal.3c02410
ACS Catal. 2023, 13, 14415−14453

since it can be easily adopted as a clean energy source to replace fossil fuels as its energy density is higher than that of gasoline, methanol, and other fuels.[382,383] With the easier ways of handling and shipping, it can replace the fuel oil-based systems in decarbonizing the existing uses to a medium of transport fuel (such as hydrogen or ammonia-hydrogen mixture) to release energy in a fuel cell by chemical reaction with oxygen or release energy in direct combustion engine, containing the only byproducts of water and nitrogen. The synthesis, storage, transportation, and transformation of NH_3 in a cyclic manner shown in Figure 17 illustrated that it could be integrated well in the hydrogen energy regime. Although its calorific value is about half that of gasoline, it has a high-octane number; being easily compressed and liquefied, it makes convenient and safe storage and transportation. Taken together, it is of practical significance for ammonia fuel to replace fossil energy in automobile engines. It has excellent antiknock performance that can save fuel while increasing the engine's output power. In the past few decades, many countries have conducted research on the feasibility of ammonia as an internal combustion engine fuel, giving considerable positive results.[384] Since ammonia has a high minimum ignition limit and slow combustion speed, it is usually necessary to use combustion accelerants such as acetylene, dimethyl ether, diesel, hydrogen, etc. when used as vehicle fuel. In existing automobile systems that use ammonia as the engine fuel, part of the ammonia will generate hydrogen through the action of a catalyst in the bypass system. After forming an ammonia-hydrogen mixed fuel with ammonia in the main system, it will enter the engine cylinder and be burned to achieve cracking hydrogen ignition. Burning ammonia fuel can improve engine combustion performance and reduce exhaust emissions, where the hydrogen and nitrogen produced after the catalytic cracking of ammonia are mixed and burned with ammonia. As a fossil alternative fuel with great potential, methyl ether has better combustion performance and is more suitable for internal combustion engines; however, its high cost hinders its large-scale promotion. Mixing liquid ammonia and methyl ether with similar densities to make fuel can not only achieve complementary combustion performance of the two but also reduce fuel costs. Currently, the Russian engine manufacturer Energomash is developing a new rocket engine that uses an ammonia-acetylene mixture as fuel, aiming to greatly reduce the cost of rocket launches and greatly improve the efficiency of the engine.

Conventional internal combustion engines running on ammonia require only minor modifications, such as changing the compression ratio and replacing fuel line materials to avoid corrosion. Compression ignition is the ideal approach when running ammonia in a dual-fuel engine with a lower autoignition temperature such as diesel, dimethyl ether, or biodiesel. Due to the high fuel nitrogen content in ammonia and the influence of clearance volume, relatively high levels of unburned ammonia and NO_X are prevalent in the exhaust gas of ammonia-doped dual-fuel engines.[382,386] Therefore, a selective catalytic reduction (SCR) post-treatment system is very necessary. The application of ammonia in gas turbines is also the most widely studied factor, including pure combustion of ammonia, mixed combustion of ammonia and hydrogen, and mixed combustion of ammonia and methane. Since, the future development of new ammonia-fueled low-nitrogen gas turbines may have the following technical application directions of staged combustion or rich-lean combustion; air preheating; higher pressure; flue gas recirculation, and staged flue gas recirculation. Similarly, ammonia usually needs to be cofired with coal in power station boilers, where all ammonia can be injected from the side wall, with the NO_X emissions in the gas equivalent to those when pulverized coal is burned alone. At present, the scale of the coal-fired boiler mixed with ammonia in the laboratory has reached 1.2MW, and the mixing ratio of ammonia is close to 50%, which is basically close to the industrial application level. In gas boilers, the lowest emission performance of 205 mg/Nm^3 NO_X and 76 mg/Nm^3 NH_3 has been achieved when pure ammonia is burned through flameless combustion technology.[383] In many uncontrollable factors during the actual combustion process, it is often difficult to avoid the generation of nitrogen oxides during ammonia combustion; therefore, treating the exhaust gas is the main challenge facing ammonia as an engine fuel. Mastering the reaction mechanism and kinetic process of mixed combustion of ammonia and various ignition aids, analyzing the formation path and treatment technology of nitrogen oxide compounds in exhaust gas, and the characteristics of various engine exhaust gases are the focus of future research on ammonia as an automobile engine fuel.

5.3. Agricultural, Industrial, and Other Different Usage. Ammonia as a rich source of nitrogen and the feedstock of ammonium nitrate, ammonium salts, and urea is usually adopted in fertilizers, antifungal agent for different foods, or facilitate in the preservation. It is also used as a neutralizer and stabilizer, applied in the treatment of wastewater, beverage, food industries, fermentation process, rubber, leather, cold storage, refrigeration system, cosmetics, and in the creation of pharmaceutical products. Being easily refrigerated to −33 °C and stored in bulk at modest pressures (10−15 bar) as a liquid, it can be adopted as an ideal chemical store for utilization in renewable energy as a transport vector and successive retransformation to the value-added routes through absorption with water/liquid to gas phase changes or solid-to-solid phase transformations. It also facilitates the manufacturing of various compounds such as nitric acid, hydrogen cyanide, ammonium carbonate, amino acids, phenol, etc. Its dissociated forms are commonly engaged in different operations of atomic hydrogen welding, furnace brazing, sintering, nitriding, carbo nitriding, and bright annealing. It is usually adopted in antiseptics or antimicrobial agents, various household cleaning products, extracting different metals, or as an anticorrosion agent for petroleum and mining industries for counterbalancing acid constituents of crude oil.

5.4. Challenges and Prospects in the Targeted Development of NH_3 as a Potential Nitrogen Derivative. The growing interest in the adoption of NH_3 as an energy carrier revives a new platform of exploring advanced strategies in profitable business avenues. However, the long route of completely decarbonizing the brown ammonia pathways or adopting an H−B free ammonia, may take at least one or two decades for the commercial scale adaption of any promising lab-scale reaction, regardless of its initial pathway (electro/photo/bio or plasma catalysts system). Most of the ammonia production units working on the narrative of green ammonia still endorsed the energy intensive (H−B) means to some extent for generating the molecule, encountering the reaction pathway of high temperatures and pressures in combining N_2 and H_2 gas over an Fe catalyst. The retrieval and decarbonizing of the rigorous (brown) ammonia regime to the sustainable avenues would be an efficient approach of finding the short-

https://doi.org/10.1021/acscatal.3c02410
ACS Catal. 2023, 13, 14415−14453

term solutions, where it can be effectively combined with current renewable energy technologies of H−B. However, the entire game must be diverted in a decent way to supply the required energy demand per metric ton of ammonia for the long-term goals of improving the sustainability of ammonia synthesis. A supposed current eHB process coupled with the often-low price of natural gas may attract attention in some modes, but the serious economic concerns of its initial high capital investment of H_2O electrolysis weakens the rest of the features of this approach. The intermittency of the power supply and utilizing the renewable power sources for electrifying the synthesis units in islanded regions carries its own operational issues, thus demanding careful consideration in the proposed plant design strategies. The field of advanced ammonia synthesis catalysts is still at the immature stages for replacing the existing inefficient catalysts. The anticipated approach of green ammonia synthesis from the sustainable energy platforms requires a holistic approach of considering both the reaction and separation strategies. The perspective synthesis means critiques the current improvement in terms of key metrics and the mechanistic discussions with advanced experimental methodology, and catalyst selection, deducing that the solutions must go with some combination of the protocol for rigorous experimentation, while suppressing the unfavorable HER reactions. The catalyst lifetime or stability is another summon to be clearly addressed for the excellent NH_3 synthesis regime, requiring an efficient and practical candidate in an electrochemical device with satisfactory stable performance. The challenging task of maintaining the high NH_3 productivity at industrially useful rates while surpassing the extremely stable N≡N triple bond (941 kJ mol^{-1}) in the presence of the easily reduced species and integrating the appropriate supply of H_2 in electrolysis with N_2 at ambient pressure in H_2O, requires the uttermost long chain of energy. Usually, the maximum H_2 pressure attained in H_2O electrolysis is relatively low (<20 bar), where the limiting principal target for process innovations constrained the NH_3 synthesis rate imposed by the thermodynamic and practical limitations in terms of unfavorable kinetics, strong thermodynamic barrier, reaction equilibrium and separation characteristics in lower operating pressures. Although the membrane in proton-exchange membrane fuel cells could be damaged or poisoned with certain contaminants of NH_3 traces, they are encountered in the process of deriving hydrogen from ammonia. Therefore, the purification or separation techniques for nominating NH_3 as the efficient H_2 carrier are critically important in rigorously mitigating the NH_3 concentration level below 1 ppm in the H_2 stream. The other designated N_2 contaminants such as nitrites and nitrates indulging the interactions with NH_3 concentrations and affecting the false positives or standardize eNRR, need the progressive establishment of benchmarking protocols for determining and eliminating the contamination sources. Moreover, conventional condensation, absorption, or separation technologies in view of the lower operating pressure limits on the catalyst, need an efficient catalyst design of operating at moderate pressures (10−30 bar). Membrane separation and effective sorbents would be further required to address the crucial removal of hydrogen and ammonia at these conditions.

Keeping in view of the intensive utilization (80%) of ammonia in fertilizers likely to be increased to ∼270 million tons per year by 2050, the current predictive analysis combined with the requirement of decarbonizing the H−B process reflects that these carbon-intensive means of industrial NH_3 production must be sorted through significant greener alternatives. The conventional synthesis route direly needs to be replaced by the new green horizons of environmentally friendly ammonia via overcoming the major challenges of low-cost sustainable approaches of hydrogen and nitrogen resources at industrial scale. However, the main determinants of the large-scale application prospects of green ammonia include the production cost of green ammonia and the maturity of application technology.[34] The manufacturing costs of green ammonia are usually influenced by plant location, size, (such as islanded, semi-islanded, and (or) variable renewable energy), the cost of distribution, and storage. Where, the production of hydrogen is a major component of ammonia production costs for dominating the both capital and operating costs (due to power consumption by the electrolyzer).[387] The H−B process based on electrolysis to synthesize green ammonia has relatively mature operating experience, where the production cost of hydrogen accounts for about 45% of the cost of electrolytic ammonia production. While the carbon intensive H−B process may have low net energy consumption, the main advantage and significance lies in "zero carbon", thus strengthening the environmental benefits of green ammonia's lifecycles. Since harnessing the low-carbon narrative by deploying some low-cost renewable (electrifying, solar, or wind) means would efficiently mutate those exhaustive carbon emissions. The possible tactics include the following: powering the reaction with renewable sources; conventionally manufacturing it with the desolation of CO_2; generating H_2 without fossil fuels in a modified small-scale H−B units by water electrification (wind, solar, and tidal wave, etc.); and adapting the efficient renewable production strategies by electro, photo, bio, or plasma catalysis, could pave their way in finding an imperatively decent route than conventional H−B. The diversity in the ammonia synthesis sector would fantastically grow quickly with the formulation of those new smart integrated plants with notable potential for rationally concerning the dramatical reducing costs by renewable energies.

In summary, ammonia, as a clean and renewable energy source with obvious advantages and broad prospects, can be directly burned in vehicle engines to provide energy and can also be used as a raw material gas for vehicle-mounted fuel cells. As a new approach, it technically puts forward higher requirements on the catalyst system: it needs to show higher catalytic activity at lower temperatures. This is directly related to the practical significance and economic benefits of ammonia as a vehicle fuel and determines the development of an ammonia decomposition reaction generator. Reducing costs, increasing efficiency, scaling up production, and expanding the pipeline infrastructure are critical for new applications and expected increased demand. Developing new methodologies for rational catalytic synthesis methods, advancement in reactor designs, and separation strategies could improve ammonia production efficiency and reduce costs, addressing the environmental and safety challenges associated with ammonia combustion, including the development and testing methods to reduce nitrogen oxide emissions. As energy carrier and fuel applications, common standards and specifications could be introduced in terms of equipment specifications, certification and accreditation, and safety requirements to further strengthen the development trend of hydrogen-ammonia linkage integration. In conclusion, developing the sustainable synthesis of nitrogen-based energy carriers such as

https://doi.org/10.1021/acscatal.3c02410
ACS Catal. 2023, 13, 14415−14453

"green" NH_3, is an environmental imperative of net-zero carbon emissions. The diversity in the ammonia synthesis sector would fantastically grow quickly with the formulation of those new smart integrated plants with notable potential for rationally concerning the dramatic reduction of costs by renewable energies. The systematic analysis of highly appealing and natural integration with renewable energy sources routes outlined above can work well under mild conditions for aspiring nitrogen derivatives (especially ammonia). However, further new strategies in developing advanced synthesis, storage, conversion, utilization, and transport systems should continually thrive for long-term applications of decarbonized commodities and energy vectors. While ammonia surely will not be the best solution for everything, it has a role to play in getting to net zero, alongside biofuels and hydrogen. Since, no matter which specific direction things go, observers expect the green ammonia market to ramp up quickly.

AUTHOR INFORMATION

Corresponding Authors

Muhammad Asif Nawaz − *Department of Inorganic Chemistry and Materials Sciences Institute, University of Seville-CSIC, 41092 Seville, Spain; Henan International Joint Laboratory of Nano-Photoelectric Magnetic Materials, Henan University of Technology, Henan, Zhengzhou 450001, China;* orcid.org/0000-0003-3234-031X; Email: mnawaz@us.es

J. A. Odriozola − *Department of Inorganic Chemistry and Materials Sciences Institute, University of Seville-CSIC, 41092 Seville, Spain;* orcid.org/0000-0002-8283-0459; Email: odrio@us.es

Authors

Rubén Blay-Roger − *Department of Inorganic Chemistry and Materials Sciences Institute, University of Seville-CSIC, 41092 Seville, Spain*

Maria Saif − *Department of Inorganic Chemistry and Materials Sciences Institute, University of Seville-CSIC, 41092 Seville, Spain*

Fanhui Meng − *State Key Laboratory of Clean and Efficient Coal Utilization, Taiyuan University of Technology, 030024 Shanxi, Taiyuan, China;* orcid.org/0000-0003-0998-5179

J. González-Arias − *Department of Inorganic Chemistry and Materials Sciences Institute, University of Seville-CSIC, 41092 Seville, Spain*

Baoji Miao − *Henan International Joint Laboratory of Nano-Photoelectric Magnetic Materials, Henan University of Technology, Henan, Zhengzhou 450001, China*

Luis F. Bobadilla − *Department of Inorganic Chemistry and Materials Sciences Institute, University of Seville-CSIC, 41092 Seville, Spain;* orcid.org/0000-0003-0085-9811

Tomas Ramirez-Reina − *Department of Inorganic Chemistry and Materials Sciences Institute, University of Seville-CSIC, 41092 Seville, Spain;* orcid.org/0000-0001-9693-5107

Complete contact information is available at: https://pubs.acs.org/10.1021/acscatal.3c02410

Notes

The authors declare no competing financial interest.

ACKNOWLEDGMENTS

This work has been supported by the Spanish Ministry of Science through the projects NICER-BIOFUELS (ref: PLEC2021-008086), sponsored by MCIN/AEI/10.13039/501100011033 Next Generation Europe, & SMART-FTS (ref: PID2021-126876OB-I00), and also sponsored by the Key Scientific Research project of Colleges and Universities in Henan Province (21A430009) & (222103810045). Authors also pay thanks to "Macrovector/Freepik" for providing the services in designing the TOC graphics. The authors declare no competing interests

REFERENCES

(1) Rosca, V.; Duca, M.; de Groot, M. T.; Koper, M. T. Nitrogen cycle electrocatalysis. *Chem. Rev.* **2009**, *109*, 2209−2244.

(2) Suryanto, B. H. R.; Du, H.-L.; Wang, D.; Chen, J.; Simonov, A. N.; MacFarlane, D. R. Challenges and prospects in the catalysis of electroreduction of nitrogen to ammonia, Nature. *Catalysis* **2019**, *2*, 290−296.

(3) Ristig, S.; Poschmann, M.; Folke, J.; Gómez-Cápiro, O.; Chen, Z.; Sanchez-Bastardo, N.; Schlögl, R.; Heumann, S.; Ruland, H. Ammonia Decomposition in the Process Chain for a Renewable Hydrogen Supply. *Chemie Ingenieur Technik* **2022**, *94*, 1413−1425.

(4) Schlögl, R. Catalytic Synthesis of Ammonia—A "Never-Ending Story"? *Angew. Chem., Int. Ed.* **2003**, *42*, 2004−2008.

(5) Ashida, Y.; Arashiba, K.; Nakajima, K.; Nishibayashi, Y. Molybdenum-catalysed ammonia production with samarium diiodide and alcohols or water. *Nature* **2019**, *568*, 536−540.

(6) Avenier, P.; Taoufik, M.; Lesage, A.; Solans-Monfort, X.; Baudouin, A.; de Mallmann, A.; Veyre, L.; Basset, J.-M.; Eisenstein, O.; Emsley, L.; Quadrelli, E. A. Dinitrogen Dissociation on an Isolated Surface Tantalum Atom. *Science* **2007**, *317*, 1056−1060.

(7) Wang, Y.; Meyer, T. J. A Route to Renewable Energy Triggered by the Haber-Bosch Process. *Chem.* **2019**, *5*, 496−497.

(8) Smil, V. Detonator of the population explosion. *Nature* **1999**, *400*, 415−415.

(9) Howarth, R. W. Coastal nitrogen pollution: a review of sources and trends globally and regionally. *Harmful algae* **2008**, *8*, 14−20.

(10) Čorić, I.; Mercado, B. Q.; Bill, E.; Vinyard, D. J.; Holland, P. L. Binding of dinitrogen to an iron−sulfur−carbon site. *Nature* **2015**, *526*, 96−99.

(11) Erisman, J. W.; Sutton, M. A.; Galloway, J.; Klimont, Z.; Winiwarter, W. How a century of ammonia synthesis changed the world. *Nature Geoscience* **2008**, *1*, 636−639.

(12) Guo, J.; Chen, P. Catalyst: NH3 as an Energy Carrier. *Chem.* **2017**, *3*, 709−712.

(13) Malmali, M.; Wei, Y.; McCormick, A.; Cussler, E. L. Ammonia Synthesis at Reduced Pressure via Reactive Separation. *Ind. Eng. Chem. Res.* **2016**, *55*, 8922−8932.

(14) Ye, L.; Nayak-Luke, R.; Bañares-Alcántara, R.; Tsang, E. Reaction: "Green" Ammonia Production. *Chem.* **2017**, *3*, 712−714.

(15) Foster, S. L.; Bakovic, S. I. P.; Duda, R. D.; Maheshwari, S.; Milton, R. D.; Minteer, S. D.; Janik, M. J.; Renner, J. N.; Greenlee, L. F. Catalysts for nitrogen reduction to ammonia. *Nature Catalysis* **2018**, *1*, 490−500.

(16) Tang, C.; Qiao, S.-Z. How to explore ambient electrocatalytic nitrogen reduction reliably and insightfully. *Chem. Soc. Rev.* **2019**, *48*, 3166−3180.

(17) Zhu, X.; Imtiaz, Q.; Donat, F.; Müller, C. R.; Li, F. Chemical looping beyond combustion − a perspective. *Energy Environ. Sci.* **2020**, *13*, 772−804.

(18) Mao, C.; Wang, J.; Zou, Y.; Shi, Y.; Viasus, C. J.; Loh, J. Y. Y.; Xia, M.; Ji, S.; Li, M.; Shang, H.; Ghoussoub, M.; Xu, Y.-F.; Ye, J.; Li, Z.; Kherani, N. P.; Zheng, L.; Liu, Y.; Zhang, L.; Ozin, G. A. Photochemical Acceleration of Ammonia Production by Pt1-Ptn-TiN Reduction and N2 Activation. *J. Am. Chem. Soc.* **2023**, *145*, 13134−13146.

(19) Marakatti, V. S.; Gaigneaux, E. M. *Recent Advances in Heterogeneous Catalysis for Ammonia Synthesis* **2020**, *12*, 5838−5857.
(20) Qi, D.; Lv, F.; Wei, T.; Jin, M.; Meng, G.; Zhang, S.; Liu, Q.; Liu, W.; Ma, D.; Hamdy, M. S.; Luo, J.; Liu, X. *High-efficiency electrocatalytic NO reduction to NH3 by nanoporous VN, Nano Research Energy* **2022**, *1*, No. e9120022.
(21) Jiao, F.; Xu, B. Electrochemical Ammonia Synthesis and Ammonia Fuel Cells. *Advanced Materials* **2019**, *31*, No. 1805173.
(22) Zhao, Y.; Setzler, B. P.; Wang, J.; Nash, J.; Wang, T.; Xu, B.; Yan, Y. An Efficient Direct Ammonia Fuel Cell for Affordable Carbon-Neutral Transportation. *Joule* **2019**, *3*, 2472−2484.
(23) Medford, A. J.; Hatzell, M. C. Photon-driven nitrogen fixation: current progress, thermodynamic considerations, and future outlook. *ACS Catal.* **2017**, *7*, 2624−2643.
(24) Kandemir, T.; Schuster, M. E.; Senyshyn, A.; Behrens, M.; Schlögl, R. Haber−Bosch Process Revisited: On the Real Structure and Stability of "Ammonia Iron" under Working Conditions. *Angew Chem. Int. Ed.* **2013**, *52*, 12723−12726.
(25) Xu, Y.; Liu, X.; Cao, N.; Xu, X.; Bi, L. Defect engineering for electrocatalytic nitrogen reduction reaction at ambient conditions. *Sustainable Materials and Technologies* **2021**, *27*, No. e00229.
(26) Li, X.; Fan, W.; Xu, D.; Ding, J.; Bai, H.; Shi, W. Boosted Photoelectrochemical N2 Reduction over Mo2C In Situ Coated with Graphitized Carbon. *Langmuir* **2020**, *36*, 14802−14810.
(27) Peng, W.; Feng, Y.; Yan, X.; Hou, F.; Wang, L.; Liang, J. Multiatom Catalysts for Energy-Related Electrocatalysis. *Advanced Sustainable Systems* **2021**, *5*, No. 2000213.
(28) Smil, V. *Enriching the Earth: Fritz Haber, Carl Bosch, and the Transformation of World Food Production*; The MIT Press 2000.
(29) Guo, J.; Chen, P. Ammonia history in the making. *Nature Catalysis* **2021**, *4*, 734−735.
(30) Giddey, S.; Badwal, S. P. S.; Munnings, C.; Dolan, M. Ammonia as a Renewable Energy Transportation Media. *ACS Sustainable Chem. Eng.* **2017**, *5*, 10231−10239.
(31) Liu, H. Ammonia synthesis catalyst 100 years: Practice, enlightenment and challenge. *Chinese journal of catalysis* **2014**, *35*, 1619−1640.
(32) Humphreys, J.; Lan, R.; Tao, S. Development and Recent Progress on Ammonia Synthesis Catalysts for Haber−Bosch Process. *Adv. Energy Sustain. Res.* **2021**, *2*, No. 2000043.
(33) Bowker, M. The 2007 Nobel Prize in Chemistry for Surface Chemistry: Understanding Nanoscale Phenomena at Surfaces. *ACS Nano* **2007**, *1*, 253−257.
(34) Smith, C.; Hill, A. K.; Torrente-Murciano, L. Current and future role of Haber−Bosch ammonia in a carbon-free energy landscape. *Energy Environ. Sci.* **2020**, *13*, 331−344.
(35) Smith, C.; Torrente-Murciano, L. Exceeding Single-Pass Equilibrium with Integrated Absorption Separation for Ammonia Synthesis Using Renewable Energy—Redefining the Haber-Bosch Loop. *Advanced Energy Materials* **2021**, *11*, No. 2003845.
(36) Schlögl, R. Catalytic Synthesis of Ammonia—A "Never-Ending Story"? *Angew Chem. Int. Ed.* **2003**, *42*, 2004−2008.
(37) Dybkjaer, I. *Ammonia, catalysis and manufacture*; Nielsen, A., Ed.; Springer: Heidelberg, 1995.
(38) Rosca, V.; Duca, M.; de Groot, M. T.; Koper, M. T. M. Nitrogen Cycle Electrocatalysis. *Chem. Rev.* **2009**, *109*, 2209−2244.
(39) Yapicioglu, A.; Dincer, I. A review on clean ammonia as a potential fuel for power generators. *Renewable and Sustainable Energy Reviews* **2019**, *103*, 96−108.
(40) Li, C.; Wang, T.; Gong, J. Alternative Strategies Toward Sustainable Ammonia Synthesis. *Transactions of Tianjin University* **2020**, *26*, 67−91.
(41) Liang, J.; Zhou, Q.; Mou, T.; Chen, H.; Yue, L.; Luo, Y.; Liu, Q.; Hamdy, M. S.; Alshehri, A. A.; Gong, F.; Sun, X. FeP nanorod array: A high-efficiency catalyst for electroreduction of NO to NH3 under ambient conditions. *Nano Research* **2022**, *15*, 4008−4013.
(42) Huang, P.; Fan, T.; Ma, X.; Zhang, J.; Zhang, Y.; Chen, Z.; Yi, X. 3D Flower-Like Zinc Cobaltite for Electrocatalytic Reduction of Nitrate to Ammonia under Ambient Conditions. *ChemSusChem* **2022**, *15*, No. e202102049.
(43) Li, Z.; Liang, J.; Liu, Q.; Xie, L.; Zhang, L.; Ren, Y.; Yue, L.; Li, N.; Tang, B.; Alshehri, A. A.; Hamdy, M. S.; Luo, Y.; Kong, Q.; Sun, X. High-efficiency ammonia electrosynthesis via selective reduction of nitrate on ZnCo2O4 nanosheet array. *Materials Today Physics* **2022**, *23*, No. 100619.
(44) Spatzal, T.; Aksoyoglu, M.; Zhang, L.; Andrade, S. L. A.; Schleicher, E.; Weber, S.; Rees, D. C.; Einsle, O. *Evidence for Interstitial Carbon in Nitrogenase FeMo Cofactor* **2011**, *334*, 940−940.
(45) van der Ham, C. J. M.; Koper, M. T. M.; Hetterscheid, D. G. H. Challenges in reduction of dinitrogen by proton and electron transfer. *Chem. Soc. Rev.* **2014**, *43*, 5183−5191.
(46) Allen, M. B.; Arnon, D. I. Studies on Nitrogen-Fixing Blue-Green Algae. I. Growth and Nitrogen Fixation by Anabaena Cylindrica Lemm. *Plant physiology* **1955**, *30*, 366−372.
(47) Houlton, B. Z.; Wang, Y.-P.; Vitousek, P. M.; Field, C. B. A unifying framework for dinitrogen fixation in the terrestrial biosphere. *Nature* **2008**, *454*, 327−330.
(48) Salvagiotti, F.; Cassman, K. G.; Specht, J. E.; Walters, D. T.; Weiss, A.; Dobermann, A. Nitrogen uptake, fixation and response to fertilizer N in soybeans: A review. *Field Crops Research* **2008**, *108*, 1−13.
(49) Iwahara, H.; Esaka, T.; Uchida, H.; Maeda, N. Proton conduction in sintered oxides and its application to steam electrolysis for hydrogen production. *Solid State Ionics* **1981**, *3*−*4*, 359−363.
(50) Jia, H.-P.; Quadrelli, E. A. Mechanistic aspects of dinitrogen cleavage and hydrogenation to produce ammonia in catalysis and organometallic chemistry: relevance of metal hydride bonds and dihydrogen. *Chem. Soc. Rev.* **2014**, *43*, 547−564.
(51) Garagounis, I.; Kyriakou, V.; Skodra, A.; Vasileiou, E.; Stoukides, M. Electrochemical Synthesis of Ammonia in Solid Electrolyte Cells. *Front. Energy Res.* **2014**, *2*, 1.
(52) Marnellos, G.; Stoukides, M. *Ammonia Synthesis at Atmospheric Pressure* **1998**, *282*, 98−100.
(53) Amar, I. A.; Lan, R.; Petit, C. T. G.; Tao, S. Solid-state electrochemical synthesis of ammonia: a review. *J. Solid State Electrochem.* **2011**, *15*, 1845−1860.
(54) Giddey, S.; Badwal, S. P. S.; Kulkarni, A. Review of electrochemical ammonia production technologies and materials. *Int. J. Hydrogen Energy* **2013**, *38*, 14576−14594.
(55) Guo, C.; Ran, J.; Vasileff, A.; Qiao, S.-Z. Rational design of electrocatalysts and photo(electro)catalysts for nitrogen reduction to ammonia (NH3) under ambient conditions. *Energy Environ. Sci.* **2018**, *11*, 45−56.
(56) Kyriakou, V.; Garagounis, I.; Vasileiou, E.; Vourros, A.; Stoukides, M. Progress in the Electrochemical Synthesis of Ammonia. *Catal. Today* **2017**, *286*, 2−13.
(57) Shipman, M. A.; Symes, M. D. Recent progress towards the electrosynthesis of ammonia from sustainable resources. *Catal. Today* **2017**, *286*, 57−68.
(58) Martín, A. J.; Shinagawa, T.; Pérez-Ramírez, J. Electrocatalytic Reduction of Nitrogen: From Haber-Bosch to Ammonia Artificial Leaf. *Chem.* **2019**, *5*, 263−283.
(59) Greenlee, L. F.; Renner, J. N.; Foster, S. L. The Use of Controls for Consistent and Accurate Measurements of Electrocatalytic Ammonia Synthesis from Dinitrogen. *ACS Catal.* **2018**, *8*, 7820−7827.
(60) Hoffman, B. M.; Lukoyanov, D.; Yang, Z.-Y.; Dean, D. R.; Seefeldt, L. C. Mechanism of Nitrogen Fixation by Nitrogenase: The Next Stage. *Chem. Rev.* **2014**, *114*, 4041−4062.
(61) Brown, K. A.; Harris, D. F.; Wilker, M. B.; Rasmussen, A.; Khadka, N.; Hamby, H.; Keable, S.; Dukovic, G.; Peters, J. W.; Seefeldt, L. C.; King, P. W. *Light-driven dinitrogen reduction catalyzed by a CdS:nitrogenase MoFe protein biohybrid* **2016**, *352*, 448−450.
(62) Hoffman, B. M.; Dean, D. R.; Seefeldt, L. C. Climbing Nitrogenase: Toward a Mechanism of Enzymatic Nitrogen Fixation. *Acc. Chem. Res.* **2009**, *42*, 609−619.

https://doi.org/10.1021/acscatal.3c02410
ACS Catal. 2023, 13, 14415−14453

(63) Xie, Y.-H.; Wang, J.-D.; Liu, R.-Q.; Su, X.-T.; Sun, Z.-P.; Li, Z.-J. Preparation of La1.9Ca0.1Zr2O6.95 with pyrochlore structure and its application in synthesis of ammonia at atmospheric pressure. *Solid State Ionics* **2004**, *168*, 117−121.
(64) Wang, J.-D.; Xie, Y.-H.; Zhang, Z.-F.; Liu, R.-Q.; Li, Z.-J. Protonic conduction in Ca2+-doped La2M2O7 (M═Ce, Zr) with its application to ammonia synthesis electrochemically. *Mater. Res. Bull.* **2005**, *40*, 1294−1302.
(65) Liu, R.-Q.; Xie, Y.-H.; Wang, J.-D.; Li, Z.-J.; Wang, B.-H. Synthesis of ammonia at atmospheric pressure with Ce0.8M0.2O2−δ (M═La, Y, Gd, Sm) and their proton conduction at intermediate temperature. *Solid State Ionics* **2006**, *177*, 73−76.
(66) Chen, C.; Ma, G. Proton conduction in BaCe1−xGdxO3−α at intermediate temperature and its application to synthesis of ammonia at atmospheric pressure. *J. Alloys Compd.* **2009**, *485*, 69−72.
(67) Marnellos, G.; Zisekas, S.; Stoukides, M. Synthesis of Ammonia at Atmospheric Pressure with the Use of Solid State Proton Conductors. *J. Catal.* **2000**, *193*, 80−87.
(68) Li, C.; Sun, Q.; Cao, F.; Ying, W.; Fang, D. Pretreatment of Alumina and Its Influence on the Properties of Co/Alumina Catalysts for Fischer−Tropsch Synthesis. *Journal of Natural Gas Chemistry* **2007**, *16*, 308−315.
(69) Xu, G.; Liu, R.; Wang, J. Electrochemical synthesis of ammonia using a cell with a Nafion membrane and SmFe0.7Cu0.3−xNixO3 (x = 0−0.3) cathode at atmospheric pressure and lower temperature. *Science in China Series B: Chemistry* **2009**, *52*, 1171−1175.
(70) Liu, R.; Xu, G. *Comparison of Electrochemical Synthesis of Ammonia by Using Sulfonated Polysulfone and Nafion Membrane with Sm1.5Sr0.5NiO4* **2010**, *28*, 139−142.
(71) Zhang, Z.; Zhong, Z.; Liu, R. Cathode catalysis performance of SmBaCuMO5+δ (M═Fe, Co, Ni) in ammonia synthesis. *Journal of Rare Earths* **2010**, *28*, 556−559.
(72) Amar, I. A.; Lan, R.; Petit, C. T. G.; Arrighi, V.; Tao, S. Electrochemical synthesis of ammonia based on a carbonate-oxide composite electrolyte. *Solid State Ionics* **2011**, *182*, 133−138.
(73) Wang, B. H.; Wang, J. D.; Liu, R.; Xie, Y. H.; Li, Z. J. Synthesis of ammonia from natural gas at atmospheric pressure with doped ceria−Ca3(PO4)2−K3PO4 composite electrolyte and its proton conductivity at intermediate temperature. *J. Solid State Electrochem.* **2007**, *11*, 27−31.
(74) Kordali, V.; Kyriacou, G.; Lambrou, C. Electrochemical synthesis of ammonia at atmospheric pressure and low temperature in a solid polymer electrolyte cell. *Chem. Commun.* **2000**, 1673−1674.
(75) Robinson, S.; Manerbino, A.; Grover Coors, W. Galvanic hydrogen pumping in the protonic ceramic perovskite BaCe0.2Zr0.7Y0.1O3−δ. *J. Membr. Sci.* **2013**, *446*, 99−105.
(76) Morejudo, S. H.; Zanón, R.; Escolástico, S.; Yuste-Tirados, I.; Malerød-Fjeld, H.; Vestre, P. K.; Coors, W. G.; Martínez, A.; Norby, T.; Serra, J. M.; Kjølseth, C. Direct conversion of methane to aromatics in a catalytic co-ionic membrane reactor. *Science* **2016**, *353*, 563−566.
(77) Kyriakou, V.; Garagounis, I.; Vourros, A.; Vasileiou, E.; Manerbino, A.; Coors, W. G.; Stoukides, M. Methane steam reforming at low temperatures in a BaZr0.7Ce0.2Y0.1O2.9 proton conducting membrane reactor. *Applied Catalysis B: Environmental* **2016**, *186*, 1−9.
(78) Vasileiou, E.; Kyriakou, V.; Garagounis, I.; Vourros, A.; Manerbino, A.; Coors, W. G.; Stoukides, M. Electrochemical enhancement of ammonia synthesis in a BaZr0.7Ce0.2Y0.1O2.9 solid electrolyte cell. *Solid State Ionics* **2016**, *288*, 357−362.
(79) Malerød-Fjeld, H.; Clark, D.; Yuste-Tirados, I.; Zanón, R.; Catalán-Martinez, D.; Beeaff, D.; Morejudo, S. H.; Vestre, P. K.; Norby, T.; Haugsrud, R.; Serra, J. M.; Kjølseth, C. Thermo-electrochemical production of compressed hydrogen from methane with near-zero energy loss. *Nature Energy* **2017**, *2*, 923−931.
(80) Kyriakou, V.; Garagounis, I.; Vourros, A.; Vasileiou, E.; Stoukides, M. An Electrochemical Haber-Bosch Process. *Joule* **2020**, *4*, 142−158.
(81) Matanović, I.; Garzon, F. H.; Henson, N. J. Electro-reduction of nitrogen on molybdenum nitride: structure, energetics, and vibrational spectra from DFT. *Phys. Chem. Chem. Phys.* **2014**, *16*, 3014−3026.
(82) Abghoui, Y.; Garden, A. L.; Hlynsson, V. F.; Björgvinsdóttir, S.; Ólafsdóttir, H.; Skúlason, E. Enabling electrochemical reduction of nitrogen to ammonia at ambient conditions through rational catalyst design. *Phys. Chem. Chem. Phys.* **2015**, *17*, 4909−4918.
(83) Abghoui, Y.; Garden, A. L.; Howalt, J. G.; Vegge, T.; Skúlason, E. Electroreduction of N2 to Ammonia at Ambient Conditions on Mononitrides of Zr, Nb, Cr, and V: A DFT Guide for Experiments. *ACS Catal.* **2016**, *6*, 635−646.
(84) Nguyen, M.-T.; Seriani, N.; Gebauer, R. Nitrogen electrochemically reduced to ammonia with hematite: density-functional insights. *Phys. Chem. Chem. Phys.* **2015**, *17*, 14317−14322.
(85) Yang, X.; Nash, J.; Anibal, J.; Dunwell, M.; Kattel, S.; Stavitski, E.; Attenkofer, K.; Chen, J. G.; Yan, Y.; Xu, B. Mechanistic Insights into Electrochemical Nitrogen Reduction Reaction on Vanadium Nitride Nanoparticles. *J. Am. Chem. Soc.* **2018**, *140*, 13387−13391.
(86) Zhang, R.; Zhang, Y.; Ren, X.; Cui, G.; Asiri, A. M.; Zheng, B.; Sun, X. High-Efficiency Electrosynthesis of Ammonia with High Selectivity under Ambient Conditions Enabled by VN Nanosheet Array. *ACS Sustainable Chem. Eng.* **2018**, *6*, 9545−9549.
(87) Zhang, X.; Kong, R.-M.; Du, H.; Xia, L.; Qu, F. Highly efficient electrochemical ammonia synthesis via nitrogen reduction reactions on a VN nanowire array under ambient conditions. *Chem. Commun.* **2018**, *54*, 5323−5325.
(88) Amar, I. A.; Lan, R.; Tao, S. Synthesis of ammonia directly from wet nitrogen using a redox stable La0.75Sr0.25Cr0.5Fe0.5O3−δ−Ce0.8Gd0.18Ca0.02O2−δ composite cathode. *RSC Adv.* **2015**, *5*, 38977−38983.
(89) Skodra, A.; Stoukides, M. Electrocatalytic synthesis of ammonia from steam and nitrogen at atmospheric pressure. *Solid State Ionics* **2009**, *180*, 1332−1336.
(90) Murakami, T.; Nishikiori, T.; Nohira, T.; Ito, Y. Electrolytic Synthesis of Ammonia in Molten Salts under Atmospheric Pressure. *J. Am. Chem. Soc.* **2003**, *125*, 334−335.
(91) Zhou, F.; Azofra, L. M.; Ali, M.; Kar, M.; Simonov, A. N.; McDonnell-Worth, C.; Sun, C.; Zhang, X.; MacFarlane, D. R. Electrosynthesis of ammonia from nitrogen at ambient temperature and pressure in ionic liquids. *Energy Environ. Sci.* **2017**, *10*, 2516−2520.
(92) Ma, J.-L.; Bao, D.; Shi, M.-M.; Yan, J.-M.; Zhang, X.-B. Reversible Nitrogen Fixation Based on a Rechargeable Lithium-Nitrogen Battery for Energy Storage. *Chem.* **2017**, *2*, 525−532.
(93) Goto, T.; Tada, M.; Ito, Y. Electrochemical Behavior of Nitride Ions in a Molten Chloride System. *J. Electrochem. Soc.* **1997**, *144*, 2271.
(94) Goto, T.; Ito, Y. Electrochemical reduction of nitrogen gas in a molten chloride system. *Electrochim. Acta* **1998**, *43*, 3379−3384.
(95) Murakami, T.; Nishikiori, T.; Nohira, T.; Ito, Y. Investigation of Anodic Reaction of Electrolytic Ammonia Synthesis in Molten Salts Under Atmospheric Pressure. *J. Electrochem. Soc.* **2005**, *152*, D75.
(96) Serizawa, N.; Miyashiro, H.; Takei, K.; Ikezumi, T.; Nishikiori, T.; Ito, Y. Dissolution Behavior of Ammonia Electrosynthesized in Molten LiCl−KCl−CsCl System. *J. Electrochem. Soc.* **2012**, *159*, No. E87.
(97) Murakami, T.; Nohira, T.; Araki, Y.; Goto, T.; Hagiwara, R.; Ogata, Y. H. Electrolytic Synthesis of Ammonia from Water and Nitrogen under Atmospheric Pressure Using a Boron-Doped Diamond Electrode as a Nonconsumable Anode. *Electrochem. Solid-State Lett.* **2007**, *10*, No. E4.
(98) Murakami, T.; Nohira, T.; Goto, T.; Ogata, Y. H.; Ito, Y. Electrolytic ammonia synthesis from water and nitrogen gas in molten salt under atmospheric pressure. *Electrochim. Acta* **2005**, *50*, 5423−5426.
(99) McEnaney, J. M.; Singh, A. R.; Schwalbe, J. A.; Kibsgaard, J.; Lin, J. C.; Cargnello, M.; Jaramillo, T. F.; Nørskov, J. K. Ammonia synthesis from N2 and H2O using a lithium cycling electrification

https://doi.org/10.1021/acscatal.3c02410
ACS Catal. 2023, 13, 14415−14453

strategy at atmospheric pressure. *Energy Environ. Sci.* **2017**, *10*, 1621−1630.
(100) Li, F.-F.; Licht, S. Advances in Understanding the Mechanism and Improved Stability of the Synthesis of Ammonia from Air and Water in Hydroxide Suspensions of Nanoscale Fe2O3. *Inorg. Chem.* **2014**, *53*, 10042−10044.
(101) Murakami, T.; Nohira, T.; Ogata, Y. H.; Ito, Y. Electrolytic Ammonia Synthesis in Molten Salts under Atmospheric Pressure Using Methane as a Hydrogen Source. *Electrochem. Solid-State Lett.* **2005**, *8*, D12.
(102) Murakami, T.; Nohira, T.; Ogata, Y. H.; Ito, Y. Electrochemical Synthesis of Ammonia and Coproduction of Metal Sulfides from Hydrogen Sulfide and Nitrogen under Atmospheric Pressure. *J. Electrochem. Soc.* **2005**, *152*, D109.
(103) Murakami, T.; Nishikiori, T.; Nohira, T.; Ito, Y. Electrolytic Ammonia Synthesis from Hydrogen Chloride and Nitrogen Gases with Simultaneous Recovery of Chlorine under Atmospheric Pressure. *Electrochem. Solid-State Lett.* **2005**, *8*, D19.
(104) Yang, J.; Weng, W.; Xiao, W. Electrochemical synthesis of ammonia in molten salts. *Journal of Energy Chemistry* **2020**, *43*, 195−207.
(105) Zhu, X.; Mou, S.; Peng, Q.; Liu, Q.; Luo, Y.; Chen, G.; Gao, S.; Sun, X. Aqueous electrocatalytic N2 reduction for ambient NH3 synthesis: recent advances in catalyst development and performance improvement. *Journal of Materials Chemistry A* **2020**, *8*, 1545−1556.
(106) Zhao, R.; Liu, C.; Zhang, X.; Zhu, X.; Wei, P.; Ji, L.; Guo, Y.; Gao, S.; Luo, Y.; Wang, Z.; Sun, X. An ultrasmall Ru2P nanoparticles−reduced graphene oxide hybrid: an efficient electrocatalyst for NH3 synthesis under ambient conditions. *Journal of Materials Chemistry A* **2020**, *8*, 77−81.
(107) Li, Y.; Li, T.; Zhu, X.; Alshehri, A. A.; Alzahrani, K. A.; Lu, S.; Sun, X. *DyF3: An Efficient Electrocatalyst for N2 Fixation to NH3 under Ambient Conditions* **2020**, *15*, 487−489.
(108) Zhang, R.; Ji, L.; Kong, W.; Wang, H.; Zhao, R.; Chen, H.; Li, T.; Li, B.; Luo, Y.; Sun, X. Electrocatalytic N2-to-NH3 conversion with high faradaic efficiency enabled using a Bi nanosheet array. *Chem. Commun.* **2019**, *55*, 5263−5266.
(109) Xie, H.; Geng, Q.; Zhu, X.; Luo, Y.; Chang, L.; Niu, X.; Shi, X.; Asiri, A. M.; Gao, S.; Wang, Z.; Sun, X. PdP2 nanoparticles−reduced graphene oxide for electrocatalytic N2 conversion to NH3 under ambient conditions. *Journal of Materials Chemistry A* **2019**, *7*, 24760−24764.
(110) Wu, T.; Zhu, X.; Xing, Z.; Mou, S.; Li, C.; Qiao, Y.; Liu, Q.; Luo, Y.; Shi, X.; Zhang, Y.; Sun, X. *Greatly Improving Electrochemical N2 Reduction over TiO2 Nanoparticles by Iron Doping* **2019**, *58*, 18449−18453.
(111) Deng, G.; Wang, T.; Alshehri, A. A.; Alzahrani, K. A.; Wang, Y.; Ye, H.; Luo, Y.; Sun, X. Improving the electrocatalytic N2 reduction activity of Pd nanoparticles through surface modification. *Journal of Materials Chemistry A* **2019**, *7*, 21674−21677.
(112) Andersen, S. Z.; Čolić, V.; Yang, S.; Schwalbe, J. A.; Nielander, A. C.; McEnaney, J. M.; Enemark-Rasmussen, K.; Baker, J. G.; Singh, A. R.; Rohr, B. A.; Statt, M. J.; Blair, S. J.; Mezzavilla, S.; Kibsgaard, J.; Vesborg, P. C. K.; Cargnello, M.; Bent, S. F.; Jaramillo, T. F.; Stephens, I. E. L.; Nørskov, J. K.; Chorkendorff, I. A rigorous electrochemical ammonia synthesis protocol with quantitative isotope measurements. *Nature* **2019**, *570*, 504−508.
(113) Lee, H. K.; Koh, C. S. L.; Lee, Y. H.; Liu, C.; Phang, I. Y.; Han, X.; Tsung, C.-K.; Ling, X. Y. Favoring the unfavored: Selective electrochemical nitrogen fixation using a reticular chemistry approach. *Sci. Adv.* **2018**, *4*, No. eaar3208.
(114) Tsuneto, A.; Kudo, A.; Sakata, T. Efficient Electrochemical Reduction of N2 to NH3 Catalyzed by Lithium. *Chem. Lett.* **1993**, *22*, 851−854.
(115) Wu, Z.-Y.; Karamad, M.; Yong, X.; Huang, Q.; Cullen, D. A.; Zhu, P.; Xia, C.; Xiao, Q.; Shakouri, M.; Chen, F.-Y.; Kim, J. Y.; Xia, Y.; Heck, K.; Hu, Y.; Wong, M. S.; Li, Q.; Gates, I.; Siahrostami, S.; Wang, H. Electrochemical ammonia synthesis via nitrate reduction on Fe single atom catalyst. *Nat. Commun.* **2021**, *12*, 2870.
(116) Chinthaginjala, J. K.; Lefferts, L. Support effect on selectivity of nitrite reduction in water. *Applied Catalysis B: Environmental* **2010**, *101*, 144−149.
(117) Li, H.; Yan, C.; Guo, H.; Shin, K.; Humphrey, S. M.; Werth, C. J.; Henkelman, G. CuxIr1−x Nanoalloy Catalysts Achieve Near 100% Selectivity for Aqueous Nitrite Reduction to NH3. *ACS Catal.* **2020**, *10*, 7915−7921.
(118) Casella, I. G.; Contursi, M. Highly dispersed rhodium particles on multi-walled carbon nanotubes for the electrochemical reduction of nitrate and nitrite ions in acid medium. *Electrochim. Acta* **2014**, *138*, 447−453.
(119) Yue, H.; Xue, L.; Chen, F. Efficiently electrochemical removal of nitrite contamination with stable RuO2-TiO2/Ti electrodes. *Applied Catalysis B: Environmental* **2017**, *206*, 683−691.
(120) Kuntke, P.; Rodrigues, M.; Sleutels, T.; Saakes, M.; Hamelers, H. V. M.; Buisman, C. J. N. Energy-Efficient Ammonia Recovery in an Up-Scaled Hydrogen Gas Recycling Electrochemical System. *ACS Sustainable Chem. Eng.* **2018**, *6*, 7638−7644.
(121) Cruz, H.; Law, Y. Y.; Guest, J. S.; Rabaey, K.; Batstone, D.; Laycock, B.; Verstraete, W.; Pikaar, I. Mainstream Ammonium Recovery to Advance Sustainable Urban Wastewater Management. *Environ. Sci. Technol.* **2019**, *53*, 11066−11079.
(122) Shin, H.; Jung, S.; Bae, S.; Lee, W.; Kim, H. Nitrite Reduction Mechanism on a Pd Surface. *Environ. Sci. Technol.* **2014**, *48*, 12768−12774.
(123) Yuan, J.; Yin, H.; Jin, X.; Zhao, D.; Liu, Y.; Du, A.; Liu, X.; O'Mullane, A. P. A practical FeP nanoarrays electrocatalyst for efficient catalytic reduction of nitrite ions in wastewater to ammonia. *Applied Catalysis B: Environmental* **2023**, *325*, No. 122353.
(124) Liu, J.; Kelley, M. S.; Wu, W.; Banerjee, A.; Douvalis, A. P.; Wu, J.; Zhang, Y.; Schatz, G. C.; Kanatzidis, M. G. Nitrogenase-mimic iron-containing chalcogels for photochemical reduction of dinitrogen to ammonia. *Proc. Natl. Acad. Sci. U. S. A.* **2016**, *113*, 5530−5535.
(125) Milton, R. D.; Cai, R.; Abdellaoui, S.; Leech, D.; De Lacey, A. L.; Pita, M.; Minteer, S. D. Bioelectrochemical Haber−Bosch Process: An Ammonia-Producing H2/N2 Fuel Cell. *Angew. Chem., Int. Ed.* **2017**, *56*, 2680−2683.
(126) Hao, Y.-C.; Guo, Y.; Chen, L.-W.; Shu, M.; Wang, X.-Y.; Bu, T.-A.; Gao, W.-Y.; Zhang, N.; Su, X.; Feng, X.; Zhou, J.-W.; Wang, B.; Hu, C.-W.; Yin, A.-X.; Si, R.; Zhang, Y.-W.; Yan, C.-H. Promoting nitrogen electroreduction to ammonia with bismuth nanocrystals and potassium cations in water. *Nature Catalysis* **2019**, *2*, 448−456.
(127) Han, C.; Qi, M.-Y.; Tang, Z.-R.; Gong, J.; Xu, Y.-J. Gold nanorods-based hybrids with tailored structures for photoredox catalysis: fundamental science, materials design and applications. *Nano Today* **2019**, *27*, 48−72.
(128) Tang, Z.-R.; Han, B.; Han, C.; Xu, Y.-J. One dimensional CdS based materials for artificial photoredox reactions. *Journal of Materials Chemistry A* **2017**, *5*, 2387−2410.
(129) Schrauzer, G. N.; Strampach, N.; Hui, L. N.; Palmer, M. R.; Salehi, J. *Nitrogen photoreduction on desert sands under sterile conditions* **1983**, *80*, 3873−3876.
(130) Dhar, N. R. Denitrification in Sunlight. *Nature* **1934**, *134*, 572−573.
(131) Dhar, N.; Pant, N. Nitrogen loss from soils and oxide surfaces. *Nature* **1944**, *153*, 115−116.
(132) Comer, B. M.; Fuentes, P.; Dimkpa, C. O.; Liu, Y.-H.; Fernandez, C. A.; Arora, P.; Realff, M.; Singh, U.; Hatzell, M. C.; Medford, A. J. Prospects and challenges for solar fertilizers. *Joule* **2019**, *3*, 1578−1605.
(133) Jewess, M.; Crabtree, R.H. Electrocatalytic nitrogen fixation for distributed fertilizer production? *ACS Sustainable Chem. Eng.* **2016**, *4*, 5855−5858.
(134) Edwards, J. G.; Davies, J. A.; Boucher, D. L.; Mennad, A. An Opinion on the Heterogeneous Photoreactions of N2 with H2O. *Angewandte Chemie International Edition in English* **1992**, *31*, 480−482.

https://doi.org/10.1021/acscatal.3c02410
ACS Catal. 2023, 13, 14415−14453

(135) Wang, A.; Edwards, J. G.; Davies, J. A. Photooxidation of aqueous ammonia with titania-based heterogeneous catalysts. *Sol. Energy* **1994**, *52*, 459−466.
(136) Augugliaro, V.; Soria, J. Concerning "an opinion on the heterogeneous photoreduction of N2 with H2O": first letter. *Angewandte Chemie International Edition in English* **1993**, *32*, 550−550.
(137) Davies, J. A.; Edwards, J. G. Reply: Standards of Demonstration for the Heterogeneous Photoreactions of N2 with H2O. *Angewandte Chemie International Edition in English* **1993**, *32*, 552−553.
(138) Zhang, G.; Sewell, C. D.; Zhang, P.; Mi, H.; Lin, Z. Nanostructured photocatalysts for nitrogen fixation. *Nano Energy* **2020**, *71*, No. 104645.
(139) Ali, M.; Zhou, F.; Chen, K.; Kotzur, C.; Xiao, C.; Bourgeois, L.; Zhang, X.; MacFarlane, D. R. Nanostructured photoelectrochemical solar cell for nitrogen reduction using plasmon-enhanced black silicon. *Nat. Commun.* **2016**, *7*, 11335.
(140) Zhu, D.; Zhang, L.; Ruther, R. E.; Hamers, R. J. Photo-illuminated diamond as a solid-state source of solvated electrons in water for nitrogen reduction. *Nat. Mater.* **2013**, *12*, 836−841.
(141) Choe, S.; Kim, S. M.; Lee, Y.; Seok, J.; Jung, J.; Lee, J. S.; Jang, Y. J. Rational design of photocatalysts for ammonia production from water and nitrogen gas. *Nano Convergence* **2021**, *8*, 22.
(142) Ithisuphalap, K.; Zhang, H.; Guo, L.; Yang, Q.; Yang, H.; Wu, G. Photocatalysis and photoelectrocatalysis methods of nitrogen reduction for sustainable ammonia synthesis. *Small Methods* **2019**, *3*, No. 1800352.
(143) John, J.; Lee, D.-K.; Sim, U. Photocatalytic and electrocatalytic approaches towards atmospheric nitrogen reduction to ammonia under ambient conditions. *Nano Convergence* **2019**, *6*, 1−16.
(144) Buscagan, T. M.; Oyala, P. H.; Peters, J. C. N2-to-NH3 Conversion by a triphos−Iron Catalyst and Enhanced Turnover under Photolysis. *Angew. Chem., Int. Ed.* **2017**, *56*, 6921−6926.
(145) Gray, H. B.; Winkler, J. R. ELECTRON TRANSFER IN PROTEINS. *Annu. Rev. Biochem.* **1996**, *65*, 537−561.
(146) Li, Y.; Li, Y.; Wang, B.; Luo, Y.; Yang, D.; Tong, P.; Zhao, J.; Luo, L.; Zhou, Y.; Chen, S.; Cheng, F.; Qu, J. Ammonia formation by a thiolate-bridged diiron amide complex as a nitrogenase mimic. *Nat. Chem.* **2013**, *5*, 320−326.
(147) Eda, G.; Fujita, T.; Yamaguchi, H.; Voiry, D.; Chen, M.; Chhowalla, M. Coherent Atomic and Electronic Heterostructures of Single-Layer MoS2. *ACS Nano* **2012**, *6*, 7311−7317.
(148) Rittle, J.; Peters, J. C. An Fe-N2 Complex That Generates Hydrazine and Ammonia via Fe═NNH2: Demonstrating a Hybrid Distal-to-Alternating Pathway for N2 Reduction. *J. Am. Chem. Soc.* **2016**, *138*, 4243−4248.
(149) Zheng, J.; Lu, L.; Lebedev, K.; Wu, S.; Zhao, P.; McPherson, I. J.; Wu, T.-S.; Kato, R.; Li, Y.; Ho, P.-L.; Li, G.; Bai, L.; Sun, J.; Prabhakaran, D.; Taylor, R. A.; Soo, Y.-L.; Suenaga, K.; Tsang, S. C. E. Fe on molecular-layer MoS2 as inorganic Fe-S2-Mo motifs for light-driven nitrogen fixation to ammonia at elevated temperatures. *Chem. Catalysis* **2021**, *1*, 162−182.
(150) Broda, H.; Tuczek, F. Catalytic Ammonia Synthesis in Homogeneous Solution—Biomimetic at Last? *Angew. Chem., Int. Ed.* **2014**, *53*, 632−634.
(151) Wang, T.; Liu, Q.; Li, T.; Lu, S.; Chen, G.; Shi, X.; Asiri, A. M.; Luo, Y.; Ma, D.; Sun, X. A magnetron sputtered Mo3Si thin film: an efficient electrocatalyst for N2 reduction under ambient conditions. *Journal of Materials Chemistry A* **2021**, *9*, 884−888.
(152) Zheng, J.; Lyu, Y.; Qiao, M.; Wang, R.; Zhou, Y.; Li, H.; Chen, C.; Li, Y.; Zhou, H.; Jiang, S. P.; Wang, S. Photoelectrochemical Synthesis of Ammonia on the Aerophilic-Hydrophilic Heterostructure with 37.8% Efficiency. *Chem.* **2019**, *5*, 617−633.
(153) Jang, Y. J.; Lindberg, A. E.; Lumley, M. A.; Choi, K.-S. Photoelectrochemical Nitrogen Reduction to Ammonia on Cupric and Cuprous Oxide Photocathodes. *ACS Energy Letters* **2020**, *5*, 1834−1839.
(154) Sethuram Markandaraj, S.; Muthusamy, T.; Shanmugam, S. Electrochemical Reduction of Nitric Oxide with 1.7% Solar-to-Ammonia Efficiency Over Nanostructured Core-Shell Catalyst at Low Overpotentials. *Advanced Science* **2022**, *9*, No. 2201410.
(155) von Liebig, J. Une note sur la nitrification. *Ann. Chem. Phys.* **1827**, *35*, 329−333.
(156) Eyde, H. S. The manufacture of nitrates from the atmosphere by the electric arc—Birkeland-Eyde process. *Journal of the Royal Society of Arts* **1909**, *57*, 568−576.
(157) Hong, J.; Pancheshnyi, S.; Tam, E.; Lowke, J. J.; Prawer, S.; Murphy, A. B. Kinetic modelling of NH3 production in N2−H2 non-equilibrium atmospheric-pressure plasma catalysis. *J. Phys. D: Appl. Phys.* **2017**, *50*, No. 154005.
(158) Carrasco, E.; Jiménez-Redondo, M.; Tanarro, I.; Herrero, V. J. Neutral and ion chemistry in low pressure dc plasmas of H 2/N 2 mixtures: routes for the efficient production of NH3 and NH 4+. *Phys. Chem. Chem. Phys.* **2011**, *13*, 19561−19572.
(159) Eliasson, B.; Kogelschatz, U. Modeling and applications of silent discharge plasmas. *IEEE transactions on plasma science* **1991**, *19*, 309−323.
(160) Ma, H.; Sharma, R. K.; Welzel, S.; van de Sanden, M. C. M.; Tsampas, M. N.; Schneider, W. F. Observation and rationalization of nitrogen oxidation enabled only by coupled plasma and catalyst. *Nat. Commun.* **2022**, *13*, 402.
(161) Mehta, P.; Barboun, P.; Herrera, F. A.; Kim, J.; Rumbach, P.; Go, D. B.; Hicks, J. C.; Schneider, W. F. Overcoming ammonia synthesis scaling relations with plasma-enabled catalysis. *Nature Catalysis* **2018**, *1*, 269−275.
(162) Peng, P.; Li, Y.; Cheng, Y.; Deng, S.; Chen, P.; Ruan, R. Atmospheric pressure ammonia synthesis using non-thermal plasma assisted catalysis. *Plasma Chemistry and Plasma Processing* **2016**, *36*, 1201−1210.
(163) Iwamoto, M.; Akiyama, M.; Aihara, K.; Deguchi, T. Ammonia synthesis on wool-like Au, Pt, Pd, Ag, or Cu electrode catalysts in nonthermal atmospheric-pressure plasma of N2 and H2. *ACS Catal.* **2017**, *7*, 6924−6929.
(164) Aihara, K.; Akiyama, M.; Deguchi, T.; Tanaka, M.; Hagiwara, R.; Iwamoto, M. Remarkable catalysis of a wool-like copper electrode for NH 3 synthesis from N 2 and H 2 in non-thermal atmospheric plasma. *Chem. Commun.* **2016**, *52*, 13560−13563.
(165) Hawtof, R.; Ghosh, S.; Guarr, E.; Xu, C.; Mohan Sankaran, R.; Renner, J. N. Catalyst-free, highly selective synthesis of ammonia from nitrogen and water by a plasma electrolytic system. *Science Advances* **2019**, *5*, No. eaat5778.
(166) Sun, J.; Alam, D.; Daiyan, R.; Masood, H.; Zhang, T.; Zhou, R.; Cullen, P. J.; Lovell, E. C.; Jalili, A.; Amal, R. A hybrid plasma electrocatalytic process for sustainable ammonia production. *Energy Environ. Sci.* **2021**, *14*, 865−872.
(167) Zhang, T.; Zhou, R.; Zhang, S.; Zhou, R.; Ding, J.; Li, F.; Hong, J.; Dou, L.; Shao, T.; Murphy, A.B.; Ostrikov, K.; Cullen, P.J. Sustainable Ammonia Synthesis from Nitrogen and Water by One-Step Plasma Catalysis. *ENERGY & ENVIRONMENTAL MATERIALS* **2023**, *6*, e12344.
(168) Wang, J.; Wen, Z.; Zi, Y.; Lin, L.; Wu, C.; Guo, H.; Xi, Y.; Xu, Y.; Wang, Z. L. Self-Powered Electrochemical Synthesis of Polypyrrole from the Pulsed Output of a Triboelectric Nanogenerator as a Sustainable Energy System. *Adv. Funct. Mater.* **2016**, *26*, 3542−3548.
(169) Fu, K.; Yao, Y.; Dai, J.; Hu, L. Progress in 3D Printing of Carbon Materials for Energy-Related Applications. *Adv. Mater.* **2017**, *29*, No. 1603486.
(170) Gao, S.; Zhu, Y.; Chen, Y.; Tian, M.; Yang, Y.; Jiang, T.; Wang, Z. L. Self-power electroreduction of N2 into NH3 by 3D printed triboelectric nanogenerators. *Mater. Today* **2019**, *28*, 17−24.
(171) Adánez, J.; Abad, A.; Mendiara, T.; Gayán, P.; De Diego, L.; García-Labiano, F. Chemical looping combustion of solid fuels. *Prog. Energy Combust. Sci.* **2018**, *65*, 6−66.
(172) Adanez, J.; Abad, A.; Garcia-Labiano, F.; Gayan, P.; De Diego, L. F. Progress in chemical-looping combustion and reforming

https://doi.org/10.1021/acscatal.3c02410
ACS Catal. 2023, 13, 14415−14453

technologies. *Progress in energy and combustion science* **2012**, *38*, 215−282.
(173) Wang, Q.; Guo, J.; Chen, P. Recent progress towards mild-condition ammonia synthesis. *Journal of Energy Chemistry* **2019**, *36*, 25−36.
(174) Zeng, L.; Cheng, Z.; Fan, J. A.; Fan, L.-S.; Gong, J. Metal oxide redox chemistry for chemical looping processes. *Nature Reviews Chemistry* **2018**, *2*, 349−364.
(175) Fan, L.-S.; Zeng, L.; Wang, W.; Luo, S. Chemical looping processes for CO 2 capture and carbonaceous fuel conversion−prospect and opportunity. *Energy Environ. Sci.* **2012**, *5*, 7254−7280.
(176) Tong, A.; Bayham, S.; Kathe, M. V.; Zeng, L.; Luo, S.; Fan, L.-S. Iron-based syngas chemical looping process and coal-direct chemical looping process development at Ohio State University. *Applied energy* **2014**, *113*, 1836−1845.
(177) Vojvodic, A.; Medford, A. J.; Studt, F.; Abild-Pedersen, F.; Khan, T. S.; Bligaard, T.; Nørskov, J. K. Exploring the limits: A low-pressure, low-temperature Haber−Bosch process. *Chem. Phys. Lett.* **2014**, *598*, 108−112.
(178) Medford, A. J.; Vojvodic, A.; Hummelshøj, J. S.; Voss, J.; Abild-Pedersen, F.; Studt, F.; Bligaard, T.; Nilsson, A.; Nørskov, J. K. From the Sabatier principle to a predictive theory of transition-metal heterogeneous catalysis. *J. Catal.* **2015**, *328*, 36−42.
(179) Wang, P.; Chang, F.; Gao, W.; Guo, J.; Wu, G.; He, T.; Chen, P. Breaking scaling relations to achieve low-temperature ammonia synthesis through LiH-mediated nitrogen transfer and hydrogenation. *Nat. Chem.* **2017**, *9*, 64−70.
(180) Michalsky, R.; Avram, A. M.; Peterson, B. A.; Pfromm, P. H.; Peterson, A. A. Chemical looping of metal nitride catalysts: low-pressure ammonia synthesis for energy storage. *Chemical Science* **2015**, *6*, 3965−3974.
(181) Gao, W.; Wang, R.; Feng, S.; Wang, Y.; Sun, Z.; Guo, J.; Chen, P. Thermodynamic and kinetic considerations of nitrogen carriers for chemical looping ammonia synthesis. *Discover Chem. Eng.* **2023**, *3*, 1.
(182) Michalsky, R.; Pfromm, P. H. Chromium as reactant for solar thermochemical synthesis of ammonia from steam, nitrogen, and biomass at atmospheric pressure. *Sol. Energy* **2011**, *85*, 2642−2654.
(183) Brown, S.; Hu, J. Review of chemical looping ammonia synthesis materials. *Chem. Eng. Sci.* **2023**, *280*, No. 119063.
(184) Ye, T.-N.; Park, S.-W.; Lu, Y.; Li, J.; Sasase, M.; Kitano, M.; Hosono, H. Contribution of nitrogen vacancies to ammonia synthesis over metal nitride catalysts. *J. Am. Chem. Soc.* **2020**, *142*, 14374−14383.
(185) Zhang, Q.; Wu, Y.; Gao, Y.; Chen, X.; Liu, D.; Fan, M. High-performance mesoporous (AlN/Al2O3) for enhanced NH3 yield during chemical looping ammonia generation technology. *Int. J. Hydrogen Energy* **2020**, *45*, 9903−9913.
(186) Xiong, C.; Wu, Y.; Feng, M.; Fang, J.; Liu, D.; Shen, L.; Argyle, M. D.; Gasem, K. A. M.; Fan, M. High thermal stability Si-Al based N-carrier for efficient and stable chemical looping ammonia generation. *Applied Energy* **2022**, *323*, No. 119519.
(187) Wang, R.; Gao, W.; Feng, S.; Guan, Y.; Wang, Q.; Guo, J.; Chen, P. Zn Promotes Chemical Looping Ammonia Synthesis Mediated by LiH−Li2NH Couple. *ChemSusChem* **2023**, No. e202300813.
(188) Gao, W.; Guo, J.; Wang, P.; Wang, Q.; Chang, F.; Pei, Q.; Zhang, W.; Liu, L.; Chen, P. Production of ammonia via a chemical looping process based on metal imides as nitrogen carriers. *Nature Energy* **2018**, *3*, 1067−1075.
(189) Tagawa, K.; Gi, H.; Shinzato, K.; Miyaoka, H.; Ichikawa, T. Improvement of kinetics of ammonia synthesis at ambient pressure by the chemical looping process of lithium hydride. *J. Phys. Chem. C* **2022**, *126*, 2403−2409.
(190) Ravi, M.; Makepeace, J. W. Lithium−nitrogen−hydrogen systems for ammonia synthesis: exploring a more efficient pathway using lithium nitride−hydride. *Chem. Commun.* **2022**, *58*, 6076−6079.
(191) Feng, S.; Gao, W.; Wang, Q.; Guan, Y.; Yan, H.; Wu, H.; Cao, H.; Guo, J.; Chen, P. A multi-functional composite nitrogen carrier for ammonia production via a chemical looping route. *Journal of Materials Chemistry A* **2021**, *9*, 1039−1047.
(192) Gao, W.; Wang, P.; Guo, J.; Chang, F.; He, T.; Wang, Q.; Wu, G.; Chen, P. Barium hydride-mediated nitrogen transfer and hydrogenation for ammonia synthesis: a case study of cobalt. *ACS Catal.* **2017**, *7*, 3654−3661.
(193) Wang, Q. R.; Guan, Y. Q.; Gao, W. B.; Guo, J. P.; Chen, P. Thermodynamic properties of ammonia production from hydrogenation of alkali and alkaline earth metal amides. *ChemPhysChem* **2019**, *20*, 1376−1381.
(194) Feng, S.; Gao, W.; Guo, J.; Cao, H.; Chen, P. Electrodriven Chemical Looping Ammonia Synthesis Mediated by Lithium Imide. *ACS Energy Letters* **2023**, *8*, 1567−1574.
(195) Brown, S.; Robinson, B.; Wang, Y.; Wildfire, C.; Hu, J. Microwave heated chemical looping ammonia synthesis over Fe and CoMo particles. *Journal of Materials Chemistry A* **2022**, *10*, 15497−15507.
(196) Wang, B.; Yin, X.; Wang, P.; Shen, L. Chemical looping ammonia synthesis at atmospheric pressure benefiting from synergistic effect of Mn- and Fe-based nitrogen carriers. *Int. J. Hydrogen Energy* **2023**, *48*, 2705−2717.
(197) Shan, N.; Chikan, V.; Pfromm, P.; Liu, B. Fe and Ni Dopants Facilitating Ammonia Synthesis on Mn4N and Mechanistic Insights from First-Principles Methods. *J. Phys. Chem. C* **2018**, *122*, 6109−6116.
(198) Laassiri, S.; Zeinalipour-Yazdi, C. D.; Catlow, C. R. A.; Hargreaves, J. S. J. The potential of manganese nitride based materials as nitrogen transfer reagents for nitrogen chemical looping. *Applied Catalysis B: Environmental* **2018**, *223*, 60−66.
(199) Aframehr, W. M.; Huang, C.; Pfromm, P. H. Chemical Looping of Manganese to Synthesize Ammonia at Atmospheric Pressure: Sodium as Promoter. *Chem. Eng. Technol.* **2020**, *43*, 2126−2133.
(200) Shan, N.; Huang, C.; Lee, R. T.; Manavi, N.; Xu, L.; Chikan, V.; Pfromm, P. H.; Liu, B. Manipulating the Geometric and Electronic Structures of Manganese Nitrides for Ammonia Synthesis. *ChemCatChem.* **2020**, *12*, 2233−2244.
(201) Wang, B.; Guo, H.; Yin, X.; Shen, L. N-Sorption Capability of Al2O3-Supported Mn-/Fe-Based Nitrogen Carriers during Chemical Looping Ammonia Synthesis Technology. *Energy Fuels* **2020**, *34*, 10247−10255.
(202) Kojima, R.; Aika, K.-i. Molybdenum nitride and carbide catalysts for ammonia synthesis. *Applied Catalysis A: General* **2001**, *219*, 141−147.
(203) Bion, N.; Can, F.; Cook, J.; Hargreaves, J.; Hector, A. L.; Levason, W.; McFarlane, A.; Richard, M.; Sardar, K. The role of preparation route upon the ambient pressure ammonia synthesis activity of Ni2Mo3N. *Applied Catalysis A: General* **2015**, *504*, 44−50.
(204) Michalsky, R.; Pfromm, P. H.; Steinfeld, A. Rational design of metal nitride redox materials for solar-driven ammonia synthesis. *Interface focus* **2015**, *5*, No. 20140084.
(205) Michalsky, R.; Parman, B. J.; Amanor-Boadu, V.; Pfromm, P. H. Solar thermochemical production of ammonia from water, air and sunlight: Thermodynamic and economic analyses. *Energy* **2012**, *42*, 251−260.
(206) Ren, X.; Cui, G.; Chen, L.; Xie, F.; Wei, Q.; Tian, Z.; Sun, X. Electrochemical N 2 fixation to NH 3 under ambient conditions: Mo 2 N nanorod as a highly efficient and selective catalyst. *Chem. Commun.* **2018**, *54*, 8474−8477.
(207) Yang, S.; Zhang, T.; Yang, Y.; Wang, B.; Li, J.; Gong, Z.; Yao, Z.; Du, W.; Liu, S.; Yu, Z. Molybdenum-based nitrogen carrier for ammonia production via a chemical looping route. *Applied Catalysis B: Environmental* **2022**, *312*, No. 121404.
(208) Swearer, D. F.; Knowles, N. R.; Everitt, H. O.; Halas, N. J. Light-Driven Chemical Looping for Ammonia Synthesis. *ACS Energy Letters* **2019**, *4*, 1505−1512.
(209) Gao, Y.; Wu, Y.; Zhang, Q.; Chen, X.; Jiang, G.; Liu, D. N-desorption or NH3 generation of TiO2-loaded Al-based nitrogen

carrier during chemical looping ammonia generation technology. *Int. J. Hydrogen Energy* **2018**, *43*, 16589−16597.
(210) Wu, Y.; Jiang, G.; Zhang, H.; Sun, Z.; Gao, Y.; Chen, X.; Liu, H.; Tian, H.; Lai, Q.; Fan, M.; Liu, D. Fe2O3, a cost effective and environmentally friendly catalyst for the generation of NH3 − a future fuel − using a new Al2O3-looping based technology. *Chem. Commun.* **2017**, *53*, 10664−10667.
(211) Chang, F.; Guan, Y.; Chang, X.; Guo, J.; Wang, P.; Gao, W.; Wu, G.; Zheng, J.; Li, X.; Chen, P. Alkali and Alkaline Earth Hydrides-Driven N2 Activation and Transformation over Mn Nitride Catalyst. *J. Am. Chem. Soc.* **2018**, *140*, 14799−14806.
(212) Brown, S.; Ahmat Ibrahim, S.; Robinson, B. R.; Caiola, A.; Tiwari, S.; Wang, Y.; Bhattacharyya, D.; Che, F.; Hu, J. Ambient Carbon-Neutral Ammonia Generation via a Cyclic Microwave Plasma Process. *ACS Appl. Mater. Interfaces* **2023**, *15*, 23255−23264.
(213) Weng, Q.; Toan, S.; Ai, R.; Sun, Z.; Sun, Z. Ammonia production from biomass via a chemical looping−based hybrid system. *Journal of Cleaner Production* **2021**, *289*, No. 125749.
(214) Gong, Y.; Li, H.; Wu, J.; Song, X.; Yang, X.; Bao, X.; Han, X.; Kitano, M.; Wang, J.; Hosono, H. Unique Catalytic Mechanism for Ru-Loaded Ternary Intermetallic Electrides for Ammonia Synthesis. *J. Am. Chem. Soc.* **2022**, *144*, 8683−8692.
(215) Wang, B.; Shen, L. Recent Advances in NH3 Synthesis with Chemical Looping Technology. *Ind. Eng. Chem. Res.* **2022**, *61*, 18215−18231.
(216) Wu, Y.; Gao, Y.; Zhang, Q.; Cai, T.; Chen, X.; Liu, D.; Fan, M. Promising zirconia-mixed Al-based nitrogen carriers for chemical looping of NH3: Reduced NH3 decomposition and improved NH3 yield. *Fuel* **2020**, *264*, No. 116821.
(217) Mohamed, A. M. O.; Bicer, Y. Coupling of a novel boron-based thermochemical cycle with chemical looping combustion to produce ammonia and power. *Int. J. Hydrogen Energy* **2021**, *46*, 28949−28960.
(218) Lai, Q.; Cai, T.; Tsang, S. C. E.; Chen, X.; Ye, R.; Xu, Z.; Argyle, M. D.; Ding, D.; Chen, Y.; Wang, J.; Russell, A. G.; Wu, Y.; Liu, J.; Fan, M. Chemical looping based ammonia production—A promising pathway for production of the noncarbon fuel. *Science Bulletin* **2022**, *67*, 2124−2138.
(219) Shinzato, K.; Tagawa, K.; Tsunematsu, K.; Gi, H.; Singh, P. K.; Ichikawa, T.; Miyaoka, H. Systematic Study on Nitrogen Dissociation and Ammonia Synthesis by Lithium and Group 14 Element Alloys. *ACS Applied Energy Materials* **2022**, *5*, 4765−4773.
(220) Yamaguchi, S.; Ichikawa, T.; Wang, Y.; Nakagawa, Y.; Isobe, S.; Kojima, Y.; Miyaoka, H. Nitrogen Dissociation via Reaction with Lithium Alloys. *ACS Omega* **2017**, *2*, 1081−1088.
(221) Tang, Z.; Meng, X.; Shi, Y.; Guan, X. Lithium-based Loop for Ambient-Pressure Ammonia Synthesis in a Liquid Alloy-Salt Catalytic System. *ChemSusChem* **2021**, *14*, 4697−4707.
(222) Chen, J. G.; Crooks, R. M.; Seefeldt, L. C.; Bren, K. L.; Bullock, R. M.; Darensbourg, M. Y.; Holland, P. L.; Hoffman, B.; Janik, M. J.; Jones, A. K.; et al. Beyond fossil fuel−driven nitrogen transformations. *Science* **2018**, *360*, No. eaar6611.
(223) Long, J.; Chen, S.; Zhang, Y.; Guo, C.; Fu, X.; Deng, D.; Xiao, J. Direct electrochemical ammonia synthesis from nitric oxide. *Angew. Chem., Int. Ed.* **2020**, *59*, 9711−9718.
(224) Cheng, S.; Gao, Y.-J.; Yan, Y.-L.; Gao, X.; Zhang, S.-H.; Zhuang, G.-L.; Deng, S.-W.; Wei, Z.-Z.; Zhong, X.; Wang, J.-G. Oxygen vacancy enhancing mechanism of nitrogen reduction reaction property in Ru/TiO2. *Journal of Energy Chemistry* **2019**, *39*, 144−151.
(225) Wang, S.; Petzold, V.; Tripkovic, V.; Kleis, J.; Howalt, J. G.; Skulason, E.; Fernández, E.; Hvolbæk, B.; Jones, G.; Toftelund, A.; et al. Universal transition state scaling relations for (de) hydrogenation over transition metals. *Phys. Chem. Chem. Phys.* **2011**, *13*, 20760−20765.
(226) Li, F.; Li, Y. C.; Wang, Z.; Li, J.; Nam, D.-H.; Lum, Y.; Luo, M.; Wang, X.; Ozden, A.; Hung, S.-F. Cooperative CO2-to-ethanol conversion via enriched intermediates at molecule−metal catalyst interfaces. *Nature Catalysis* **2020**, *3*, 75−82.
(227) Liu, J.-X.; Richards, D.; Singh, N.; Goldsmith, B. R. Activity and selectivity trends in electrocatalytic nitrate reduction on transition metals. *ACS Catal.* **2019**, *9*, 7052−7064.
(228) Kitano, M.; Inoue, Y.; Yamazaki, Y.; Hayashi, F.; Kanbara, S.; Matsuishi, S.; Yokoyama, T.; Kim, S.-W.; Hara, M.; Hosono, H. Ammonia synthesis using a stable electride as an electron donor and reversible hydrogen store. *Nat. Chem.* **2012**, *4*, 934−940.
(229) Inoue, Y.; Kitano, M.; Kim, S.-W.; Yokoyama, T.; Hara, M.; Hosono, H. Highly Dispersed Ru on Electride [Ca24Al28O64]-4+(e−)4 as a Catalyst for Ammonia Synthesis. *ACS Catal.* **2014**, *4*, 674−680.
(230) Inoue, Y.; Kitano, M.; Tokunari, M.; Taniguchi, T.; Ooya, K.; Abe, H.; Niwa, Y.; Sasase, M.; Hara, M.; Hosono, H. Direct Activation of Cobalt Catalyst by 12CaO·7Al2O3 Electride for Ammonia Synthesis. *ACS Catal.* **2019**, *9*, 1670−1679.
(231) Kitano, M.; Inoue, Y.; Ishikawa, H.; Yamagata, K.; Nakao, T.; Tada, T.; Matsuishi, S.; Yokoyama, T.; Hara, M.; Hosono, H. Essential role of hydride ion in ruthenium-based ammonia synthesis catalysts. *Chemical Science* **2016**, *7*, 4036−4043.
(232) Murakami, K.; Tanaka, Y.; Sakai, R.; Toko, K.; Ito, K.; Ishikawa, A.; Higo, T.; Yabe, T.; Ogo, S.; Ikeda, M.; et al. The important role of N2H formation energy for low-temperature ammonia synthesis in an electric field. *Catal. Today* **2020**, *351*, 119−124.
(233) Taylor, D. W.; Smith, P. J.; Dowden, D. A.; Kemball, C.; Whan, D. A. Ammonia synthesis and related reactions over iron-cobalt and iron-nickel alloy catalysts. Part I. Catalysts reduced at 853 K. *Applied Catalysis* **1982**, *3*, 161−176.
(234) McKay, D.; Hargreaves, J. S. J.; Rico, J. L.; Rivera, J. L.; Sun, X. L. The influence of phase and morphology of molybdenum nitrides on ammonia synthesis activity and reduction characteristics. *J. Solid State Chem.* **2008**, *181*, 325−333.
(235) Kitano, M.; Kujirai, J.; Ogasawara, K.; Matsuishi, S.; Tada, T.; Abe, H.; Niwa, Y.; Hosono, H. Low-Temperature Synthesis of Perovskite Oxynitride-Hydrides as Ammonia Synthesis Catalysts. *J. Am. Chem. Soc.* **2019**, *141*, 20344−20353.
(236) Hagen, S.; Barfod, R.; Fehrmann, R.; Jacobsen, C. J. H.; Teunissen, H. T.; Chorkendorff, I. Ammonia synthesis with barium-promoted iron−cobalt alloys supported on carbon. *J. Catal.* **2003**, *214*, 327−335.
(237) Humphreys, J.; Lan, R.; Chen, S.; Tao, S. Improved stability and activity of Fe-based catalysts through strong metal support interactions due to extrinsic oxygen vacancies in Ce0.8Sm0.2O2−δ for the efficient synthesis of ammonia. *Journal of Materials Chemistry A* **2020**, *8*, 16676−16689.
(238) McAulay, K.; Hargreaves, J. S. J.; McFarlane, A. R.; Price, D. J.; Spencer, N. A.; Bion, N.; Can, F.; Richard, M.; Greer, H. F.; Zhou, W. Z. The influence of pre-treatment gas mixture upon the ammonia synthesis activity of Co−Re catalysts. *Catal. Commun.* **2015**, *68*, 53−57.
(239) Kojima, R.; Aika, K.-i. Cobalt molybdenum bimetallic nitride catalysts for ammonia synthesis: Part 1. Preparation and characterization. *Applied Catalysis A: General* **2001**, *215*, 149−160.
(240) Al Sobhi, S.; Bion, N.; Hargreaves, J. S. J.; Hector, A. L.; Laassiri, S.; Levason, W.; Lodge, A. W.; McFarlane, A. R.; Ritter, C. The reactivity of lattice nitrogen within the Ni2Mo3N and NiCoMo3N phases. *Mater. Res. Bull.* **2019**, *118*, No. 110519.
(241) Ye, T.-N.; Park, S.-W.; Lu, Y.; Li, J.; Sasase, M.; Kitano, M.; Tada, T.; Hosono, H. Vacancy-enabled N2 activation for ammonia synthesis on an Ni-loaded catalyst. *Nature* **2020**, *583*, 391−395.
(242) Al Sobhi, S.; Hargreaves, J. S. J.; Hector, A. L.; Laassiri, S. Citrate-gel preparation and ammonia synthesis activity of compounds in the quaternary (Ni,M)2Mo3N (M = Cu or Fe) systems. *Dalton Transactions* **2019**, *48*, 16786−16792.
(243) Cao, H.; Guo, J.; Chang, F.; Pistidda, C.; Zhou, W.; Zhang, X.; Santoru, A.; Wu, H.; Schell, N.; Niewa, R.; Chen, P.; Klassen, T.; Dornheim, M. Transition and Alkali Metal Complex Ternary Amides for Ammonia Synthesis and Decomposition. *Chemistry − A European Journal* **2017**, *23*, 9766−9771.

https://doi.org/10.1021/acscatal.3c02410
ACS Catal. 2023, 13, 14415−14453

(244) Ouzounidou, M.; Skodra, A.; Kokkofitis, C.; Stoukides, M. Catalytic and electrocatalytic synthesis of NH3 in a H+ conducting cell by using an industrial Fe catalyst. *Solid State Ionics* **2007**, *178*, 153−159.
(245) Liu, J.; Li, Y.; Wang, W.; Wang, H.; Zhang, F.; Ma, G. Proton conduction at intermediate temperature and its application in ammonia synthesis at atmospheric pressure of BaCe1-x Ca x O3-α. *J. Mater. Sci.* **2010**, *45*, 5860−5864.
(246) Chen, C.-H.; Chang, S.-J.; Chang, S.-P.; Li, M.-J.; Chen, I. C.; Hsueh, T.-J.; Hsu, C.-L. Novel fabrication of UV photodetector based on ZnO nanowire/p-GaN heterojunction. *Chem. Phys. Lett.* **2009**, *476*, 69−72.
(247) Guo, Y.; Liu, B.; Yang, Q.; Chen, C.; Wang, W.; Ma, G. Preparation via microemulsion method and proton conduction at intermediate-temperature of BaCe1-xYxO3-α. *Electrochem. Commun.* **2009**, *11*, 153−156.
(248) Chen, C.; Wang, W.; Ma, G. Proton conduction in La0.9M0.1Ga0.8 Mg0.2O3-alpha; at intermediate temperature and its application to synthesis of ammonia at atmospheric pressure. *Acta Chimica Sinica* **2009**, *67*, 623−628.
(249) Xie, Y. H.; Wang, J. D.; Liu, R. Q.; Su, X. T.; Sun, Z. P.; Li, Z. J. Preparation of La1.9Ca0.1Zr2O 6.95 with pyrochlore structure and its application in synthesis of ammonia at atmospheric pressure. *Solid State Ionics* **2004**, *168*, 117−121.
(250) Wang, W. B.; Cao, X. B.; Gao, W. J.; Zhang, F.; Wang, H. T.; Ma, G. L. Ammonia synthesis at atmospheric pressure using a reactor with thin solid electrolyte BaCe0.85Y0.15O3-α membrane. *J. Membr. Sci.* **2010**, *360*, 397−403.
(251) Vasileiou, E.; Kyriakou, V.; Garagounis, I.; Vourros, A.; Stoukides, M. Ammonia synthesis at atmospheric pressure in a BaCe0.2Zr0.7Y0.1O2.9 solid electrolyte cell. *Solid State Ionics* **2015**, *275*, 110−116.
(252) Zhang, F.; Yang, Q.; Pan, B.; Xu, R.; Wang, H.; Ma, G. Proton conduction in La0.9Sr0.1Ga0.8Mg0.2O3-α ceramic prepared via microemulsion method and its application in ammonia synthesis at atmospheric pressure. *Mater. Lett.* **2007**, *61*, 4144−4148.
(253) Marnellos, G.; Stoukides, M. Ammonia synthesis at atmospheric pressure. *Science* **1998**, *282*, 98−100.
(254) Jeoung, H.; Kim, J. N.; Yoo, C. Y.; Joo, J. H.; Yu, J. H.; Song, K. C.; Sharma, M.; Yoon, H. C. Electrochemical synthesis of ammonia from water and nitrogen using a Pt/GDC/Pt cell. *Korean Chemical Engineering Research* **2014**, *52*, 58−62.
(255) Skodra, A.; Stoukides, M. Electrocatalytic synthesis of ammonia from steam and nitrogen at atmospheric pressure. *Solid State Ionics* **2009**, *180*, 1332−1336.
(256) Amar, I. A.; Lan, R.; Tao, S. Synthesis of ammonia directly from wet nitrogen using a redox stable La0.75Sr0.25Cr0.5Fe0.5O3-δ-Ce0.8Gd0.18Ca0.02O2-δ composite cathode. *RSC Adv.* **2015**, *5*, 38977−38983.
(257) Lan, R.; Alkhazmi, K. A.; Amar, I. A.; Tao, S. Synthesis of ammonia directly from wet air at intermediate temperature. *Applied Catalysis B: Environmental* **2014**, *152*−*153*, 212−217.
(258) Yun, D. S.; Joo, J. H.; Yu, J. H.; Yoon, H. C.; Kim, J. N.; Yoo, C. Y. Electrochemical ammonia synthesis from steam and nitrogen using proton conducting yttrium doped barium zirconate electrolyte with silver, platinum, and lanthanum strontium cobalt ferrite electrocatalyst. *J. Power Sources* **2015**, *284*, 245−251.
(259) Yang, L.; Wu, T.; Zhang, R.; Zhou, H.; Xia, L.; Shi, X.; Zheng, H.; Zhang, Y.; Sun, X. Insights into defective TiO 2 in electrocatalytic N 2 reduction: combining theoretical and experimental studies. *Nanoscale* **2019**, *11*, 1555−1562.
(260) Zhang, R.; Ren, X.; Shi, X.; Xie, F.; Zheng, B.; Guo, X.; Sun, X. Enabling effective electrocatalytic N2 conversion to NH3 by the TiO2 nanosheets array under ambient conditions. *ACS Appl. Mater. Interfaces* **2018**, *10*, 28251−28255.
(261) Wu, T.; Zhu, X.; Xing, Z.; Mou, S.; Li, C.; Qiao, Y.; Liu, Q.; Luo, Y.; Shi, X.; Zhang, Y.; Sun, X. Greatly improving electrochemical N2 reduction over TiO2 nanoparticles by iron doping. *Angew. Chem., Int. Ed.* **2019**, *58*, 18449−18453.
(262) Kong, W.; Gong, F. F.; Zhou, Q.; Yu, G.; Ji, L.; Sun, X.; Asiri, A. M.; Wang, T.; Luo, Y.; Xu, Y. An MnO 2−Ti 3 C 2 T x MXene nanohybrid: an efficient and durable electrocatalyst toward artificial N 2 fixation to NH 3 under ambient conditions. *Journal of Materials Chemistry A* **2019**, *7*, 18823−18827.
(263) Liu, G.; Cui, Z.; Han, M.; Zhang, S.; Zhao, C.; Chen, C.; Wang, G.; Zhang, H. Ambient Electrosynthesis of Ammonia on a Core−Shell-Structured Au@ CeO2 Catalyst: Contribution of Oxygen Vacancies in CeO2. *Chemistry−A European Journal* **2019**, *25*, 5904−5911.
(264) Xie, H.; Wang, H.; Geng, Q.; Xing, Z.; Wang, W.; Chen, J.; Ji, L.; Chang, L.; Wang, Z.; Mao, J. Oxygen vacancies of Cr-doped CeO2 nanorods that efficiently enhance the performance of electrocatalytic N2 fixation to NH3 under ambient conditions. *Inorg. Chem.* **2019**, *58*, 5423−5427.
(265) Zhang, S.; Zhao, C.; Liu, Y.; Li, W.; Wang, J.; Wang, G.; Zhang, Y.; Zhang, H.; Zhao, H. Cu doping in CeO 2 to form multiple oxygen vacancies for dramatically enhanced ambient N 2 reduction performance. *Chem. Commun.* **2019**, *55*, 2952−2955.
(266) Lv, C.; Yan, C.; Chen, G.; Ding, Y.; Sun, J.; Zhou, Y.; Yu, G. An amorphous noble-metal-free electrocatalyst that enables nitrogen fixation under ambient conditions. *Angew. Chem.* **2018**, *130*, 6181−6184.
(267) Suryanto, B. H.; Wang, D.; Azofra, L. M.; Harb, M.; Cavallo, L.; Jalili, R.; Mitchell, D. R.; Chatti, M.; MacFarlane, D. R. MoS2 polymorphic engineering enhances selectivity in the electrochemical reduction of nitrogen to ammonia. *ACS Energy Letters* **2019**, *4*, 430−435.
(268) Li, L.; Zhang, M.; Zhang, T.; Gao, Y.; Ni, J.; Zhou, Y.; Lin, J.; Wang, X.; Jiang, L. Strong Ruδ+−Ce3+ electronic interaction induced by a CeOy overlayer for enhanced low-temperature N2-to-NH3 conversion. *Catalysis Science & Technology* **2023**, *13*, 2134−2141.
(269) Wang, R.; Gao, W.; Feng, S.; Guan, Y.; Wang, Q.; Guo, J.; Chen, P. Zn Promotes Chemical Looping Ammonia Synthesis Mediated by LiH−Li2NH Couple, *ChemSusChem* **2023**, e202300813.
(270) Gorky, F.; Best, A.; Jasinski, J.; Allen, B. J.; Alba-Rubio, A. C.; Carreon, M. L. Plasma catalytic ammonia synthesis on Ni nanoparticles: The size effect. *J. Catal.* **2021**, *393*, 369−380.
(271) Cai, W.; Jiang, Y.-F.; Zhang, J.; Yang, H.; Zhang, J.; Xu, C.-Q.; Liu, W.; Li, J.; Liu, B. Ruthenium/titanium oxide interface promoted electrochemical nitrogen reduction reaction. *Chem. Catalysis* **2022**, *2*, 1764−1774.
(272) He, W.; Zhang, J.; Dieckhöfer, S.; Varhade, S.; Brix, A. C.; Lielpetere, A.; Seisel, S.; Junqueira, J. R. C.; Schuhmann, W. Splicing the active phases of copper/cobalt-based catalysts achieves high-rate tandem electroreduction of nitrate to ammonia. *Nat. Commun.* **2022**, *13*, 1129.
(273) Croisé, C.; Alabd, K.; Tencé, S.; Gaudin, E.; Villesuzanne, A.; Courtois, X.; Bion, N.; Can, F. Influence of the Rare Earth (R) Element in Ru-supported RScSi Electride-like Intermetallic Catalysts for Ammonia Synthesis at Low Pressure: Insight into NH3 Formation Mechanism. *ChemCatChem.* **2023**, *15*, No. e202201172.
(274) Li, H.; Gong, Y.; Yang, H.; Yang, X.; Li, K.; Wang, J.; Hosono, H. Ammonia Synthesis on Ternary LaSi-based Electrides: Tuning the Catalytic Mechanism by the Third Metal, *ChemSusChem* **2023**, e202301016.
(275) Gupta, D.; Kafle, A.; Nagaiah, T. C. Dinitrogen Reduction Coupled with Methanol Oxidation for Low Overpotential Electrochemical NH3 Synthesis Over Cobalt Pyrophosphate as Bifunctional Catalyst. *Small* **2023**, *19*, No. 2208272.
(276) Gao, W.; Wang, Q.; Guan, Y.; Yan, H.; Guo, J.; Chen, P. Barium hydride activates Ni for ammonia synthesis catalysis. *Faraday Discuss.* **2023**, *243*, 27−37.
(277) Miyazaki, M.; Ikejima, K.; Ogasawara, K.; Kitano, M.; Hosono, H. Ammonia Synthesis over Fe-Supported Catalysts Mediated by Face-Sharing Nitrogen Sites in $BaTiO_{3-x}N_y$ Oxynitride, *ChemSusChem* **2023**, e202300551.
(278) Ye, T.-N.; Park, S.-W.; Lu, Y.; Li, J.; Wu, J.; Sasase, M.; Kitano, M.; Hosono, H. Dissociative and Associative Concerted Mechanism

for Ammonia Synthesis over Co-Based Catalyst. *J. Am. Chem. Soc.* **2021**, *143*, 12857−12866.
(279) Jiang, Y.; Takashima, R.; Nakao, T.; Miyazaki, M.; Lu, Y.; Sasase, M.; Niwa, Y.; Abe, H.; Kitano, M.; Hosono, H. Boosted Activity of Cobalt Catalysts for Ammonia Synthesis with BaAl2O4−xHy Electrides. *J. Am. Chem. Soc.* **2023**, *145*, 10669−10680.
(280) Nazemi, M.; Panikkanvalappil, S. R.; El-Sayed, M. A. Enhancing the rate of electrochemical nitrogen reduction reaction for ammonia synthesis under ambient conditions using hollow gold nanocages. *Nano Energy* **2018**, *49*, 316−323.
(281) Geng, Z.; Liu, Y.; Kong, X.; Li, P.; Li, K.; Liu, Z.; Du, J.; Shu, M.; Si, R.; Zeng, J. Achieving a Record-High Yield Rate of 120.9 for N2 Electrochemical Reduction over Ru Single-Atom Catalysts. *Adv. Mater.* **2018**, *30*, No. 1803498.
(282) Han, J.; Ji, X.; Ren, X.; Cui, G.; Li, L.; Xie, F.; Wang, H.; Li, B.; Sun, X. MoO3 nanosheets for efficient electrocatalytic N2 fixation to NH3. *Journal of Materials Chemistry A* **2018**, *6*, 12974−12977.
(283) Zhang, L.; Ji, X.; Ren, X.; Ma, Y.; Shi, X.; Tian, Z.; Asiri, A. M.; Chen, L.; Tang, B.; Sun, X. Electrochemical Ammonia Synthesis via Nitrogen Reduction Reaction on a MoS2 Catalyst: Theoretical and Experimental Studies. *Adv. Mater.* **2018**, *30*, No. 1800191.
(284) Wu, X.; Xia, L.; Wang, Y.; Lu, W.; Liu, Q.; Shi, X.; Sun, X. Mn3O4 Nanocube: An Efficient Electrocatalyst Toward Artificial N2 Fixation to NH3. *Small* **2018**, *14*, No. 1803111.
(285) Han, J.; Liu, Z.; Ma, Y.; Cui, G.; Xie, F.; Wang, F.; Wu, Y.; Gao, S.; Xu, Y.; Sun, X. Ambient N2 fixation to NH3 at ambient conditions: Using Nb2O5 nanofiber as a high-performance electrocatalyst. *Nano Energy* **2018**, *52*, 264−270.
(286) Liu, F.; Shan, W.; Pan, D.; Li, T.; He, H. Selective catalytic reduction of NOx by NH3 for heavy-duty diesel vehicles. *Chinese Journal of Catalysis* **2014**, *35*, 1438−1445.
(287) Zhao, B.; Wang, S. X.; Liu, H.; Xu, J. Y.; Fu, K.; Klimont, Z.; Hao, J. M.; He, K. B.; Cofala, J.; Amann, M. NOx emissions in China: historical trends and future perspectives. *Atmos. Chem. Phys.* **2013**, *13*, 9869−9897.
(288) Granger, P.; Parvulescu, V. I. Catalytic NOx Abatement Systems for Mobile Sources: From Three-Way to Lean Burn after-Treatment Technologies. *Chem. Rev.* **2011**, *111*, 3155−3207.
(289) Li, Y.; Cheng, H.; Li, D.; Qin, Y.; Xie, Y.; Wang, S. WO3/CeO2-ZrO2, a promising catalyst for selective catalytic reduction (SCR) of NOx with NH3 in diesel exhaust. *Chem. Commun.* **2008**, 1470−1472.
(290) Qiu, W.; Xie, X.-Y.; Qiu, J.; Fang, W.-H.; Liang, R.; Ren, X.; Ji, X.; Cui, G.; Asiri, A. M.; Cui, G.; Tang, B.; Sun, X. High-performance artificial nitrogen fixation at ambient conditions using a metal-free electrocatalyst. *Nat. Commun.* **2018**, *9*, 3485.
(291) Hong, W. T.; Risch, M.; Stoerzinger, K. A.; Grimaud, A.; Suntivich, J.; Shao-Horn, Y. Toward the rational design of non-precious transition metal oxides for oxygen electrocatalysis. *Energy Environ. Sci.* **2015**, *8*, 1404−1427.
(292) Zhang, X.; Liu, Q.; Shi, X.; Asiri, A. M.; Luo, Y.; Sun, X.; Li, T. TiO2 nanoparticles−reduced graphene oxide hybrid: an efficient and durable electrocatalyst toward artificial N2 fixation to NH3 under ambient conditions. *Journal of Materials Chemistry A* **2018**, *6*, 17303−17306.
(293) Wang, Y.; Jia, K.; Pan, Q.; Xu, Y.; Liu, Q.; Cui, G.; Guo, X.; Sun, X. Boron-Doped TiO2 for Efficient Electrocatalytic N2 Fixation to NH3 at Ambient Conditions. *ACS Sustainable Chem. Eng.* **2019**, *7*, 117−122.
(294) Zhang, Y.; Qiu, W.; Ma, Y.; Luo, Y.; Tian, Z.; Cui, G.; Xie, F.; Chen, L.; Li, T.; Sun, X. High-Performance Electrohydrogenation of N2 to NH3 Catalyzed by Multishelled Hollow Cr2O3Microspheres under Ambient Conditions. *ACS Catal.* **2018**, *8*, 8540−8544.
(295) Li, J.; Meng, X.; Xiao, F.-S. Zeolites for control of NOx emissions: Opportunities and challenges. *Chem. Catalysis* **2022**, *2*, 253−261.
(296) Lv, C.; Yan, C.; Chen, G.; Ding, Y.; Sun, J.; Zhou, Y.; Yu, G. An Amorphous Noble-Metal-Free Electrocatalyst that Enables Nitrogen Fixation under Ambient Conditions. *Angew. Chem., Int. Ed.* **2018**, *57*, 6073−6076.
(297) Li, X.; Li, T.; Ma, Y.; Wei, Q.; Qiu, W.; Guo, H.; Shi, X.; Zhang, P.; Asiri, A. M.; Chen, L.; Tang, B.; Sun, X. Boosted Electrocatalytic N2 Reduction to NH3 by Defect-Rich MoS2 Nanoflower. *Adv. Energy Mater.* **2018**, *8*, No. 1801357.
(298) (a) Luo, Y.; Chen, G.; Ding, L.; Chen, X.; Ding, L.; Wang, H. *Joule* **2019**, *3*, 279−289. (i) Liu, H.-M.; Han, S.-H.; Zhao, Y.; Zhu, Y.-Y.; Tian, X.-L.; Zeng, J.-H.; Jiang, J.-X.; Xia, B. Y.; Chen, Y. Surfactant-free atomically ultrathin rhodium nanosheet nanoassemblies for efficient nitrogen electroreduction. *J. Mater. Chem. A* **2018**, *6*, 3211−3217.
(299) Yu, X.; Han, P.; Wei, Z.; Huang, L.; Gu, Z.; Peng, S.; Ma, J.; Zheng, G. Boron-doped graphene for electrocatalytic N2 reduction. *Joule* **2018**, *2*, 1610−1622.
(300) Chen, G.-F.; Cao, X.; Wu, S.; Zeng, X.; Ding, L.-X.; Zhu, M.; Wang, H. Ammonia Electrosynthesis with High Selectivity under Ambient Conditions via a Li+ Incorporation Strategy. *J. Am. Chem. Soc.* **2017**, *139*, 9771−9774.
(301) Tao, H.; Choi, C.; Ding, L.-X.; Jiang, Z.; Han, Z.; Jia, M.; Fan, Q.; Gao, Y.; Wang, H.; Robertson, A. W.; Hong, S.; Jung, Y.; Liu, S.; Sun, Z. Nitrogen Fixation by Ru Single-Atom Electrocatalytic Reduction. *Chem.* **2019**, *5*, 204−214.
(302) Chen, S.; Perathoner, S.; Ampelli, C.; Mebrahtu, C.; Su, D.; Centi, G. Electrocatalytic Synthesis of Ammonia at Room Temperature and Atmospheric Pressure from Water and Nitrogen on a Carbon-Nanotube-Based Electrocatalyst. *Angew. Chem., Int. Ed.* **2017**, *56*, 2699−2703.
(303) Cheng, H.; Ding, L.-X.; Chen, G.-F.; Zhang, L.; Xue, J.; Wang, H. Molybdenum Carbide Nanodots Enable Efficient Electrocatalytic Nitrogen Fixation under Ambient Conditions. *Adv. Mater.* **2018**, *30*, No. 1803694.
(304) Zhang, H.; Liu, G.; Shi, L.; Ye, J. Single-Atom Catalysts: Emerging Multifunctional Materials in Heterogeneous Catalysis. *Adv. Energy Mater.* **2018**, *8*, No. 1701343.
(305) Han, L.; Liu, X.; Chen, J.; Lin, R.; Liu, H.; Lü, F.; Bak, S.; Liang, Z.; Zhao, S.; Stavitski, E.; Luo, J.; Adzic, R. R.; Xin, H. L. Atomically Dispersed Molybdenum Catalysts for Efficient Ambient Nitrogen Fixation. *Angew. Chem., Int. Ed.* **2019**, *58*, 2321−2325.
(306) Cui, X.; Tang, C.; Zhang, Q. A review of electrocatalytic reduction of dinitrogen to ammonia under ambient conditions. *Adv. Energy Mater.* **2018**, *8*, No. 1800369.
(307) Gao, K.; Wang, B.; Tao, L.; Cunning, B. V.; Zhang, Z.; Wang, S.; Ruoff, R. S.; Qu, L. Efficient metal-free electrocatalysts from N-doped carbon nanomaterials: mono-doping and co-doping. *Adv. Mater.* **2019**, *31*, No. 1805121.
(308) Li, W.; Wu, T.; Zhang, S.; Liu, Y.; Zhao, C.; Liu, G.; Wang, G.; Zhang, H.; Zhao, H. Nitrogen-free commercial carbon cloth with rich defects for electrocatalytic ammonia synthesis under ambient conditions. *Chem. Commun.* **2018**, *54*, 11188−11191.
(309) Liu, Y.; Su, Y.; Quan, X.; Fan, X.; Chen, S.; Yu, H.; Zhao, H.; Zhang, Y.; Zhao, J. Facile ammonia synthesis from electrocatalytic N2 reduction under ambient conditions on N-doped porous carbon. *ACS Catal.* **2018**, *8*, 1186−1191.
(310) Wort, C. J.; Balmer, R. S. Diamond as an electronic material. *Mater. Today* **2008**, *11*, 22−28.
(311) Einaga, Y. Diamond electrodes for electrochemical analysis. *Journal of applied electrochemistry* **2010**, *40*, 1807−1816.
(312) Liu, B.; Zheng, Y.; Peng, H.-Q.; Ji, B.; Yang, Y.; Tang, Y.; Lee, C.-S.; Zhang, W. Nanostructured and Boron-Doped Diamond as an Electrocatalyst for Nitrogen Fixation. *ACS Energy Letters* **2020**, *5*, 2590−2596.
(313) Reyter, D.; Bélanger, D.; Roué, L. Study of the electroreduction of nitrate on copper in alkaline solution. *Electrochim. Acta* **2008**, *53*, 5977−5984.
(314) Pérez-Gallent, E.; Figueiredo, M. C.; Katsounaros, I.; Koper, M. T. Electrocatalytic reduction of Nitrate on Copper single crystals in acidic and alkaline solutions. *Electrochim. Acta* **2017**, *227*, 77−84.

https://doi.org/10.1021/acscatal.3c02410
ACS Catal. 2023, 13, 14415−14453

(315) Zhang, X.; Wang, Y.; Liu, C.; Yu, Y.; Lu, S.; Zhang, B. Recent advances in non-noble metal electrocatalysts for nitrate reduction. *Chemical Engineering Journal* **2021**, *403*, No. 126269.
(316) Martínez, J.; Ortiz, A.; Ortiz, I. State-of-the-art and perspectives of the catalytic and electrocatalytic reduction of aqueous nitrates. *Applied Catalysis B: Environmental* **2017**, *207*, 42−59.
(317) Xing, Y.; Guo, X.; Jia, G.; Fang, S.; Zhao, C.; Liu, Z. Investigations on the Zn/Fe ratio and activation route during CO hydrogenation over porous iron/spinel catalysts, Reaction Kinetics. *Mechanisms and Catalysis* **2020**, *129*, 755−772.
(318) Zhou, M.; Cai, L.; Bajdich, M.; García-Melchor, M.; Li, H.; He, J.; Wilcox, J.; Wu, W.; Vojvodic, A.; Zheng, X. Enhancing Catalytic CO Oxidation over Co3O4 Nanowires by Substituting Co2+ with Cu2+. *ACS Catal.* **2015**, *5*, 4485−4491.
(319) Gao, C.; Meng, Q.; Zhao, K.; Yin, H.; Wang, D.; Guo, J.; Zhao, S.; Chang, L.; He, M.; Li, Q.; Zhao, H.; Huang, X.; Gao, Y.; Tang, Z. Co3O4 Hexagonal Platelets with Controllable Facets Enabling Highly Efficient Visible-Light Photocatalytic Reduction of CO2. *Adv. Mater.* **2016**, *28*, 6485−6490.
(320) Zhang, B.; Cheng, M.; Liu, G.; Gao, Y.; Zhao, L.; Li, S.; Wang, Y.; Liu, F.; Liang, X.; Zhang, T.; Lu, G. Room temperature NO2 gas sensor based on porous Co3O4 slices/reduced graphene oxide hybrid. *Sens. Actuators, B* **2018**, *263*, 387−399.
(321) Ma, L.; Seo, C. Y.; Chen, X.; Sun, K.; Schwank, J. W. Indium-doped Co3O4 nanorods for catalytic oxidation of CO and C3H6 towards diesel exhaust. *Applied Catalysis B: Environmental* **2018**, *222*, 44−58.
(322) Nawaz, M. A.; Saif, M.; Li, M.; Song, G.; Zihao, W.; Liu, D. Tailoring the synergistic dual-decoration of (Cu−Co) transition metal auxiliaries in Fe-oxide/zeolite composite catalyst for the direct conversion of syngas to aromatics. *Catalysis Science & Technology* **2021**, *11*, 7992−8006.
(323) Nawaz, M. A.; Li, M.; Saif, M.; Song, G.; Wang, Z.; Liu, D. Harnessing the Synergistic Interplay of Fischer−Tropsch Synthesis (Fe-Co) Bimetallic Oxides in Na-FeMnCo/HZSM-5 Composite Catalyst for Syngas Conversion to Aromatic Hydrocarbons. *ChemCatChem.* **2021**, *13*, 1966−1980.
(324) Guo, W.; Liang, Z.; Zhao, J.; Zhu, B.; Cai, K.; Zou, R.; Xu, Q. Hierarchical Cobalt Phosphide Hollow Nanocages toward Electrocatalytic Ammonia Synthesis under Ambient Pressure and Room Temperature. *Small Methods* **2018**, *2*, No. 1800204.
(325) Zhang, S.; Gong, W.; Lv, Y.; Wang, H.; Han, M.; Wang, G.; Shi, T.; Zhang, H. A pyrolysis−phosphorization approach to fabricate carbon nanotubes with embedded CoP nanoparticles for ambient electrosynthesis of ammonia. *Chem. Commun.* **2019**, *55*, 12376−12379.
(326) Chu, K.; Liu, Y.-p.; Li, Y.-b.; Zhang, H.; Tian, Y. Efficient electrocatalytic N2 reduction on CoO quantum dots. *Journal of Materials Chemistry A* **2019**, *7*, 4389−4394.
(327) Gao, J.; Lv, X.; Wang, F.; Luo, Y.; Lu, S.; Chen, G.; Gao, S.; Zhong, B.; Guo, X.; Sun, X. Enabling electrochemical conversion of N2 to NH3 under ambient conditions by a CoP3 nanoneedle array. *Journal of Materials Chemistry A* **2020**, *8*, 17956−17959.
(328) Wang, Y.; Zhou, W.; Jia, R.; Yu, Y.; Zhang, B. Unveiling the activity origin of a copper-based electrocatalyst for selective nitrate reduction to ammonia. *Angew. Chem., Int. Ed.* **2020**, *59*, 5350−5354.
(329) Lin, B.; Heng, L.; Fang, B.; Yin, H.; Ni, J.; Wang, X.; Lin, J.; Jiang, L. Ammonia synthesis activity of alumina-supported ruthenium catalyst enhanced by alumina phase transformation. *ACS Catal.* **2019**, *9*, 1635−1644.
(330) Zheng, J.; Liao, F.; Wu, S.; Jones, G.; Chen, T. Y.; Fellowes, J.; Sudmeier, T.; McPherson, I. J.; Wilkinson, I.; Tsang, S. C. E. Efficient non-dissociative activation of dinitrogen to ammonia over lithium-promoted ruthenium nanoparticles at low pressure. *Angew. Chem., Int. Ed.* **2019**, *58*, 17335−17341.
(331) Tang, Y.; Kobayashi, Y.; Masuda, N.; Uchida, Y.; Okamoto, H.; Kageyama, T.; Hosokawa, S.; Loyer, F.; Mitsuhara, K.; Yamanaka, K.; et al. Metal-Dependent Support Effects of Oxyhydride-Supported Ru, Fe, Co Catalysts for Ammonia Synthesis, Advanced Energy. *Materials* **2018**, *8*, No. 1801772.
(332) Sato, K.; Imamura, K.; Kawano, Y.; Miyahara, S.-i.; Yamamoto, T.; Matsumura, S.; Nagaoka, K. A low-crystalline ruthenium nano-layer supported on praseodymium oxide as an active catalyst for ammonia synthesis. *Chemical science* **2017**, *8*, 674−679.
(333) Bielawa, H.; Hinrichsen, O.; Birkner, A.; Muhler, M. The ammonia-synthesis catalyst of the next generation: barium-promoted oxide-supported ruthenium. *Angew. Chem., Int. Ed.* **2001**, *40*, 1061−1063.
(334) Aika, K.-i.; Takano, T.; Murata, S. Preparation and characterization of chlorine-free ruthenium catalysts and the promoter effect in ammonia synthesis: 3. A magnesia-supported ruthenium catalyst. *J. Catal.* **1992**, *136*, 126−140.
(335) Dowben, P.; Miller, A.; Ruppender, H.-J.; Grunze, M. The influence of surface metal composition of Fe— Cr alloys on the dissociative adsorption of N2. *Surf. Sci.* **1988**, *193*, 336−352.
(336) Skulason, E.; Bligaard, T.; Gudmundsdóttir, S.; Studt, F.; Rossmeisl, J.; Abild-Pedersen, F.; Vegge, T.; Jónsson, H.; Nørskov, J. K. A theoretical evaluation of possible transition metal electro-catalysts for N 2 reduction. *Phys. Chem. Chem. Phys.* **2012**, *14*, 1235−1245.
(337) Vojvodic, A.; Medford, A. J.; Studt, F.; Abild-Pedersen, F.; Khan, T. S.; Bligaard, T.; Nørskov, J. Exploring the limits: A low-pressure, low-temperature Haber−Bosch process. *Chem. Phys. Lett.* **2014**, *598*, 108−112.
(338) Guan, Y.; Zhang, W.; Wang, Q.; Weidenthaler, C.; Wu, A.; Gao, W.; Pei, Q.; Yan, H.; Cui, J.; Wu, H.; Feng, S.; Wang, R.; Cao, H.; Ju, X.; Liu, L.; He, T.; Guo, J.; Chen, P. Barium chromium nitride-hydride for ammonia synthesis. *Chem. Catalysis* **2021**, *1*, 1042−1054.
(339) Chu, K.; Liu, Y.-p.; Li, Y.-b.; Wang, J.; Zhang, H. Electronically Coupled SnO2 Quantum Dots and Graphene for Efficient Nitrogen Reduction Reaction. *ACS Appl. Mater. Interfaces* **2019**, *11*, 31806−31815.
(340) Xu, Y.; Liu, J.; Wang, J.; Ma, G.; Lin, J.; Yang, Y.; Li, Y.; Zhang, C.; Ding, M. Selective Conversion of Syngas to Aromatics over Fe_3O_4@MnO_2 and Hollow HZSM-5 Bifunctional Catalysts. *ACS Catal.* **2019**, *9*, 5147−5156.
(341) Chang, B.; Liu, Q.; Chen, N.; Yang, Y. A Flower-like Bismuth Oxide as an Efficient, Durable and Selective Electrocatalyst for Artificial N2 Fixation in Ambient Condition. *ChemCatChem.* **2019**, *11*, 1884−1888.
(342) Yao, D.; Tang, C.; Li, L.; Xia, B.; Vasileff, A.; Jin, H.; Zhang, Y.; Qiao, S.-Z. In Situ Fragmented Bismuth Nanoparticles for Electrocatalytic Nitrogen Reduction. *Adv. Energy Mater.* **2020**, *10*, No. 2001289.
(343) Sun, Z.; Ma, T.; Tao, H.; Fan, Q.; Han, B. Fundamentals and challenges of electrochemical CO2 reduction using two-dimensional materials. *Chem.* **2017**, *3*, 560−587.
(344) Tsai, M.-C.; Nguyen, T.-T.; Akalework, N. G.; Pan, C.-J.; Rick, J.; Liao, Y.-F.; Su, W.-N.; Hwang, B.-J. Interplay between molybdenum dopant and oxygen vacancies in a TiO2 support enhances the oxygen reduction reaction. *ACS catalysis* **2016**, *6*, 6551−6559.
(345) Li, J.; Zhou, H.; Zhuo, H.; Wei, Z.; Zhuang, G.; Zhong, X.; Deng, S.; Li, X.; Wang, J. Oxygen vacancies on TiO 2 promoted the activity and stability of supported Pd nanoparticles for the oxygen reduction reaction. *Journal of Materials Chemistry A* **2018**, *6*, 2264−2272.
(346) Liu, L.; Jiang, Y.; Zhao, H.; Chen, J.; Cheng, J.; Yang, K.; Li, Y. Engineering coexposed {001} and {101} facets in oxygen-deficient TiO2 nanocrystals for enhanced CO2 photoreduction under visible light. *ACS Catal.* **2016**, *6*, 1097−1108.
(347) Geng, Z.; Kong, X.; Chen, W.; Su, H.; Liu, Y.; Cai, F.; Wang, G.; Zeng, J. Oxygen vacancies in ZnO nanosheets enhance CO2 electrochemical reduction to CO. *Angew. Chem.* **2018**, *130*, 6162−6167.
(348) Sun, Z.; Talreja, N.; Tao, H.; Texter, J.; Muhler, M.; Strunk, J.; Chen, J. Catalysis of carbon dioxide photoreduction on nanosheets:

https://doi.org/10.1021/acscatal.3c02410
ACS Catal. 2023, 13, 14415−14453

fundamentals and challenges. *Angew. Chem., Int. Ed.* **2018**, *57*, 7610−7627.
(349) Liu, Y.; Miao, C.; Yang, P.; He, Y.; Feng, J.; Li, D. Synergetic promotional effect of oxygen vacancy-rich ultrathin TiO2 and photochemical induced highly dispersed Pt for photoreduction of CO2 with H2O. *Applied Catalysis B: Environmental* **2019**, *244*, 919−930.
(350) Hirakawa, H.; Hashimoto, M.; Shiraishi, Y.; Hirai, T. Photocatalytic conversion of nitrogen to ammonia with water on surface oxygen vacancies of titanium dioxide. *J. Am. Chem. Soc.* **2017**, *139*, 10929−10936.
(351) Li, H.; Shang, J.; Ai, Z.; Zhang, L. Efficient visible light nitrogen fixation with BiOBr nanosheets of oxygen vacancies on the exposed {001} facets. *J. Am. Chem. Soc.* **2015**, *137*, 6393−6399.
(352) Zhao, Y.; Zhao, Y.; Waterhouse, G. I.; Zheng, L.; Cao, X.; Teng, F.; Wu, L. Z.; Tung, C. H.; O'Hare, D.; Zhang, T. Layered-double-hydroxide nanosheets as efficient visible-light-driven photocatalysts for dinitrogen fixation. *Adv. Mater.* **2017**, *29*, No. 1703828.
(353) Li, C.; Wang, T.; Zhao, Z. J.; Yang, W.; Li, J. F.; Li, A.; Yang, Z.; Ozin, G. A.; Gong, J. Promoted fixation of molecular nitrogen with surface oxygen vacancies on plasmon-enhanced TiO2 photoelectrodes. *Angew. Chem., Int. Ed.* **2018**, *57*, 5278−5282.
(354) Can, F.; Berland, S.; Royer, S.; Courtois, X.; Duprez, D. Composition-Dependent Performance of CexZr1−xO2Mixed-Oxide-Supported WO3 Catalysts for the NOx Storage Reduction−Selective Catalytic Reduction Coupled Process. *ACS Catal.* **2013**, *3*, 1120−1132.
(355) Shan, W.; Liu, F.; Yu, Y.; He, H. The use of ceria for the selective catalytic reduction of NOx with NH3. *Chinese Journal of Catalysis* **2014**, *35*, 1251−1259.
(356) Si, Z.; Weng, D.; Wu, X.; Yang, J.; Wang, B. Modifications of CeO2−ZrO2 solid solutions by nickel and sulfate as catalysts for NO reduction with ammonia in excess O2. *Catal. Commun.* **2010**, *11*, 1045−1048.
(357) Yan, H.; Zhang, N.; Wang, D. Highly efficient CeO2-supported noble-metal catalysts: From single atoms to nanoclusters. *Chem. Catalysis* **2022**, *2*, 1594−1623.
(358) Zhao, S.; Liu, H. X.; Qiu, Y.; Liu, S. Q.; Diao, J. X.; Chang, C. R.; Si, R.; Guo, X. H. An oxygen vacancy-rich two-dimensional Au/TiO2 hybrid for synergistically enhanced electrochemical N2 activation and reduction. *Journal of Materials Chemistry A* **2020**, *8*, 6586−6596.
(359) Fang, Y.; Liu, Z.; Han, J.; Jin, Z.; Han, Y.; Wang, F.; Niu, Y.; Wu, Y.; Xu, Y. High-Performance Electrocatalytic Conversion of N 2 to NH 3 Using Oxygen-Vacancy-Rich TiO 2 In Situ Grown on Ti 3 C 2 T x MXene. *Adv. Energy Mater.* **2019**, *9*, 1803406.
(360) Fang, C.; Bi, T.; Xu, X.; Yu, N.; Cui, Z.; Jiang, R.; Geng, B. Oxygen Vacancy−Enhanced Electrocatalytic Performances of TiO_2 Nanosheets toward N_2 Reduction Reaction. *Advanced Materials Interfaces* **2019**, *6*, 1901034.
(361) Chu, K.; Liu, Y. P.; Cheng, Y. H.; Li, Q. Q. Synergistic boron-dopants and boron-induced oxygen vacancies in MnO2 nanosheets to promote electrocatalytic nitrogen reduction. *Journal of Materials Chemistry A* **2020**, *8*, 5200−5208.
(362) Zhang, J.; Yang, L.; Wang, H.; Zhu, G.; Wen, H.; Feng, H.; Sun, X.; Guan, X.; Wen, J.; Yao, Y. In Situ Hydrothermal Growth of TiO2 Nanoparticles on a Conductive Ti3C2Tx MXene Nanosheet: A Synergistically Active Ti-Based Nanohybrid Electrocatalyst for Enhanced N2 Reduction to NH3 at Ambient Conditions. *Inorg. Chem.* **2019**, *58*, 5414−5418.
(363) Han, Z.; Choi, C.; Hong, S.; Wu, T.-S.; Soo, Y.-L.; Jung, Y.; Qiu, J.; Sun, Z. Activated TiO2 with tuned vacancy for efficient electrochemical nitrogen reduction. *Applied Catalysis B: Environmental* **2019**, *257*, No. 117896.
(364) Wu, T.; Zhao, H.; Zhu, X.; Xing, Z.; Liu, Q.; Liu, T.; Gao, S.; Lu, S.; Chen, G.; Asiri, A.M.; Zhang, Y.; Sun, X. Identifying the Origin of Ti3+ Activity toward Enhanced Electrocatalytic N2 Reduction over TiO2 Nanoparticles Modulated by Mixed-Valent Copper. *Adv. Mater.* **2020**, *32*, 2000299.
(365) Cao, N.; Chen, Z.; Zang, K.; Xu, J.; Zhong, J.; Luo, J.; Xu, X.; Zheng, G. Doping strain induced bi-Ti3+ pairs for efficient N2 activation and electrocatalytic fixation. *Nat. Commun.* **2019**, *10*, 2877.
(366) Xu, B.; Liu, Z.; Qiu, W.; Liu, Q.; Sun, X.; Cui, G.; Wu, Y.; Xiong, X. La 2 O 3 nanoplate: An efficient electrocatalyst for artificial N 2 fixation to NH 3 with excellent selectivity at ambient condition. *Electrochim. Acta* **2019**, *298*, 106−111.
(367) Li, L.; Chen, H.; Li, L.; Li, B.; Wu, Q.; Cui, C.; Deng, B.; Luo, Y.; Liu, Q.; Li, T.; Zhang, F.; Asiri, A. M.; Feng, Z.-S.; Wang, Y.; Sun, X. La-doped TiO2 nanorods toward boosted electrocatalytic N2-to-NH3 conversion at ambient conditions. *Chinese Journal of Catalysis* **2021**, *42*, 1755−1762.
(368) Wang, Q.; Pan, J.; Guo, J.; Hansen, H. A.; Xie, H.; Jiang, L.; Hua, L.; Li, H.; Guan, Y.; Wang, P.; Gao, W.; Liu, L.; Cao, H.; Xiong, Z.; Vegge, T.; Chen, P. Ternary ruthenium complex hydrides for ammonia synthesis via the associative mechanism. *Nature Catalysis* **2021**, *4*, 959−967.
(369) Valov, I.; Luerssen, B.; Mutoro, E.; Gregoratti, L.; De Souza, R. A.; Bredow, T.; Günther, S.; Barinov, A.; Dudin, P.; Martin, M.; Janek, J. Electrochemical activation of molecular nitrogen at the Ir/YSZ interface. *Phys. Chem. Chem. Phys.* **2011**, *13*, 3394−3410.
(370) Zeng, L.; Li, X.; Chen, S.; Wen, J.; Huang, W.; Chen, A. Unique hollow Ni−Fe@MoS2 nanocubes with boosted electrocatalytic activity for N2 reduction to NH3. *Journal of Materials Chemistry A* **2020**, *8*, 7339−7349.
(371) Luo, Y.; Liang, S.; Wang, X.; Lin, B.; Chen, C.; Jiang, L. Facile Synthesis and High-Value Utilization of Ammonia. *Chin. J. Chem.* **2022**, *40*, 953−964.
(372) Nayak-Luke, R. M.; Forbes, C.; Cesaro, Z.; Bañares-Alcántara, R.; Rouwenhorst, K. H. R. Chapter 8 - Techno-Economic Aspects of Production, Storage and Distribution of Ammonia. In *Techno-Economic Challenges of Green Ammonia as an Energy Vector*; Valera-Medina, A., Banares-Alcantara, R., Eds.; Academic Press, 2021; pp 191−207.
(373) Yüzbaşıoğlu, A. E.; Avşar, C.; Gezerman, A. O. The current situation in the use of ammonia as a sustainable energy source and its industrial potential. *Current Research in Green and Sustainable Chemistry* **2022**, *5*, No. 100307.
(374) Salmon, N.; Bañares-Alcántara, R. Green ammonia as a spatial energy vector: a review. *Sustainable Energy & Fuels* **2021**, *5*, 2814−2839.
(375) Rathore, S. S.; Biswas, S.; Fini, D.; Kulkarni, A. P.; Giddey, S. Direct ammonia solid-oxide fuel cells: A review of progress and prospects. *Int. J. Hydrogen Energy* **2021**, *46*, 35365−35384.
(376) Wojcik, A.; Middleton, H.; Damopoulos, I.; Van herle, J. Ammonia as a fuel in solid oxide fuel cells. *J. Power Sources* **2003**, *118*, 342−348.
(377) Jeerh, G.; Zhang, M.; Tao, S. Recent progress in ammonia fuel cells and their potential applications. *Journal of Materials Chemistry A* **2021**, *9*, 727−752.
(378) Smith, C.; Torrente-Murciano, L. Guidance for targeted development of ammonia synthesis catalysts from a holistic process approach. *Chem. Catalysis* **2021**, *1*, 1163−1172.
(379) Mukherjee, S.; Devaguptapu, S. V.; Sviripa, A.; Lund, C. R. F.; Wu, G. Low-temperature ammonia decomposition catalysts for hydrogen generation. *Applied Catalysis B: Environmental* **2018**, *226*, 162−181.
(380) David, W. I. F.; Makepeace, J. W.; Callear, S. K.; Hunter, H. M. A.; Taylor, J. D.; Wood, T. J.; Jones, M. O. Hydrogen Production from Ammonia Using Sodium Amide. *J. Am. Chem. Soc.* **2014**, *136*, 13082−13085.
(381) Guo, Y.; Pan, Z.; An, L. Carbon-free sustainable energy technology: Direct ammonia fuel cells. *J. Power Sources* **2020**, *476*, No. 228454.
(382) Tornatore, C.; Marchitto, L.; Sabia, P.; De Joannon, M. Ammonia as Green Fuel in Internal Combustion Engines: State-of-the-Art and Future Perspectives. *Frontiers in Mechanical Engineering* **2022**, *8*, 944201.

https://doi.org/10.1021/acscatal.3c02410
ACS Catal. 2023, 13, 14415−14453

(383) Kobayashi, H.; Hayakawa, A.; Somarathne, K.D. K. A.; Okafor, E. C. Science and technology of ammonia combustion. *Proceedings of the Combustion Institute* **2019**, *37*, 109−133.
(384) Cardoso, J. S.; Silva, V.; Rocha, R. C.; Hall, M. J.; Costa, M.; Eusébio, D. Ammonia as an energy vector: Current and future prospects for low-carbon fuel applications in internal combustion engines. *Journal of Cleaner Production* **2021**, *296*, No. 126562.
(385) Guo, J.; Chen, P. Catalyst: NH3 as an Energy Carrier. *Chem.* **2017**, *3*, 709−712.
(386) Erdemir, D.; Dincer, I. A perspective on the use of ammonia as a clean fuel: Challenges and solutions. *International Journal of Energy Research* **2021**, *45*, 4827−4834.
(387) Osorio-Tejada, J.; Tran, N. N.; Hessel, V. Techno-environmental assessment of small-scale Haber-Bosch and plasma-assisted ammonia supply chains. *Science of The Total Environment* **2022**, *826*, No. 154162.

https://doi.org/10.1021/acscatal.3c02410
ACS Catal. 2023, 13, 14415−14453